The University Of Sheffield.

How is limb development timed between different species?

By:

Holly Stainton

A thesis submitted in partial fulfilment of the requirements for the degree of Doctor of Philosophy

The University of Sheffield
Faculty of Science
Department of Biomedical Science

September 2019

Acknowledgements

I would like to express my very great appreciation to my supervisor, Dr Matthew Towers for his patience, guidance and support throughout my PhD. Your enthusiasm and useful critique have been invaluable in encouraging my scientific career. I would also like to thank my advisors, Professor Marysia Placzek and Dr Ivana Barbaric for their advice and valuable feedback. I am particularly grateful also to Dr Caitlin McQueen and Dr Joe Pickering for their patience and help with learning procedures in the lab. Thanks also should be extended to the past and present members of the Towers, Placzek, and Furley labs for their friendship and assistance in the lab over the years.

Finally, a special thanks to my parents, brother, and Seb for their continued and invaluable support and encouragement, without you all this would not have been possible.

INDEX

Chapter 2.

Materials and Methods

Abbreviations

AER Apical ectodermal ridge

A-P Antero-posterior

BMP Bone morphogenetic protein

CC Chick to chick (grafts)

CS Carnegie stage

CQ Chick to quail (grafts)

Cyp26b1 Cytochrome P450 26B1

DEAB N,N-diethylaminobenzaldehyde

DEPC Diethylpyrocarbonate

DMEM Dulbecco's modified Eagle's medium

DNA Deoxyribonucleic acid

En1 Engrailed-1

Fgf Fibroblast growth factor

GFP Green fluorescent protein

Gli3R Glioma-associated oncogene-3 (repressor)

Grem1 Gremlin-1

HH Hamburger-Hamilton stage

Lmx1b LIM homeobox transcription factor 1-beta

P-D Proximo-distal

QC Quail to chick (graft)

QQ Quail to quail (graft)

RA *all-trans* retinoic acid

RALDH2 retinaldehyde dehydrogenase-2

RAR Retinoic acid receptor

RNA Ribonucleic acid

Shh Sonic hedgehog

Sox9 SRY-Box-9

Wnt Wingless-related integration site

Abstract

How patterning is timed during embryonic development is a fundamental question in developmental biology. To understand this, I have compared the development of the wings of different sized avian species: quails, chicks and turkeys. I find that development is accelerated in the smaller quail compared to the larger chick, and this occurs during the first 12 hours of limb outgrowth. Using tissue grafting techniques and gene expression analyses I have implicated the extrinsic signal, retinoic acid, in setting developmental timing in avian wings, in relation to a fixed growth rate between species. However, retinoic acid does not appear to set species-specific growth during the time frame analysed in my study. My work elucidates the influence of extrinsic signals on intrinsic timing mechanisms in specifying cell fates in the wing, and has significant implications for how patterning is timed and scaled in different sized species during embryonic development.

Chapter 1.

Introduction

1.1 Limb development

The limb bud develops as a core of mesenchymal cells covered by ectoderm which is first visible in the chick at day 3 - Hamburger-Hamilton stage 16/17 (HH16/17) (Hamburger and Hamilton, 1951). The forelimb bud is derived from the somatopleural cells of the lateral plate mesoderm, which spans the anterior to posterior axis of the developing embryo. In vertebrates, the forelimb forms at the cervico-thoracic boundary, which is positioned between somites 15-20 in the chick embryo.

Retinoic acid (all trans retinoic acid - RA), is an important signalling molecule in embryonic development, and is involved in forelimb bud initiation and patterning. In order for RA to exert its effect in limb development, it must first be derived from vitamin A (retinol) and then to retinal. RALDH2 converts retinal to all-trans retinoic acid throughout the lateral plate mesoderm (Nakajima, 2019, Swindell, Thaller et al., 1999). In chick development, RA signalling in the lateral plate mesoderm is required for initiating the forelimb (wing) bud, and ensuring the correct expression of *Tbx5*, which marks the presumptive forelimb territory (Mic, Sirbu et al., 2004, Niederreither, Vermot et al., 2002, Stratford, Logan et al., 1999, Zhao, Sirbu et al., 2009). In addition to RA, *Tbx5* also acts downstream of Hox proteins that segment and establish the body plan and studies in the mouse have shown that Hox4 and 5 regulate *Tbx5* expression. (Burke, Nelson et al., 1995, Moreau, Caldarelli et al., 2019)Gibson-Brown, Agulnik et al., 1998, (Izpisua-Belmonte, Tickle et al., 1991, Minguillon, Nishimoto et al., 2012).

Tbx5 then induces *Fgf10* in the forelimb bud field mesenchyme, which induces *Fgf8* in the overlying ectoderm (Agarwal, Wylie et al., 2003). Fgf10 and Fgf8 then form a positive feedback loop between the limb mesenchyme and ectoderm, which is necessary for the

outgrowth of the wing bud (Figure 1.1) (Moon and Capecchi, 2000, Nishimoto, Wilde et al., 2015).

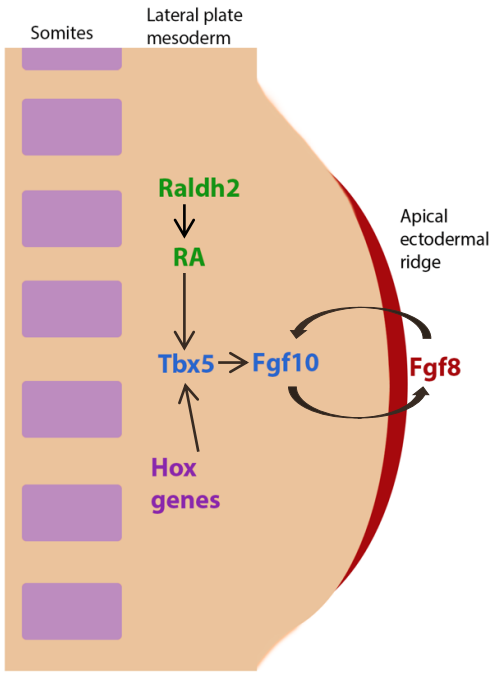

Figure 1.1. Schematic depicting initiation of the forelimb (wing) bud.

Raldh2 in the lateral plate mesoderm synthesises retinoic acid (RA) from retinal. RA acts along with Hox genes to induce *Tbx5* expression in the presumptive forelimb field. Tbx5 then induces Fgf10, which induces Fgf8 in the overlying ectoderm. A positive feedback loop between Fgf10 in the mesenchyme and Fgf8 in the ectoderm drives the initial outgrowth of the wing bud.

Growth and patterning of the wing bud to form a fully patterned wing (Figure 1.2) requires the interaction of embryonic signalling centres including the apical ectodermal ridge (the thickened ectodermal ridge located at the distal tip), the polarising region (also referred sometimes as the zone of polarising activity) and the dorsal and ventral ectoderm. These signalling centres pattern the limb along three principle axes: the antero-posterior axis, the proximo-distal axis, and the dorso-ventral axis, detailed below.

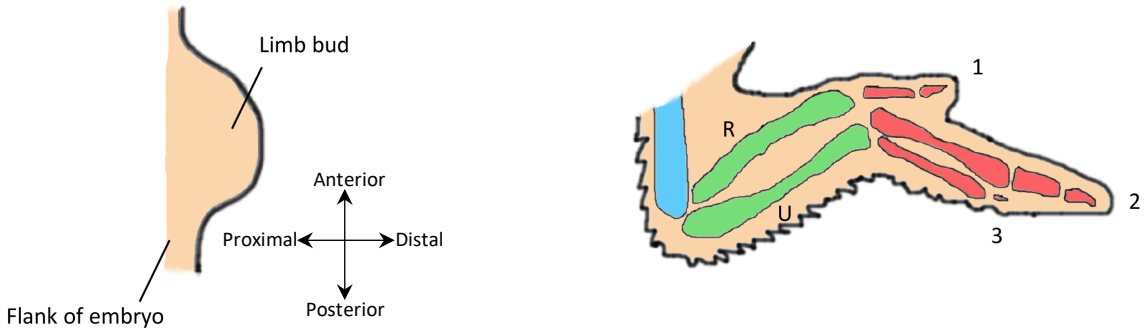

Figure 1.2. Schematic depicting the wing bud and developed wing.
Schematic of the right chick wing bud at early stages of development (shortly after wing bud initiation and outgrowth) and late stages (e.g. day 10 incubation). Over time the wing bud develops into a characteristic wing shape (pictured right), with recognisable skeletal elements, the stylopod (humerus) – blue, zeugopod (ulna (U) and radius (R)) – green, and autopod (digits, labelled as 1, 2 and 3 – carpals not shown) – red.

1.2 Antero-posterior patterning

The antero-posterior axis of the limb runs from the thumb to the little finger. However, the number of digits varies between species, with the chick having three digits in the wing (1, 2 and 3 - anterior to posterior) and four digits in the leg, compared to mice and human limbs that both have five digits.

One of the major advances in understanding antero-posterior patterning of the limb was the discovery of the embryonic signalling centre, the polarising region (Saunders and Gasseling, 1968). It was shown that a complete mirror-image duplication of the three chick digits occurred (i.e. 3-2-1-1-2-3) when the posterior-distal portion of the wing bud was transplanted to the anterior margin of the wing bud of another embryo (Figure 1.3). Lewis Wolpert interpreted the outcome of this experiment to help formulate his concept of positional information, whereby cells acquire positional values and use them to instruct their differentiation into a particular structure. Therefore, it was hypothesised that this area

of tissue (the polarising region) produces a morphogenic signal that acts to provide mesenchyme with antero-posterior positional values in a concentration-dependent manner (Wolpert, 1969). In the positional information model, cells interpret a gradient of different concentration thresholds and differentiate into the appropriate digit identity. This model could therefore explain the mirror image duplication of digits seen when transplanting the posterior distal tissue. Subsequent experiments in which the polarising region was grafted at different positions (Tickle, Summerbell et al., 1975), or polarising region cells were irradiated (Smith, Tickle et al., 1978) resulted in variations in the number of digits produced in the wing. This revealed that the number of polarising region cells is important in specifying digit fates. Thus, providing further evidence for the polarising region as the source of a morphogenic signal and supporting the idea of digit specification by a gradient of positional values. Furthermore, the concentration of this morphogenic signal was shown to be important, as the number of digits duplicated is dependent on the number of cells transplanted (Saunders and Gasseling, 1968, Tickle, 1981, Tickle, Summerbell et al., 1975).

The first molecule found to mimic the effects of polarising region grafts was RA. In a series of experiments in which RA was applied on carriers to the anterior margin of the wing, a mirror image duplication of the digit pattern was achieved, similar to those obtained with polarising region grafts (Tickle, Lee et al., 1985). However, it was later discovered that RA acts to induce the formation of a new polarising region (Noji, Nohno et al., 1991, Riddle, Johnson et al., 1993, Stratford, Logan et al., 1999, Wanek, Gardiner et al., 1991). Subsequently, the Tabin group found that *Shh* is expressed in the polarising region (Riddle, Johnson et al., 1993). In addition, grafting *Shh* expressing cells and beads soaked in Shh protein to the anterior margin of the wing was found to induce mirror image duplications of digits. (Riddle, Johnson et al., 1993, Yang, Drossopoulou et al., 1997). These findings provided strong evidence that Shh acts as the morphogenic signal produced by the polarising region.

Shh emanates from the polarising region and forms a concentration gradient across the anterior-posterior (A-P) axis of the wing bud, which provides cells with positional values

of the digits (in the chick, digits 1, 2 and 3). Application of Shh protein for various lengths of time in the chick wing showed that not only the concentration, but also the exposure time was important in specifying digit fates (Yang, Drossopoulou et al., 1997). It was also shown that during the specification of positional values, cells are initially specified with anterior positional values and are promoted to more posterior values every four hours. (Towers, Signolet et al., 2011, Yang, Drossopoulou et al., 1997). Furthermore, inhibiting Shh signalling by cyclopamine also revealed that Shh signalling from the polarising region has an important role in stimulating proliferation and the expansion of adjacent mesenchyme in the digit-forming field. This is necessary for the correct amount of growth across the antero-posterior axis to occur, and thus, the ability to form the full range of positional values. (Towers, Mahood et al., 2008). Therefore, it has been shown that Shh acts to integrate growth and specification during antero-posterior patterning.

Using genetic approaches, two different models of how Shh patterns the antero-posterior axis of the mouse limb have also been proposed. The biphasic model proposed that Shh specifies the pattern of digits over a short period of time (approximately 3 hours) but is then primarily required to promote cell proliferation and maintenance of the digit-forming cells (Zhu, Nakamura et al., 2008). On the other hand, the temporal expansion model suggested specification occurs over a longer time, and that a concentration gradient of Shh specifies the anterior digits (1, 2 and 3) and the duration of signalling specifies the posterior digits (4 and 5), which arise from the polarising region (Harfe, Scherz et al., 2004). This, however, does not appear to be the case in the three digit chick wing, as no digits arise from the polarising region itself. Furthermore, it is unclear if the biphasic model can be applied to the chick model as there is no evidence that Shh is required after digit specification.

The transcriptional effectors of Shh are the Gli proteins (1-3), Gli2 and Gli3 have both activator and repressor forms. High levels of Gli repressors are found in the anterior wing bud where Shh signalling is absent. However in the posterior wing, Gli proteins are converted to their activator forms in response to Shh signalling (Lee, Zhao et al., 2016, Tickle

and Towers, 2017). The ratio of activator/repressor forms in the posterior wing is reflective of the Shh concentration gradient i.e. a higher proportion of Gli activators posteriorly (Wang, Fallon et al., 2000). Gli3 is the key repressor in the chick wing bud, and Shh operates by preventing Gli3 being processed to the repressor form (Gli3R). Thus, it has been shown that Shh mediates its effects through alleviating repression by Gli3, facilitating the specification of digit identities (Litingtung, Dahn et al., 2002, te Welscher, Zuniga et al., 2002).

However, currently it is not well understood how positional values are then interpreted to allow the appropriate digit to form at a later stage of development. There is evidence that signalling pathways downstream of Shh, such as BMPs and FGFs may be involved. For example, BMP signalling in the interdigital mesoderm has been suggested to confer posterior and anterior digit identity, with higher levels of BMP signalling being sufficient to transform anterior into posterior digit identities (Dahn and Fallon, 2000).

Furthermore, a Turing-type reaction-diffusion mechanism has been implicated in determining digit number in the limb (Gierer and Meinhardt, 1972, Newman and Frisch, 1979, Sheth, Marcon et al., 2012, Turing, 1952). Using the mouse model, interactions between Sox9, Bmps and Wnts have recently been proposed to make up the components of this Turing mechanism and provide a self-organised pre-pattern, which determines the number of digits across the antero-posterior field (Raspopovic, Marcon et al., 2014).

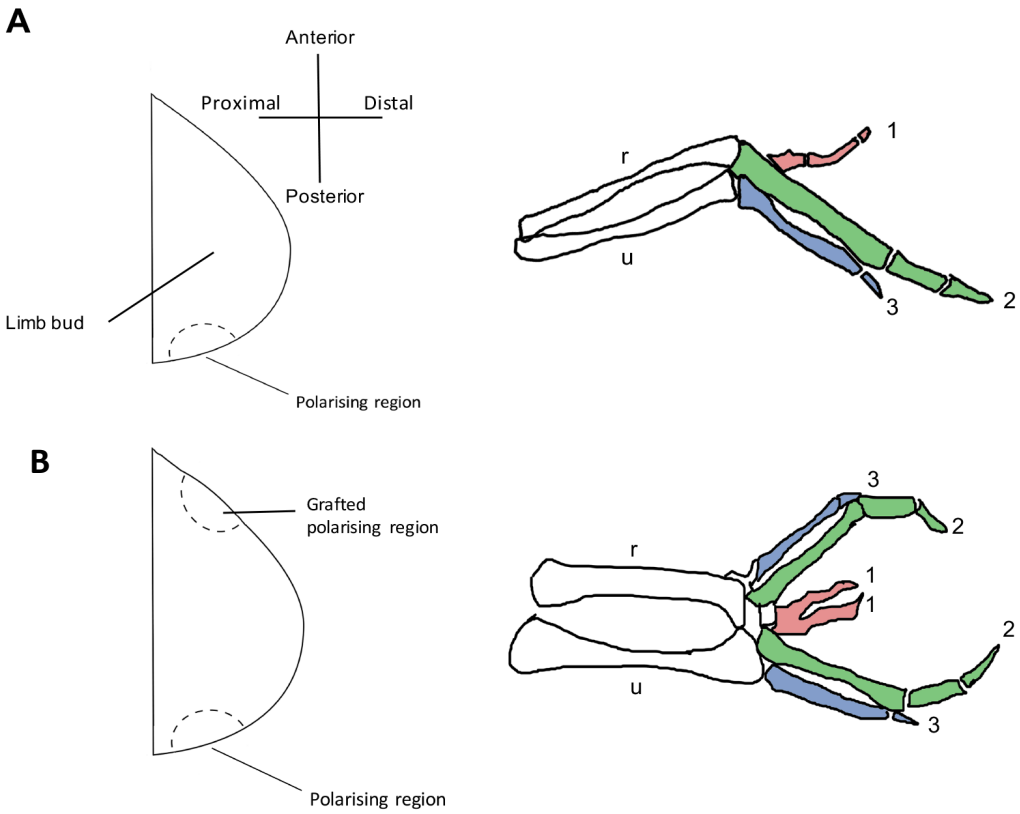

Figure 1.3. Transplantation of the polarising region to the anterior margin results in mirror-image duplication of the digits.

A) During normal development, the polarising region is located in the posterior limb bud and the typical morphology of digits 1, 2 and 3 (anterior to posterior) is formed. **B)** In experiments, such as the transplantation experiments conducted by Saunders and Gasseling, a second polarising region is grafted to the anterior margin of the limb bud. This results in a duplication digit pattern - 3, 2, 1, 1, 2, 3 (anterior to posterior). Adapted from Stainton and Towers, 2018**.**

1.3 Proximal-distal patterning

The structures of the limb are laid down in a proximal to distal sequence (P-D) and can be divided into three principle segments, the proximal stylopod (i.e. humerus), the

zeugopod (i.e. ulna/radius) and the most distal autopod (i.e. wrist and digits). It is widely accepted that expression of the 5' Hoxa and Hoxd genes are associated with patterning and specification of the proximo-distal axis of the developing limb bud. Similar to expression of Hox genes along the primary body axis, Hoxa and Hoxd genes are expressed with spatial and temporal collinearity in the limb bud, thus are expressed according to their location along the chromosome. *Hoxa10* is expressed first in the prospective stylopod, followed by *Hoxa11* in the zeugopod, and finally *Hoxa13* in the prospective autopod (Nelson, Morgan et al., 1996, Yokouchi, Sasaki et al., 1991). However, the specification of specification of skeletal elements along the proximo-distal axis has remained a controversial subject and multiple conflicting models have been proposed.

1.3.1 Progress zone model

It was discovered that the removal of the overlying apical ectodermal ridge in the chick wing at different time points led to the truncation of the limb at different P-D levels, i.e. early removal resulted only in proximal development, and later stage removal resulted in progressively more distal development (Saunders, 1948). This discovery was interpreted in terms of positional information and led to the progress zone model (Summerbell, Lewis et al., 1973). As opposed to antero-posterior patterning, in which positional values are specified by a concentration gradient, proximo-distal positional values were considered to be specified sequentially through an autonomous timing mechanism that operates in the undifferentiated mesenchyme below the apical ectodermal ridge. This area, known as the progress zone, is exposed to signals from the apical ectodermal ridge (now known to include FGFs), which acts to maintain the outgrowth of the limb. The AER was demonstrated to be maintained by a factor expressed in the mesenchyme (Zwilling, 1956). Over time, cells are progressively specified with proximal to more-distal positional values, before being displaced by proliferation from the progress zone (Figure 1.4a) (Summerbell, Lewis et al., 1973). This model therefore suggests that specification of P-D positional values is dependent on the time cells spend in the progress zone while being exposed to apical ectodermal signals (Summerbell, Lewis et al., 1973, Wolpert, Tickle et al., 1979). The idea that the

progress zone behaves autonomously was supported by the finding that cells maintain an autonomous progression through P-D axis positional values when distal tips are transplanted between wings of different ages (Summerbell and Lewis, 1975). Additionally, transplanting older stage apical ectodermal ridges to younger limb buds and vice versa showed that the apical ectodermal ridge has a permissive role in permitting the outgrowth of the wing, rather than in actively specifying positional values (Rubin and Saunders, 1972). Furthermore, evidence that the cell cycle may be linked to the autonomous timing mechanism came from experiments which produced fate maps based on the mitotic index, and showed that each limb segment is derived from tissue generated by one round of the cell cycle in the progress zone (Lewis, 1975).

1.3.2 Early Specification Model

An alternative interpretation of the progress zone model, is that specification of positional values occurs very early in the undifferentiated limb mesenchyme - at around HH19 (Figure 1.4b) (Dudley, Ros et al., 2002). Specified cells then proliferate and expand as the limb develops. In the early specification model, it was unclear if this involved instructive or permissive signalling. However, later fate maps revealed that cells in the early limb bud are not lineage-restricted, as predicted in the early specification model, and have the capacity to contribute to both the autopod and zeugopod (Sato, Koizumi et al., 2007). Additionally, the early specification model does not account for the progressive nature of how each element is laid down in a proximal to distal fashion. Thus *5' Hox* genes, which provide a readout of positional identity along the proximo-distal axis, are progressively switched on, beginning with *Hoxa10* (stylopod marker) at HH19 and finally with *Hoxa13* (autopod marker) expressed at HH22. (Vargesson, Kostakopoulou et al., 2001). These considerations provide persuasive evidence against the early specification model; instead suggesting that cell fates are progressively specified.

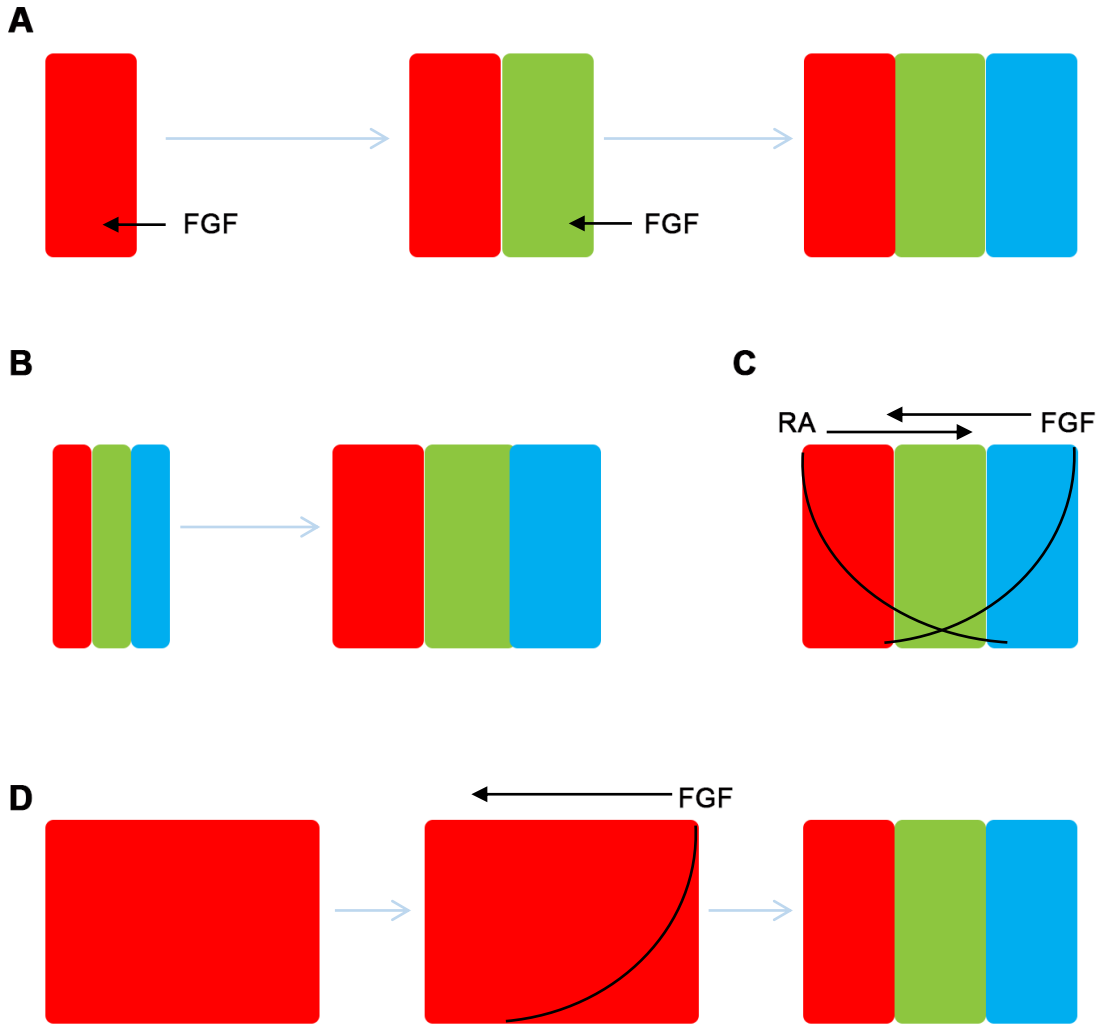

Figure 1.4. Previous models of proximo-distal patterning of the limb bud.

Red – cells specified to stylopod fate. Green – cells specified to zeugopod fate. Blue – cells specified to autopod fate. **A)** Progress zone model, permissive distal FGF signals from the apical ectodermal ridge act on underlying proliferating mesenchyme in the progress zone. Cells are specified depending on how long they have been proliferating in the progress zone. **B)** Early specification model, the specification of cell fates occurs very early in the developing wing bud, cells proliferate and over time populations expand. **C)** Two signal model, RA from the flank of the embryo and FGFs from the apical ectodermal ridge form opposing gradients across the wing bud providing positional information. **D)** One signal model, the limb is initially set up to a default proximal programme, FGFs then act to remove RA signalling and allow specification of more distal fates.

1.3.3 Two-signal model

The two-signal model proposed an instructive role for extrinsic signalling from the apical ectodermal ridge in specifying proximo-distal positional values. Retinoic acid (RA) signalling, emanating from the flank of the embryo, was proposed to be involved in specifying the positional value of the proximal stylopod by inducing *Meis1/2* expression in the proximal limb. Over-expression of *Meis1* and *Meis2* leads to truncation of the limb or inhibition of distal elements, revealing their role in proximal patterning. (Capdevila, Tsukui et al., 1999, Mercader, Leonardo et al., 1999, Mercader, Leonardo et al., 2000). Furthermore, in cultured chick limb bud cells and recombinant limbs, RA has been shown to be necessary for the induction of *Meis1* and in the specification of proximal skeletal elements (Cooper, Hu et al., 2011). FGFs derived from the apical ectodermal ridge were then proposed to instructively specify the positional values of distal structures (zeugopod and autopod), by acting in a morphogenic gradient and inducing the Hox genes, *Hoxa10*, *Hoxa11* and *Hoxa13*. In this model, RA is opposed by the antagonistic action of the distal signal, Fgf8. Fgf8 activates transcription of the enzyme Cyp26b1, which breaks down RA distally, restricting *Meis* gene expression to the proximal region of the limb and allows the specification of distal positional values (Mic, Sirbu et al., 2004). This model implicates an instructive role for extrinsic signals rather than a permissive role as suggested in the progress zone model (Figure 1.4c). However, although there is evidence supporting a role for RA acting as an instructive signal, no strong evidence has been presented to show that FGFs are instructive signals. Indeed, experiments in which the FGF signalling was manipulated in the chick wing failed to alter the timing of *Hoxa13* expression, which is implicated in autopod specification (Vargesson, 2001).

1.3.4 One-signal model

Based on genetic analyses in the mouse, an alternative one signal model has also been proposed as a variant to the two-signal model. The model states that before FGFs are expressed in the apical ectodermal ridge, the whole limb bud is exposed to RA and expresses *Meis1/*2. FGFs from neighbouring tissues, including the heart field, act to remove RA from the limb and thus prevent teratogenesis (Cunningham and Duester, 2015). FGFs from the apical ectodermal ridge then act to inhibit RA and act as permissive signals to allow outgrowth and positional value specification (Figure 1.4d). In this model, patterning of prospective skeletal elements occurs independently of RA signalling. However, this conflicts with evidence gained from experiments using the chick, where *Meis1* is induced in limb buds when RA is ectopically placed in distal regions. (Rosello-Diez, Ros et al., 2011, Tamura, Yokouchi et al., 1997) (Cooper, Hu et al., 2011).

Furthermore, the one signal model is based on experiments in the mouse *Raldh2-/-* , which is a knockout of a major RA synthesising enzyme (Zhao et al, 2009). However, the complete depletion of RA in *Raldh2-/-* mice resulted in the failure of limb development, and so the mice were treated with a functional level of RA, which also possibly contributed to outgrowth and patterning. Indeed, later experiments in the chick in which re-aggregated early chick wing mesenchymal cells were transplanted in proximity to the RA-rich region of the somites, showed that RA was necessary and sufficient to pattern proximal structures. However, caution is needed with this experiment as it involved transplanting cells to an artificial signalling environment (Rosello-Diez, Ros et al., 2011).

1.3.5 Signal-time model for proximo-distal patterning

The current model for proximo-distal patterning comes from the interpretation of recent data from the Towers/Ros labs, which builds on the progress zone model, and has provided further evidence for the involvement of an intrinsic timer in proximo-distal patterning. The authors provided evidence that zeugopod and autopod positional values are

specified by an intrinsic timing mechanism as predicted in the progress zone model and the one-signal model. However, the positional value of the stylopod is specified by the extrinsic signal, RA, as in the two-signal model.

Through a series of experiments, in which older stage and younger stage distal mesenchyme were grafted between chick wing buds, distal positional values were shown to be specified by an autonomous timing mechanism. Grafts of early stage (HH20) distal mesenchyme, fated to give rise to the zeugopod, were transplanted underneath the distal ectoderm of later stage (HH24) host. The experiments revealed that the autopod marker, *Hoxa13,* and that cell cycle kinetics, are intrinsically timed in the donor graft and not re-set by extrinsic host signals. It was also shown that Fgf8 from the apical ectodermal ridge has no instructive role on the mesenchyme, and in fact, the grafted mesenchyme dictated the duration of the host apical ectodermal ridge. The stability and intrinsic nature of *Hoxa13* timing and cell cycle rates in the distal mesenchyme were also seen in similar grafting experiments using even later stage HH27 wings to HH20 wings (Saiz-Lopez, Chinnaiya et al., 2015, Saiz-Lopez, Chinnaiya et al., 2017).

The evidence that positional values are specified by an intrinsic mechanism was also demonstrated in an experiment in which HH24 wing bud cells and *Gfp*-expressing HH20 cells were disaggregated, then randomly re-aggregated, and grafted to the distal tip a HH24 host wing bud. It was shown that cells of different ages in the graft had sorted out from one another, with HH20 cells moving to the periphery of the graft to integrate with host cells of the same age. These findings fit with the widely accepted idea that a cells proximo-distal positional value is encoded by its surface properties (1984, Nardi, 1984, Wada, 2011, Wada and Ide, 1994), which allow cells with different positional values to sort out when confronted with cells of a different positional value. The products of the 5' *Hoxa* genes regulate molecules that are involved in cell adhesion, inducing *Ephrin* receptors in distal cells. (Saiz-Lopez, Chinnaiya et al., 2017, Stadler, Higgins et al., 2001) This provides a mechanism by which the progressive activation of 5'Hox genes could specify proximo-distal positional values.

The signal-time model incorporates ideas from previous models, suggesting that trunk derived RA could act as an instructive extrinsic signal to specify the stylopod via *Meis1/2*; and that the specification of distal fates occurs by an intrinsic timer operating in the distal mesenchyme (Figure 1.5). The model involves a switch from early extrinsic signal based specification of proximal limb elements (stylopod), to an intrinsic timing mechanism, which specifies distal cell (zeugopod and autopod) fates. However, how the switch from extrinsic proximal specification to intrinsic distal specification occurs has not yet been shown.

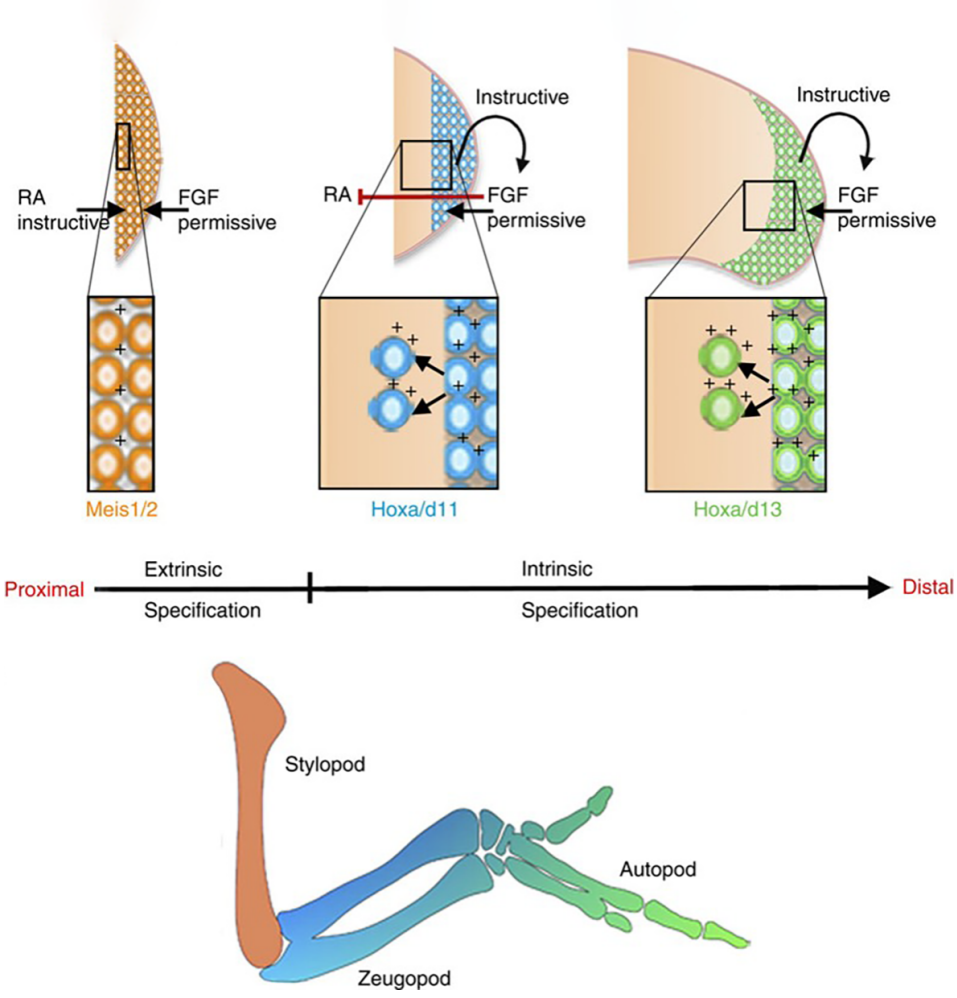

Figure 1.5. Signal-time model of proximo-distal patterning of the limb bud.

In the current model of proximo-distal patterning RA acts instructively to pattern the proximal limb via *Meis1/2* expression. FGFs from the apical ectodermal ridge then act permissively to allow cell proliferation and outgrowth and to inhibit RA signalling, allowing

more distal fates to be specified by an autonomous timer (e.g. *Hoxa11* and *Hoxa13* marking the zeugopod and autopod, respectively). The mesenchyme also signals to the apical ectodermal ridge, determining the age of the tissue. Adapted from Saiz-Lopez et al 2015.

Furthermore, recently it has been shown that the intrinsic timer operating in the distal mesenchyme is involved in terminating limb bud outgrowth during the patterning phase of chick wing development. It was found that cells complete their proliferative programme regardless of the age of the overlying ectoderm, which acts permissively to allow the cell cycle timer to run. Analysis of BMP signalling in these cells indicated that there is a switch from inhibition of BMP signalling, to BMP signalling which is involved in decreasing proliferation and terminating the intrinsic cell cycle programme (Pickering, Rich et al., 2018, Saiz-Lopez, Chinnaiya et al., 2017).

1.4 Dorso-ventral patterning

Correct patterning of the dorso-ventral axis is important in creating a functional morphological structure. For example, the correct muscle patterns in the limb, the nails/claws which are present on the dorsal side of the finger tips, and also hair on the dorsal side of the hand in mammalian species.

As the limb bud emerges, the ectoderm is split into dorsal ectoderm expressing *Wnt7a*, and the ventral ectoderm which expresses *En1* via BMP signalling. Polarity is achieved by Wnt7a in the dorsal ectoderm inducing *Lmx1b* in the underlying mesoderm. (Figure 1.6) (Parr and McMahon, 1995, Riddle, Ensini et al., 1995, Vogel, Rodriguez et al., 1995). Loss of function mouse studies have shown that ventral identity is imparted by *En1* which acts to inhibit *Wnt7a* expression and thus, restricts *Wnt7a* expression to the dorsal ectoderm (Figure 1.6). (Cygan, Johnson et al., 1997, Dealy, Roth et al., 1993, Loomis, Harris et al., 1996)

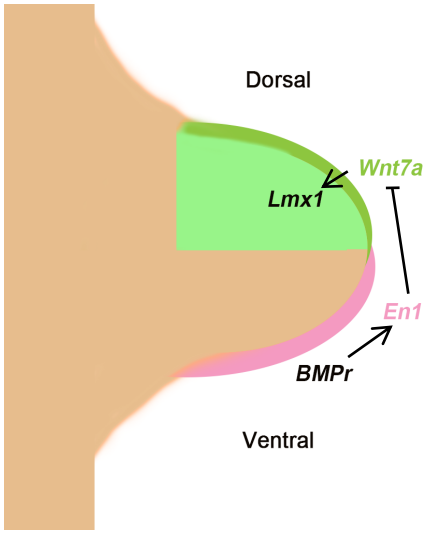

Figure 1.6. Schematic depicting dorso-ventral patterning of the limb bud.
In the ventral ectoderm BMP signalling induces *En1* expression via BMPr. *En1* in the ventral ectoderm inhibits *Wnt7a* and restricts its expression to the dorsal ectoderm. *Wnt7a* then acts to impart dorsal identity by inducing *Lmx1b* expression in the underlying mesoderm.

1.5 Integration of the axes

Growth and specification of the axes of the limb do not occur independently of one another. Early grafting experiments found that the polarising region needs to be grafted in contact with the apical ectodermal ridge in order to provide positional information and therefore showed that antero-posterior and proximo-distal patterning is integrated (Summerbell, 1974). It was later discovered that a positive feedback loop exists between the polarising region and the apical ectodermal ridge, whereby Fgf4 regulates *Shh* expression in the polarising region, and *Shh* feeds back to maintain the apical ectodermal ridge via the AER maintenance factor and BMP antagonist, *Grem1.* (Laufer, Nelson et al., 1994, Niswander, Jeffrey et al., 1994, Zuniga, Haramis et al., 1999, Zwilling, 1956). It has been proposed that loss of signalling between the apical ectodermal ridge and the polarising region occurs due to the breakdown in the *Grem1/Fgf4/Shh* feedback loop between the two

embryonic signalling centres. However, recently an alternative model has been suggested, based on grafting experiments showing that the duration of *Shh* expression in the polarising region is intrinsically determined and linked to a proliferation timer (Chinnaiya, Tickle et al., 2014) The mechanism underpinning this cell cycle timing mechanism is unclear although a recent paper implicates Shh controlling antagonistic regulators of the G1-S phase transition over time (Pickering, 2019)

In addition dorso-ventral and antero-posterior/proximo-distal axes are linked, as it has also been shown that Wnt7a in the dorsal ectoderm acts with Fgf4 from the apical ectodermal ridge to maintain *Shh* expression in the polarising region, and thus shows how the three axes are integrated during growth and patterning (Yang and Niswander, 1995).

1.6 Timing limb development

The aim of my thesis is to understand how patterning events are timed in the developing wing. Therefore, the extensive research on limb development has provided an excellent model to determine the influence of intrinsic timing mechanisms and extrinsic signals. A useful method to gain insight into how timing is controlled is through comparing development across different species with different sized limbs. Development varies between species and often depending on the size of the organism and the length of the incubation/gestation period, generally following the trend that larger species with longer incubation times have a slower rate of development. The avian family therefore provides a useful model due to the wide range of limb sizes and correlating incubation periods.

1.6.1 Comparative staging of avian embryos

Although the limbs of different avian species grow to markedly different sizes, it is largely unknown how this occurs. The quail incubation period is 14 days and adult wings attain a size of approximately 17.5cm in length, whereas the chicken incubation period is 21

days and their wings are approximately 31cm. Despite the use of quails and other avian species as model systems, there is only a comprehensive literature describing the timing and staging of chicken embryonic development. Although early studies described different morphological aspects of quail embryonic development, there are a number of issues with these studies (Padgett and Ivey, 1960, Zacchei, 1961) (Nakane and Tsudzuki, 1999). For example, studies used broad, non-specific time points such as recording the staging of embryos every 24 hours (Padgett and Ivey, 1960). According to the Hamburger-Hamilton system chicks can pass through up to 4 or 5 stages in the space of 24 hours. Recording stages over shorter time intervals would therefore be more useful. Furthermore, staging of the quail was not performed in reference to the well-established chicken model making cross-species comparisons limited.

A more recent study has analysed and compared the development of multiple avian species including the quail, turkey and chick (Sellier, 2006). This study used the Hamburger Hamilton (HH) staging system—a widely used morphology-based system which characterises the development of chick from oviposition (laying of the egg) until hatching (Hamburger and Hamilton, 1951). The results revealed only a negligible difference in the development of the quail and chick at 72 hours incubation (noted as HH20 in the chick and HH19 in the quail), but due to lack of statistical tests, it was unclear if this result was significant. Furthermore, according to the Hamburger Hamilton system, chick embryos should only be at HH18-19 after 72 hours incubation (Hamburger and Hamilton, 1951), as opposed to HH20 stated in the study. This suggests that embryos were staged inaccurately, or the temperature the eggs were incubated at was higher than the normal 37-38˚C. Additionally, analyses in this study were limited to only the first 72 hours after oviposition, and while this may provide a useful comparison of very early embryonic development, many of the major organs and appendages (including the limb buds) would not have developed or become visible during this time.

Other developmental studies appear to suggest that there is heterogeneity between the development of avian species which correlates to incubation length until hatching. A

study exploring skeleton formation in the Japanese quail, although not directly compared to the chick, showed that quail skeletons develop faster, with chondrification occurring at day 4 of incubation in quail compared to 5.5 in chick (Nakane, 1999; (Hamburger and Hamilton, 1951), consistent with the shorter incubation period seen in the quail. Furthermore, initiation of the wing bud in the emu occurs at day 7 of incubation, compared to just over 2 days (51-56 hours incubation) in the chick at HH16. Again, this is consistent with the longer incubation period for the emu (Nagai, 2010). However, a comprehensive study in 2010 compared the appearance of developmental features in quail embryos to landmarks highlighted in the Hamburger-Hamilton staging of chicks, such as the appearance of somites, limb buds and feather germs (Ainsworth, Stanley et al., 2010). The authors concluded that, based on these parameters, quail and chick development appears equivalent until HH28 (day 7) stating no obvious delays or accelerated development between either species. After which point, the quail has an accelerated rate of development, reaching HH46 (the final HH stage before hatching) one hundred hours earlier than the chick (Ainsworth, 2010). Interestingly, the authors noted that it takes approximately 8-9 days for the quail to reach HH36, compared to 10 days in the chick. However, after this time point the Hamburger Hamilton staging system could not be accurately compared to the quail, due to differences in morphology of the developing quail. For example, the black pigmentation that arises in quail feathers from HH36, is not present in the chick feathers. From this study, it can be taken that the Hamburger Hamilton staging system is a useful tool to analyse quail development up until HH36.

In the previously described studies, all of the analyses focused on the morphology of different avian embryos and how it changes over time. Although these studies provide a useful starting point for comparing embryonic growth and scaling between the species, the comparison of broad morphology only provides a limited analysis. It is not currently known if molecular signalling events such as providing cells with positional information, or the duration of embryonic signalling centres, are timed alongside the progression through HH stages. It is also unknown how these patterning events are specifically timed in the wings of different avian species compared to the chick. Thus, characterisation and comparison of the

development of the forelimb between different avian species may elucidate how patterning and growth is timed in different sized limbs.

1.6.2 The use of inter-species transplantation to study developmental timing

The transplantation of cells and tissues between different species with distinctive developmental times is a useful technique to understand the role of intrinsic and extrinsic factors in developmental timing. Some of the first experiments to address the issue of species-specific developmental timing and growth involved the transplantation of limb buds between different sized salamander species (Harrison, 1924, Twitty, 1931). The researchers found that grafted limbs developed closer to the size to the limbs of the donor species than the limbs of the host species, but with a slight influence from host-derived factors resulting in limbs that were larger than the host, but not quite as large as the donor species. Therefore, it was concluded that mechanisms 'intrinsic' to the limb were important in scaling development yet there was also an influence from 'extrinsic' factors derived from the body of the host. However, in these studies no control grafts were performed between the same species, and therefore it is difficult to draw conclusions about how grafted tissue behaves in another host environment.

Nevertheless, more recent studies analysing species-specific growth of wings in different bird species also found similar results to the early salamander experiments. In quail and chick chimeric grafts of developing wing buds, the resulting skeletal elements in the wing largely maintained the size of the original donor, however influence from the host body could be seen (Le Douarin, Dieterlen-Lievre et al., 2000, Ohki-Hamazaki, Katsumata et al., 1997). The research also indicated that the size of wing itself was intrinsic to the proliferating mesenchyme of the wing bud and could not be affected by the overlying ectoderm of a different species. However, only the length of the zeugopod (specifically, the ulna) was measured a month after hatching, no data measuring the length of the whole limb is described in the paper and there is no mention of the size of wing during embryonic

development. It is difficult to speculate why this may be, however it could suggest abnormal or missing skeletal elements after the grafting procedure as the study also indicates a low rate of survival and integration of the wing buds – 22%. (Martin, Ohki-Hamazaki et al., 1991)

Taken together, these studies have revealed how transplantation studies can provide a useful technique to study species-specific developmental timing However, the role and relative influence of 'extrinsic' signals and 'intrinsic' timing remains unclear, and whether species-specific timing can be altered by these signals is currently unknown.

1.6.3 Timing wing development between different avian species

To summarise, how embryonic development is timed, and how this differs between species is an enigmatic question in developmental biology. Previous studies have determined that cell autonomous mechanisms are important in timing wing development, however there is a small but significant influence from extrinsic signals. Comparing the development of limbs between different sized species provides a useful method for elucidating how differences in developmental time occur and transplanting these structures between the species is an effective technique for observing and determining the relative importance of cell autonomous intrinsic timing, and whether this can be affected by extrinsic signals.

The developing avian limb is an appropriate model organ to study developmental timing as there is extensive research on the mechanisms of patterning in the chick wing, the limb is also accessible to manipulate in the egg, and is amenable to transplantation studies. In addition to this, there is a wide range of avian species with different sized wings, which can be compared with the well-established Hamburger Hamilton chick staging system in order to provide a reference for developmental age across avian species.

The molecular mechanisms involved in patterning and growth of the wing are well understood, however, it remains unclear if they influence the timing of limb development between species. Despite morphological staging of avian species progression through

developmental stages, questions still remain regarding how developmental age relates to the timing of cellular and molecular patterning events in patterning the limb.

1.7 Aims of the thesis:

- To compare morphological, cellular, and molecular developmental events in different sized avian wings in comparison to developmental age (HH stages), in order to determine when differences in developmental timing arise.

- To determine how the switch from extrinsic signal-based patterning, to an autonomous timer occurs in timing and patterning the outgrowth wing.

- Through tissue grafting techniques, determine whether developmental time is intrinsically controlled in the developing wing bud, and through manipulation of signalling pathways and analysis of gene expression, determine the role of extrinsic signals and intrinsic timers in setting species-specific time.

Chapter 2.

Materials and Methods

2.1 Avian embryo husbandry

2.1.1 Incubation of avian embryos

Wild type fertilised chick eggs were obtained from Henry Stewart and Co. (UK), wild type fertilised quail embryos obtained from Quails in Essex (Essex, UK), wild type turkey eggs were obtained from Rutland Organic Poultry, and also as a gift from Nicola Hemmings (UK). *Gfp*-expressing chicken eggs were obtained from the Roslin Institute (Edinburgh, UK; (McGrew, Sherman et al., 2004).

Eggs were incubated in a Panasonic MIR-262-PE incubator set to 37°C with 95% humidity. All experiments involving live chick embryos conformed to the relevant regulatory standards (University of Sheffield).

2.1.2 Staging of avian embryos

Embryos were windowed at day 3 incubation (72 hours). To window the eggs, blunt forceps were used to make a small hole in the base of the egg and approximately 1-1.5ml of serum was removed, the eggs were then laid on their sides and a hole was cut into the side of the egg using scissors. The embryos were then staged according to the Hamburger-Hamilton system (Hamburger and Hamilton, 1951) to determine if they were at the appropriate age of HH18/19. There is some level of stage variability in early embryo stages and so outliers were discarded at this point. The remaining eggs were sealed using sellotape, then left to develop until the appropriate time. In order to ensure windowing eggs did not cause disruption in development, unwindowed eggs were compared against

windowed eggs to ensure the same rate of development. Eggs were also removed from the incubator for short periods of time before being returned so as not to disrupt development. For my analyses on the quail and chick embryos the 72 hour point (day 3) - shortly after the limb bud becomes visible – is at the equivalent stage HH18/19, and is noted as time 0. In the turkey, the equivalent stage HH18/19 occurs at the 96 hour point and is noted as time 0. After which time point, analyses were performed every subsequent 12 hours.

2.1.3 Fixation of avian embryos

At the appropriate time points, embryos were cut out of the egg and placed in a Petri dish containing phosphate buffered saline solution (PBS). The head, membranes and internal organs were then carefully removed, and the embryos stored in 4% Para-formaldehyde (PFA) at 4°C.

2.2 Cartilage staining

Embryos collected on either day 9 or day 10 incubation were removed from the egg and dissected in PBS, removing the head and internal organs. The embryos were then fixed overnight at room temperature (RT) in 90-100% ethanol. The next day the ethanol was removed and replaced with 0.05% Alcian blue staining solution (pH 2.5, 0.05% Alcian blue powder 8GX Sigma/20% acetic acid/80% ethanol) and left overnight. The following day the Alcian blue stain was removed and replaced with 100% ethanol, after 2 hours this was replaced by 50% ethanol and 2 hours later in 100% H20. After 2 hours Embryos were places in 0.1-1% KOH and the solution was changed over the next 1-3 days until the embryos cleared. Cartilage stains were then stored in 50% glycerol in PBS.

2.3 Measuring limb size

2.3.1 Measuring the proximal-distal and antero-posterior axes

Embryos of the appropriate age were dissected and stored in 4% PFA for a maximum of 1 day or used as fresh samples. To measure the limbs, embryos were placed in a Petri dish containing 1.5% agarose and PBS. Using fly pins, the embryos were pinned out so the dorsal side faced upwards and the limbs were outstretched and flat. Using a Leica MZ16F microscope, measurements of the proximo-distal axis were taken from the proximal boundary of the limb with the body wall, to the distal tip of the limb bud (consistent with measurements taken in (Lewis, 1975). The proximal boundary here is defined as the groove between the flank of the body wall and the limb bud, to ensure samples were comparable, measurements were taken consistently from this point. Antero-posterior measurements were taken from the anterior tip to the posterior boundary at the widest point (Figure 2.1).

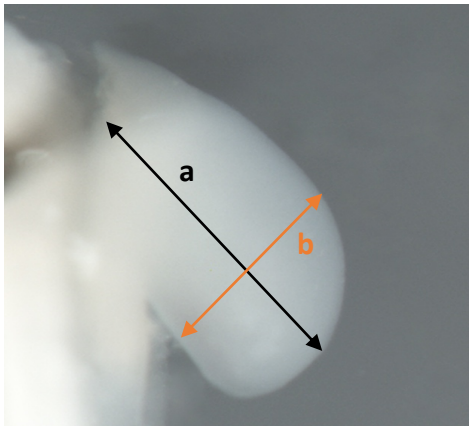

Figure 2.1. Measurements of proximo-distal and antero-posterior axes. Straight lines were drawn from the proximal flank boundary to the distal tip (a), and the anterior edge to the posterior edge (b).

2.3.2 Measuring skeletal elements

Cartilage stains of the appropriately staged embryos were placed in Petri dishes containing PBS. Using a Leica MZ16F microscope, lines were drawn down the centre of each of the skeletal elements (figure 2.2). To measure the full length of the limb, the lengths of the humerus, ulna and digit 2 were combined.

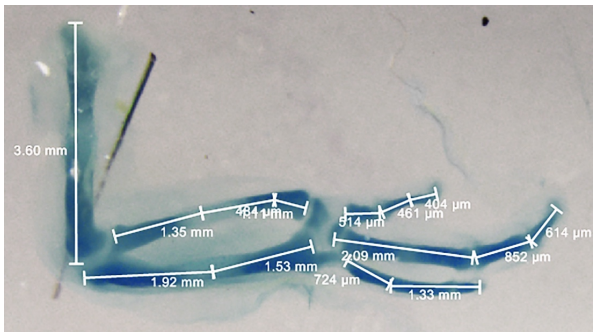

Figure 2.2. Alcian blue cartilage stain of day 9 chick embryos. Straight lines were drawn through the middle of each skeletal element.

2.4 Measuring cell size

Chick and quail embryos were collected at the 12 hour time point and dissected in a Petri dish containing PBS, the limb buds were then removed and a 200µm block of mesenchymal tissue was removed using fine dissecting scissors from the distal tip. Tissue from 6-10 embryos were pooled for each repeat of the experiment. The tissue was then transferred to 0.05% trypsin (Sigma) and gently pipetted before being left at room temperature for 30 minutes to allow disaggregation. The disaggregated cells were then pelleted at 7000rpm for 5 mins at 4°C in a 5417R centrifuge. Trypsin was then removed, and PBS added to the pelleted cells. The cells were then centrifuged again and PBS was removed and the pellet re-suspended in PSB.

Analysis of cell size was performed at the Flow cytometry core facility at the University of Sheffield. Doublet cells were used as a positive control reference. Cell size of both species was compared using the FSC (forward scatter) measuring the average fluorescence in arbitrary units.

2.5 Manipulation of RA signalling through bead implantation

AGX1-2 beads were soaked for 1 hour in 0.1mM (0.05mg/ml) TTNPB (Sigma) to enrich in RA, then washed in 1% Penicillin Streptomycin in DMEM. TTNPB is an active RA

analogue, 0.1mM of TTNPB has been shown to diffuse from AGX1-2 beads over a 20 hour period and can be used to model RA distribution in chick wing buds due to comparable patterning effects kinetics and diffusion constants. (Eichele and Thaller, 1987, Eichele, Tickle et al., 1985).

Embryos were then staged according to the time of incubation, referencing the Hamburger-Hamilton system, and the membranes and chorion removed with forceps from over the limb bud. Using a sharp tungsten needle a hole was made in the appropriate place in the limb bud (centre or proximal-anterior). The beads were then implanted into the limb bud before the egg was resealed and left to develop for the appropriate amount of time.

2.6 Analysis of cell death

Chick and quail wing buds were collected at the appropriate time point and dissected in PBS. Wing buds were then transferred to pre-warmed Lysotracker staining solution in PBS (1:1000) and incubated in the dark at 37°c for 1 hour. Wing bud samples were then washed in PBS and fixed in 4% PFA O/N at 4°c. The following day samples were rehydrated in a decreasing methanol series and imaged for RFP staining on a Leica MZ16F microscope.

2.7 Analysis of gene expression

2.7.1 RNA probe synthesis

The quail and chick are closely related and belong to the Galliformes bird order, due to this, there is a high homology between gene sequences. Comparison of quail and chick sequences using BLAST alignment revealed a high similarity between gene sequences, for example, the quail *Shh g*ene shares a 99% homology to the chick sequence. Therefore, chicken anti-sense RNA probes can therefore be used successfully in *in situ* hybridisation experiments in quail wings.

Plasmid DNA in vectors were transformed into *E.coli* DH5α competent cells, plated in LB agar with ampicillin antibiotic, and cultured at 37°c O/N. The next day, one colony was selected and inoculated in LB broth. With ampicillin antibiotic and incubated at 37°c O/N on a shaker. Plasmid purification was performed using QIAGEN mini or maxiprep kits.

DNA templates were generated either by linearising 5µg of the plasmid using the appropriate restriction enzymes (NEB enzymes were used), or by extracting the template using polymerase chain reaction (PCR). For PCR, M13 forward and reverse primers were used to isolate and amplify the template sequence. Biomix (Bioline), was used for PCR reactions, and 25-50ng of plasmid was used in 50µl reaction solutions in accordance with the manufacturers protocol. PCR settings were used as follows:

1. 94˚C 5 min
2. 94˚C 1 min (denature)
3. 55˚C 1 min (annealing primers)
4. 72˚C 40 seconds (extension)
5. Go to step 2 x34
6. 72˚ 10 mins (elongation)
7. End 4˚

The resulting template DNA was purified by phenol-chloroform extraction and ethanol precipitation. DNA pellets were then resuspended in miliQ water (MQ) to final concentration of 1µg/µl.

Anti-sense digoxigenin (DIG)-labelled ribiprobes were synthesised by *in vitro* transcription in a 20µl reaction containing 1ug of DNA template. Promega 5x transcription buffer (4µl), RNase inhibitor (1µl) and appropriate RNA polymerase (2µl) were used in addition to 2µl of 10X DIG label mix (Roche) and DEPC treated MQ water. Reactions were incubated in a 37°C water bath for 2 hours. Purified probes were obtained using a purification column (illustra ProbeQuant G-50 Micro Column, GE) in accordance with the manufacturer's protocol. The resulting probed was then diluted in approximately 7ml of

prehybridization buffer solution. This solution was used directly for *in situ* hybridisation experiments.

Probe name	***Restriction enzyme***	***RNA polymerase***	***Source (Many thanks to the following labs)***
Shh (pSport)	*Sal1*	*Sp6*	*Cheryll Tickle*
Fgf8 (pBS)	*Not1*	*T7*	*Cheryll Tickle*
Sox9 (pGEM)	*Nco1*	*Sp6*	*Cheryll Tickle*
Grem1 (pGEM)	*Sal1*	*T7*	*Cheryll Tickle*
Hoxa13 (pGEM)	*(M13 primers)*	*T3*	*Cheryll Tickle*
Meis1 (pGEM)	*ClaI*	*Sp6*	*Gift from Marian Ros*
Cyp26b1	*KnpI*	*T7*	*Gift from Miguel Torres*
Fgf4 (pBS)	*BamHI*	*T7*	*Cheryll Tickle*

Table 2.1. Antisense probes for chick genes used in this study

The probe name, and plasmid vector where known is listed above, along with appropriate restriction enzyme or primer, and RNA polymerase and source.

2.7.2 Whole mount *in situ* hybridization

At the appropriate time point embryos were fixed in 4% PFA overnight at 4°C. They were then washed in 0.1% PBT and dehydrated in a series of methanol washes (50% and 100%) and left for a minimum overnight at −20°C. Embryos were rehydrated through a series of methanol washes and PBT, then treated with 20µg/µl proteinase K (Sigma) for a maximum of 25 minutes (the time embryos were left in proteinase K depended on the age of the embryos). Embryos were then washed in PBT, fixed for 30 min in 4% PFA at room temperature and then prehybridised at 69°C for 2 hours (50% formamide/50% 2× SSC). Antisense DIG-labelled mRNA probes (1 µg) was added in 1 ml of hybridisation buffer at 69°C overnight. The following day, embryos were washed twice in hybridisation buffer, twice in 50:50 hybridization buffer and MABT buffer, and then twice in MABT buffer, before being transferred to blocking buffer (2% blocking reagent (Roche), 20% fetal bovine serum (Sigma), 80% MABT buffer) for 3 hours at room temperature. Embryos were transferred to blocking buffer containing anti-digoxigenin antibody (1:2000, Roche) at 4°C overnight, then washed in MABT buffer overnight before being transferred to NTMT buffer (100 mM NaCl, 100 mM Tris-HCl, pH 9.5, 50 mM $MgCl_2$) containing Nitro Blue tetrazolium/BCIP.
mRNA distribution was visualized using a Leica MZ16F microscope.

2.7.3 RNA extraction

Control and treated whole limb buds at the appropriate time point were dissected in PBS on ice and transferred to 100% Trizol reagent (Ambion). Samples were then homogenized and left at room temperature. RNA was extracted and isolated using Zymo

Direct-zol RNA miniprep kit as per the manufacturer's instructions and eluted in 30µl of DEPC treated MQ water. The concentration of RNA was determined using a nanodrop.

2.7.4 cDNA synthesis

cDNA was synthesized using Superscript III (Invitrogen) according to manufacturer's instructions in 20µl reactions. 500ng of RNA was added up each reaction. Reactions were incubated as follows

1. 25˚C 10 mins
2. 50˚C 30 mins
3. 85˚C 5 mins

1u of RNAse H was then added to each reaction and incubated at 37 ˚c for 20 minutes before qPCR analysis.

2.7.5 qPCR

Exon sequences for chick and quail genes were compared using ensemble and primers were designed using Primer 3Web using sequences with 100% homology.

The following primers were used in this study.

Gene	**Primer Sequences (5'-3')**	**Amplicon Size (bp)**
Meis1	F: aggcgatgtttgctcctcc R: tcgggattagaggaaaagaggg	96
Cyp26b1	F: cctgcaagctaccaatccct R: ttgccgtacttctcccgtc	115
18S	F: tgtgccgctagaggtgaaatt R: tggcaaatgctttcgcttt	Unknown – sequence as used in (Kuchipudi, Tellabati et al., 2012)

Table 2.2. Primer sequence
(primers were validated by producing a standard curve).

20µl reactions were set up in triplicate in 48 well plates. Using Step1 software, each qPCR reaction was set up according to the system instructions; 10µl 2x Sybr green master mix, 0.4µl 0.01nm forward primer, 0.4µl 0.01nm reverse primer, 7.1µl PRC grade H20, 0.1µl ROX passive fluorescent dye and 2µl of 1:5 dilution of cDNA. Gene expression was standardised in comparison to the control gene, 18S.

2.7.6 Measuring the extent of *Meis1* expression in the wing

Quantification of the percentage of the wing expressing *Meis1* was performed by analysing the *in situ* hybridisation images on a Leica MZ16F microscope and measuring along the proximo-distal axis from the flank of the embryo to the end of strong *Meis1* expression.

2.8 Cell cycle analysis

2.8.1 Measuring cell cycle rate

Embryos were collected at the appropriate times and dissected in a Petri dish containing PBS, the limb buds were then removed and a 150-200µm block of tissue was removed using fine dissecting scissors from either the polarising region or the distal tip. Tissue from 8-12 embryos were pooled for each repeat of the experiment. The tissue was then transferred to 0.05% trypsin (Gibco) and gently pipetted before being left at room temperature for 30 minutes to allow disaggregation. The disaggregated cells were then pelleted at 7000rpm for 5 mins at 4°C in a 5417R centrifuge. Trypsin was then removed, and PBS added to the pelleted cells. The cells were then centrifuged again and PBS was removed and the pellet re-suspended in 70% ethanol and stored for a minimum overnight at -20°C. On the day of the flow cytometry analysis, cells were centrifuged then re-suspended in

0.5ml of staining buffer (50 µg/µl propidium iodide (Roche), 50µg/µl RNAase A (Sigma), 0.1% Triton X (Sigma).
Analysis of the cell cycle was performed at the Flow cytometry core facility at the University of Sheffield, the proportion at cells in G1, S and G2M were determined from 10,000 cells gated for analysis, and statistical analysis was performed using Pearson's Chi squared test and Student's t-tests.

2.8.2 Cell cycle manipulation

The G1-S phase cell cycle inhibitor, PD0332991 (Sigma) was made up to a stock solution of 1mg/ml in MQ water, then diluted in DMEM to a concentration of 0.1mg/ml. Following the removal of the chorion and vitelline membranes, 10µl was pipetted directly onto embryos over the limb bud. The eggs were then resealed and left to develop for the appropriate amount of time. Control embryos received the carrier, DMEM.

2.9 Tissue grafts

2.9.1 Polarising region grafts

Polarising region grafts were performed as described in (Stainton and Towers, 2018). The donor embryos were dissected in PBS and the polarising regions removed using sharpened tungsten needles then transferred to the host egg where they were grafted to equivalently sized holes in the host anterior limb bud then held in place with 25µm diameter platinum pins

2.9.2 Whole limb grafts

At the appropriate time point, the chorion and vitelline membranes were removed over the wing bud of host embryos, the right wing bud of the host embryo was then

removed using fine tungsten needles. Donor embryos were dissected in PBS and whole limbs buds were removed using dissecting scissors and held in place on the donor embryo using two 25µm platinum pins. The eggs were resealed with Sellotape and left to develop for the appropriate amount of time.

Chapter 3.

Morphological and cellular comparisons of quail and chick wing development

3.1 Introduction

How embryonic development is timed on a species-specific level is a fundamental question in developmental biology. The wings of different avian species grow to markedly different sizes, however how this occurs is largely unknown. The quail incubation period is 14 days and adult wings attain a size of approximately 17.5cm in length, whereas the chicken incubation period is 21 days and their wings are approximately 31cm. Previous studies describing the timing and staging of quail embryonic development did not cross-reference its development to the well-established chick model. (Padgett and Ivey, 1960, Zacchei, 1961) (Nakane and Tsudzuki, 1999). However, more recent studies comparing development of other bird species to the chick staging system, confirmed that the Hamburger-Hamilton stages could be used to accurately stage developing avian embryos other than the chick (Ainsworth, Stanley et al., 2010, Li, Bai et al., 2019, Sellier, 2006). By comparing the morphology of the entire embryo, these studies recorded only minor differences in the development of the quail compared to the chick until day 7 incubation. However, statistical tests were not used to determine whether there is a significant difference in developmental rates (Ainsworth, Stanley et al., 2010, Sellier, 2006).

In order to determine how wings of different species grow to different sizes and when in embryonic development these differences become apparent, I have compared the development of the smaller quail wing to the larger chick wing. To do this, I have built on earlier morphological studies (Ainsworth, Stanley et al., 2010, Nakane and Tsudzuki, 1999, Padgett and Ivey, 1960, Sellier, 2006, Zacchei, 1961) by comparing the external

morphological features of the quail to the chick in reference to the Hamburger Hamilton staging system over the incubation time. I have also analysed a range of developmental events including outgrowth of the wing, rates of cell proliferation, apoptosis and cell size in the wing buds of both species. By analysing developmental events, I aim to elucidate the timing of patterning events in the limbs of differently-sized species, and to identify when differences in the limb sizes are established during embryogenesis.

3.2 Results

3.2.1 Comparison of wing morphology in relation to the Hamburger Hamilton staging system indicates accelerated development of the quail wing

At day 3 of incubation (72 hours), quail and chick embryos are at an equivalent Hamburger Hamilton stage (HH18-19), which is determined by the appearance of the allantois (extra-embryonic membrane sac attaching to the hindgut), the wing bud and the formation of 30-36 somite pairs (Ainsworth, Stanley et al., 2010, Hamburger and Hamilton, 1951, Sellier, 2006). At around stage HH18/19 in development, the wing buds can be identified as slight bulges on the lateral sides of the embryos at appropriate axial levels. I have defined this equivalent point of chick and quail wing bud outgrowth as time '0 hours', with all other times referenced as hours incubation after this point. Note that I will continue to use this timing for the remainder of my thesis.

I compared the morphology of quail and chick wings from time 0 to 144 hours of wing growth which corresponds to day 9 incubation – the time limit quail embryos can be allowed to develop. During this time, both quail and chick wing buds form the characteristic pattern of the stylopod (humerus), zeugopod (radius and ulna) and autopod (wrist and digits 1, 2 and 3). My analyses show that quail and chick wing buds appear identical in morphology at time 0 – HH18/19, but after this time point, the quail wing bud becomes more

morphologically-defined, with a characteristic shape being recognisable at an earlier time compared to the chick (Figure 3.1). Thus, the distal part of the quail wing forms a paddle-like shape at an earlier time point than the chick wing and the contours of the digits become distinguishable earlier (96 hours in the quail compared to 108 hours in the chick). Furthermore, feather follicles along the posterior margin of the quail wing become visible earlier than in the chick (seen at 132 hours in the quail compared to 144 hours in the chick). Moreover, by 144 hours, black pigmentation is seen in the quail feathers, but not in the chick wing feathers (Figure 3.1).

To better characterise the morphological differences outlined in Figure 3.1, I applied the Hamburger Hamilton staging system of the chick to the quail wing. Along with other morphological features, the Hamburger Hamilton system uses characteristics of limb development to define embryonic stages, such as the presence of elbow joints, symmetry of the wing bud, presence of cartilage and the separation of the digits. Using this system, previous studies suggested that the development of the quail and chick embryo is equivalent up until day 7 incubation, equating to HH27 (Ainsworth, Stanley et al., 2010) (Figure 3.2a). However, as mentioned earlier, this staging was based on overall morphology of the embryo with little attention paid to the wing. I have plotted my data on how quail and chick wings progress through the HH stages over time and this shows that development is equivalent at time 0, after which time point, the quail progresses through the Hamburger Hamilton stages faster than the chick (Figure 3.2b, c). Interestingly, the quail wing reaches stage HH22 at 12 hours incubation, but the chick wing does not reach this developmental stage until 24 hours incubation (Figure 3.2b, c , *n*=20). However, after 12 hours, quail and chick wings progress through the HH stages at a similar rate (Figure 3.2c, *n*=20). Thus, it takes the same amount of time for quail and chick wings to progress from HH22 to HH30 – 60 hours. Similarly, the appearance of distinct morphological features described in the Hamburger Hamilton system appear earlier in the quail wing compared to the chick wing, such as the elbow joint, which is visible at HH25: the quail reaches this stage at 36 hours, and the chick at approximately 48 hours (Figures 3.1 and 3.2b, *n*=20).

0
12
24
36
48
60
72
84
96
108
Chick
Quail
20/21
22
24
26
27/28
29
30
31
32/33
22
24
26
27/28
29
30
32
34
34/35
120
132
144
Chick
Quail
33/34
35
35/36
35
35/36
36

Figure 3.1. Morphology of the quail and chick wing from 0 hours HH18/19 to 144 hours.

Chick and quail eggs were incubated for equivalent times. Right wing buds from quails and chicks were then removed and photographed every 12 hours of development from 0 hours to 144 hours (0 hour refers to day 3 incubation i.e 72 hours - see materials and methods). Hamburger Hamilton stages are also recorded below each wing bud. Scale bars represent 1mm.

3.2.2 Quail wing outgrowth is accelerated compared to the chick

To determine if advanced progression through HH stages in quail wings is also reflected in differences in growth rates between chick and quail wings, I measured the wing along the proximo-distal (P-D) axis (body wall to wing bud tip) over time (Figures 3.3a and b). These results show that wing bud lengths are equivalent at time 0 when both quail and chicks are at HH18/19, however, after this time point, the quail wing bud grows at a faster rate than the chick wing bud. Interestingly, the first significant difference in length occurs very early, between 0 and 12 hours (Figure 3.3ai). An average chick wing bud grows from 0.33mm at 0 hours (HH18/19) to 0.41mm at 12 hours (HH20/21). Note, the similar outgrowth of the chick wing has also been recorded previously (Lewis, 1975). By contrast, the quail wing grows significantly longer along the P-D axis, from an average of 0.33mm to 0.56mm at 12 hours, reflective of the more advanced embryological stage of HH22 quail wings compared to HH20/21 chick wings (Figure 3.3aii). The quail wing is longer until 120 hours incubation (HH35 quail, HH33/34 chick), but after this, the length of the chick wing surpasses that of the quail wing (Figure 3b, also visible in Figure 3.1).

I also measured the width of wing buds along their widest point, i.e. most-anterior to most-posterior point (A-P axis) at each time point from 0 to 72 hours. The quail wing has a significantly narrower A-P axis from 0 to 36 hours (HH18/19 to HH26) compared to the chick (HH18/19 to HH24), after which time, there is no significant difference in the width of quail and chick wing buds. Also note that the A-P axis decreases in width in both species – in the chick from 1.38mm at 0 hours to 1.25mm at 36 hours, and in the quail from 1.82mm at 0 hours to 1.13mm. By 48 hours, there is no significant difference in the width of the wings (in

the quail and chick 1.183mm and 1.208mm, respectively), which corresponds to different Hamburger Hamilton stages i.e. HH26 in the chick and HH27/28 in the quail). Furthermore, from 48 hours the A-P axis grows wider in both the quail and the chick wing (Figure 3.3c, *n*=16).

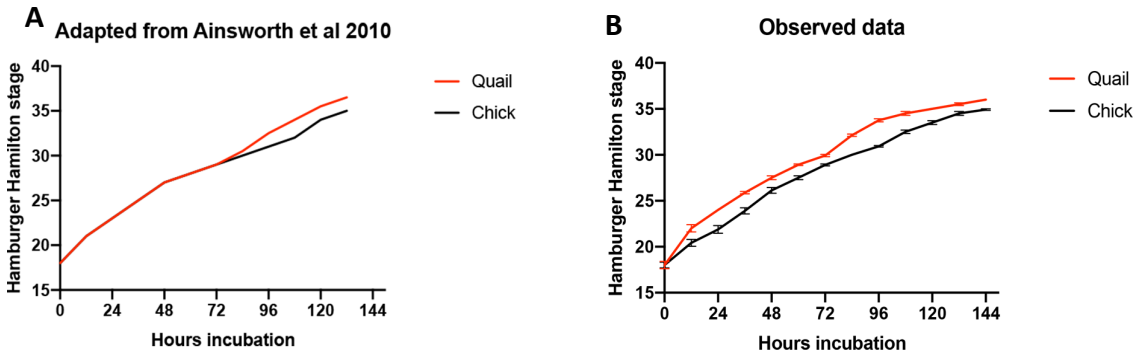

C

Hours incubation	Chicks (HH stage)	Quail (HH stage)
0	18/19	18/19
+12	20/21	22
+24	22	24
+36	24	26
+48	26	27/28
+60	27/28	29
+72	29	30
+84	30	31/32

Figure 3.2. Quail wings progress through the Hamburger Hamilton stages faster than the chick.

A) Average Hamburger Hamilton stages were plotted against incubation time from 0 hours. Adapted graph from (Ainsworth, Stanley et al., 2010) suggests development is equivalent between the quail and the chick until just before day 7 (84 hours incubation). **B)** My observations show that the quail wing bud progresses through the Hamburger Hamilton stages at a faster rate than the chick wing bud between 0 and 12 hours. Students *t*-tests show there is no significant difference between the stages at 0 hours, however for all points after, the quail has a significantly more advanced HH stage (*p*= ***= <0.001), *p* values not included on graph. **C)** The Hamburger Hamilton stages of the quail and chick are noted from 0 hours. *n*=20.

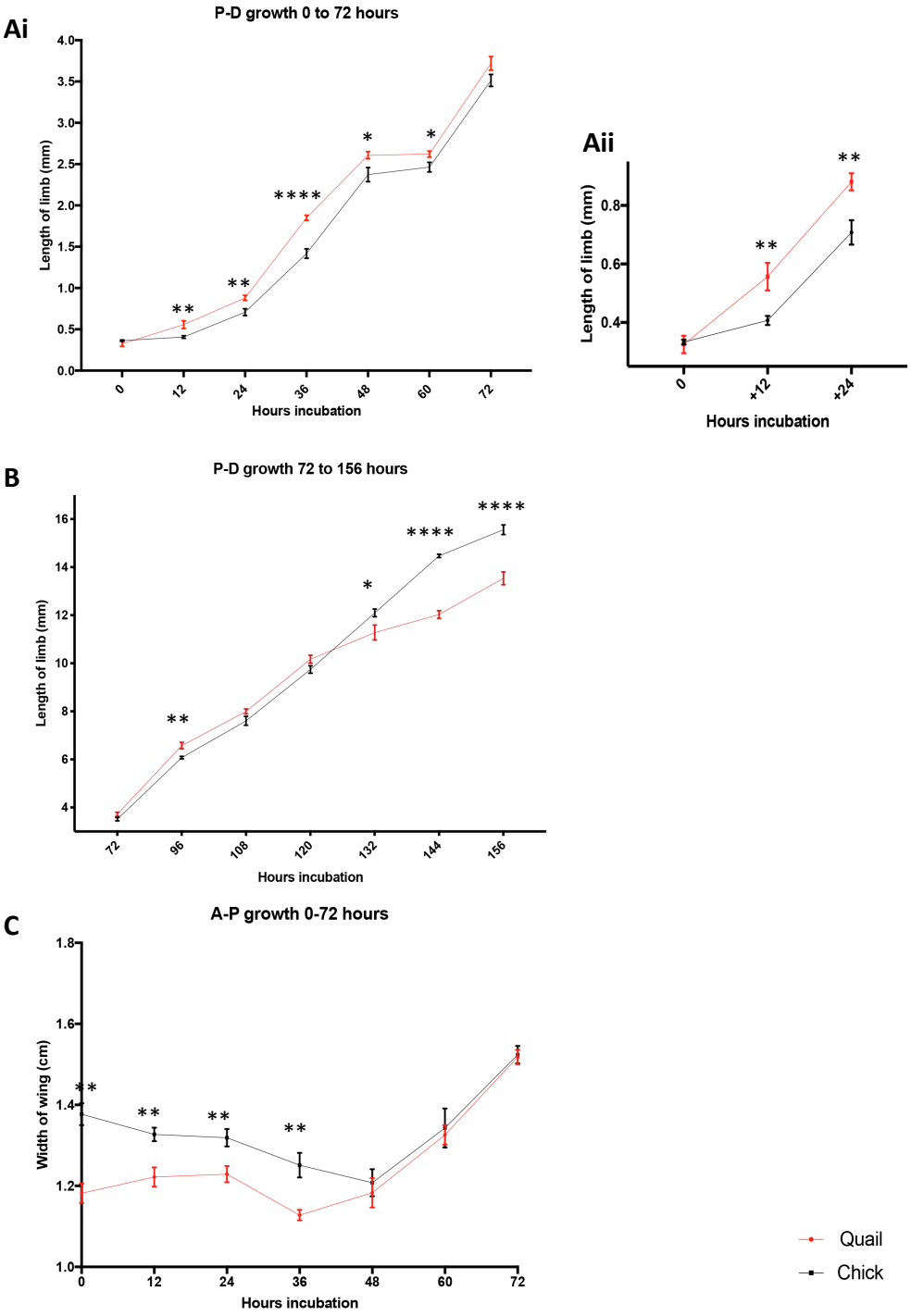

Figure 3.3. Quail wing outgrowth is accelerated compared to the chick

Ai and ii) Quail and chick wing buds were measured along the proximo-distal (P-D) axis (body wall to tip of wing bud) every 12 hours after the 0 hour time point. At 0 hours there is no significant difference, and from 12 hours the quail wing is significantly longer

than the chick wing. Student's *t*-tests show significant differences in wing bud lengths from 12 to 72 hours, *n*= 4-8. **B)** Quail wings are significantly longer than chick wings until approximately 132 hours, after which time the chick wing bud growth surpasses the quail wing and becomes significantly longer at 144 hours, *n*=4-8. **C)** Quail and chick wing buds were measured along the anterior-posterior (A-P) axis (width of the wing bud) every 12 hours after the 0 hour time point. Student's *t*-tests reveal no significant difference in the width of the wing after 48 hours *n*=4-18. *p* values: *=<0.05, **=<0.01 ***= <0.001 ****= <0.0001.

3.2.3 Accelerated quail wing outgrowth is associated with a faster proliferation rate in distal mesenchymal cells

In order to determine if the accelerated outgrowth of quail wing buds between 0-12 hours (HH18/19-HH22 in the quail; HH18/19-HH20 in the chick) can be accounted for by differences in the cell size or cell number, I measured the diameter of undifferentiated distal mesenchymal wing bud cells using flow cytometry. A 200μm block of tissue was taken from the distal mesenchyme of 12 hour quail and chick wing buds (Figure 3.4a) and was then trypsinised to form a live single cell suspension. In flow cytometric analysis, the forward scatter signal is a measure of cell size as it quantifies how light is diffracted around the diameter of a single cell in suspension (Collier, 2000). This is shown in Figure 3.4b as fluorescence (arbitrary units) and is plotted against cell count. My analyses reveal no significant difference in the forward scatter signal intensity between the two species, showing that quail and chick wing bud mesenchymal cells are equivalently sized (Figure 3.4c*, n*=3).

To determine if differences in growth rates can be explained by differences in proliferation, I measured DNA content of proliferating distal mesenchyme cells of the wing bud by flow cytometry (tissue taken as shown in Figure 3.4a). Figure 3.5 depicts the proportion of cells in G1-phase at each time point (data for S-phase can be found in the appendix). The percentage of cells in G1-phase was chosen due to repeats being highly reproducible and is considered to give a better indication of proliferation (Chinnaiya, Tickle et al., 2014, Saiz-Lopez, Chinnaiya et al., 2015) A lower percentage of cells in G1 phase (the

rate-limiting rest phase of the cell cycle) is indicative of a faster cell cycle rate (Crowley, Chojnowski et al., 2016). Figure 3.5 shows that as development progresses, the cell cycle slows down as determined by increasing proportions of cells in G1 in both quail and chick wings. Note that comparable cell cycle rates over time have been reported previously in the chick wing (Saiz-Lopez, Chinnaiya et al., 2015).

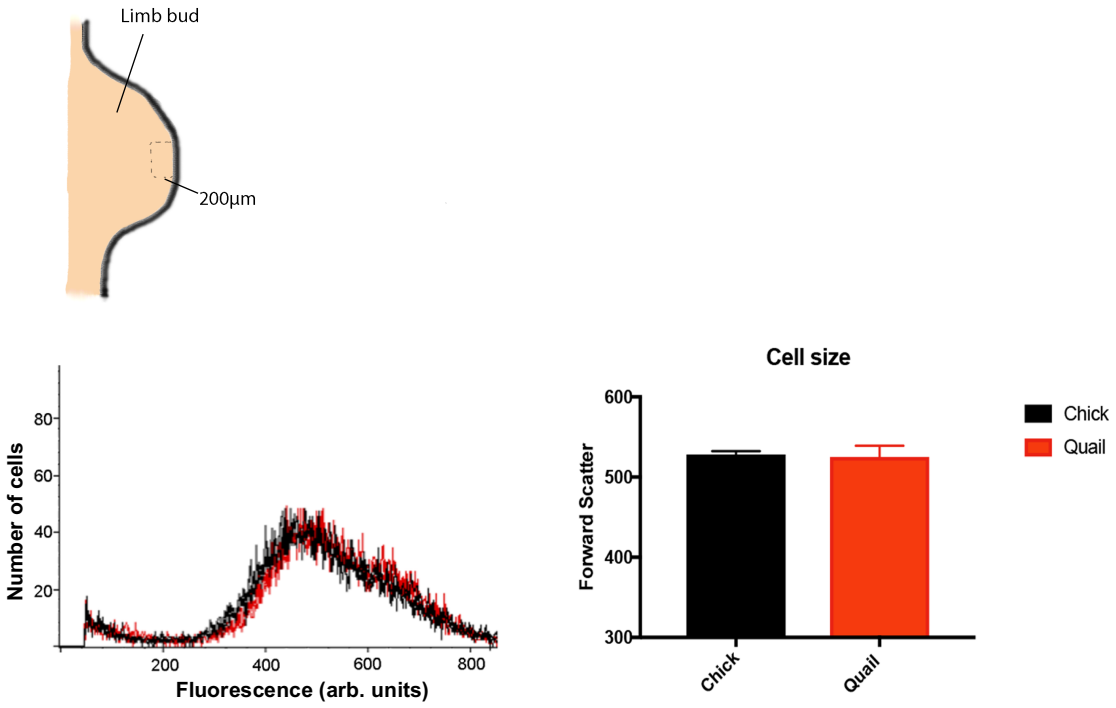

Figure 3.4. Quail and chick wing bud mesenchyme cells are not significantly different in size.

A) Schematic depicting the right wing bud and the block of proliferating distal mesenchyme cells dissected out for flow cytometric analyses (dashed line). **B)** Cell size was measured by assessing forward scatter intensity by flow cytometry, an overlay of the 3 experimental repeats can be seen plotted as fluorescent intensity against cell number (counts). **C)** The average intensity of fluorescence is plotted as a bar chart on the left (chick = 528.2 fluorescent intensity SEM= 4.24, quail = 525 fluorescent intensity SEM= 14). No significant difference was detected in cell size. (*n*=3 - three experimental repeats, *n*= 8-12 - each experimental repeat contained 8-12 pooled embryos). *p* values: *=<0.05, **=<0.01 ***= <0.001 ****= <0.0001.

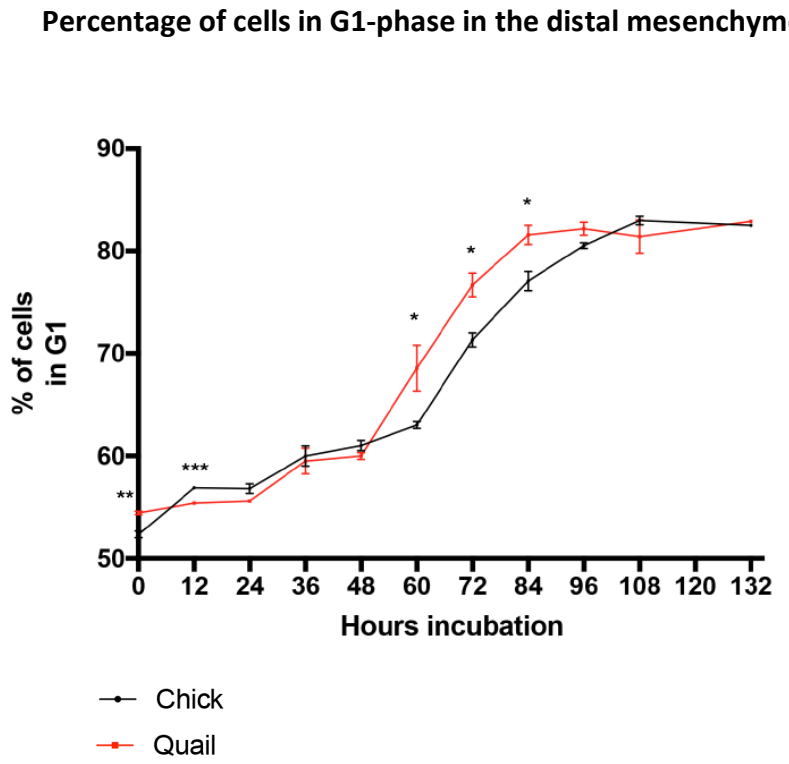

Figure 3.5. Cell cycle rates in quail and chick wing bud distal mesenchyme.
The proportion of cells in G1-phase (rest phase) is lower in quail wing bud distal mesenchyme than in the chick distal mesenchyme at 12 hours incubation indicating a faster cell cycle rate in the quail wing bud. Student *t* tests were performed on the percentage of cells in each phase of the cell cycle. *n*=3 experimental repeats each containing *n*=8-12 pooled blocks of distal mesenchyme. *p* values: *=<0.05, **=<0.01 ***= <0.001 ****= <0.0001.

It is interesting to note that from approximately HH34 onwards, both the quail and chick wing have a very similar percentage of cells in G1-phase (higher % is indicative of a slower cycle rate) (Figure 3.5, *n*= 3). However, the quail wing bud reaches this stable proliferation rate at 84-96 hours incubation, which is approximately 12 hours earlier than the chick wing bud does at around 108 hours incubation.

It has been shown that distinct areas of the chick (and also mouse) limb mesenchyme exhibit different rates of proliferation (Boehm, Westerberg et al., 2010, Fernandez-Teran, Hinchliffe et al., 2006, Hornbruch and Wolpert, 1970). Therefore, in addition to the distal mesenchyme at the tip of the wing, I have also analysed cell cycle rates in both quail and chick polarising regions from 0 to 72 hours (Figure 3.6). The polarising region is located at the posterior part of the distal mesenchyme in the wing bud and expresses *Sonic hedgehog* (*Shh*). Even after the time-point when the polarising region has switched of *Shh*, I continued to measure cell cycle parameters in the posterior distal region.

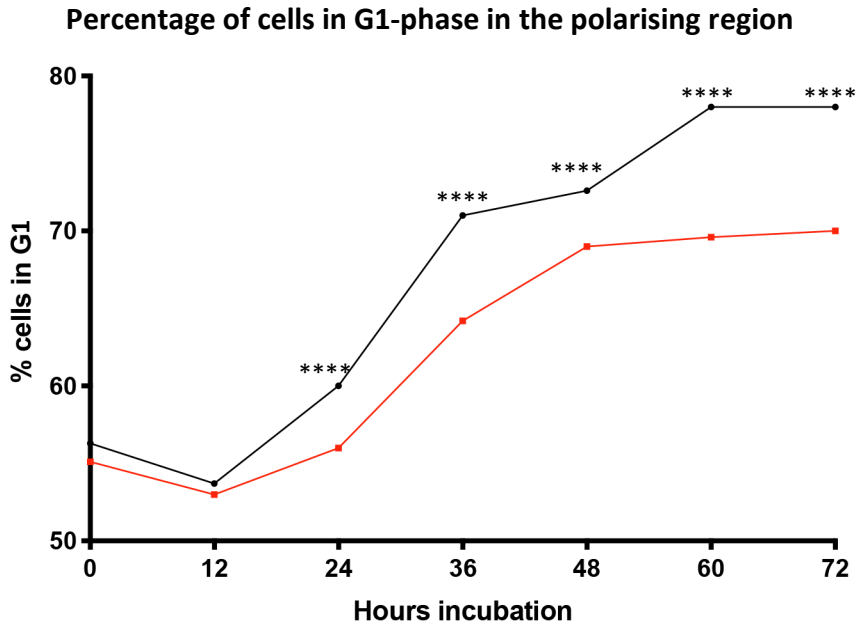

Figure 3.6. Cell cycle rates in quail and chick polarising regions.
The proportion of cells in G1-phase (rest phase) of the cell cycle decreases between 0 and 12 hours in both the quail and chick. However, from 12 hours increases in both species. Student's *t* tests were performed on the percentage of cells in G1, revealing that from 12 to 72 hours the chick has a significantly larger percentage of cells in G1 compared to the quail. *n*=8-12 pooled blocks of distal mesenchyme. *p* values: *=<0.05, **=<0.01 ***= <0.001 ****= <0.0001.

The percentage of cells in G1-phase of the cell cycle is lower in the quail wing polarising region than in the chick wing polarising region, and this is maintained throughout

the 72 hour time-course, suggesting a faster cell cycle rate. (Figure 3.6). By the end of 72 hour period (HH29 chick, HH30 quail), the chick polarising region maintains a rate of approximately 78% of cells in G1-phase, compared to a significantly lower 70% of cells in the quail. Therefore, as also seen in the distal mesenchyme, proliferation rates in the polarising region decrease over time.

3.2.4 Cell death in the developing quail and chick wing

In the developing chick wing, several regions of cell death are observed including the anterior necrotic zone (ANZ) and posterior necrotic zone (PNZ), which contribute to the paddle-like shape of the digit field and in giving the wing characteristic contours (Hurle, Ros et al., 1996, Hurle, Ros et al., 1995, Saunders and Gasseling, 1962). In Figures 3.2 and 3.3, I showed that these aspects of wing morphology become more pronounced at an earlier time in the quail compared to the chick. In order to further investigate if these changes are associated with the timing of the ANZ and PNZ, I have used lysotracker staining of apoptotic cells in wing bud tissue between 36 hours and 84 hours, equating to HH26-HH30 - chick and HH26-HH31/32 – quail, when these changes in wing morphology become apparent. Lysotracker is a permeable small molecule which stains lysosomes during apoptosis, and due to its penetrative ability, is particularly useful in staining thick sections or whole mount embryos (Fogel, Thein et al., 2012) (See Materials). Figure 3.7 shows that at 36 hours (HH24 in the chick) both the ANZ and the PNZ are undetectable in the chick wing bud, whereas a weak patch of apoptotic tissue can be seen in the ANZ of the quail wing bud at this time – HH26 (arrow). The ANZ is then visible 12 hours later in both the quail and chick wings, now stages HH27/28 and HH26, respectively (*n*=3).

At 60 hours in the quail (HH29), the contour of digit 1 can be distinguished and the ANZ is no longer detectable, but a similar pattern can then be seen 12 hours later when the chick reaches HH29, at 72 hours. By contrast, at 72 hours in the quail wing, the emergence of the PNZ can be seen (as indicated by the arrow) along with the contour of the developing

digit 3, and again, a similar pattern of apoptosis occurs 12 hours later in the chick at 84 hours.

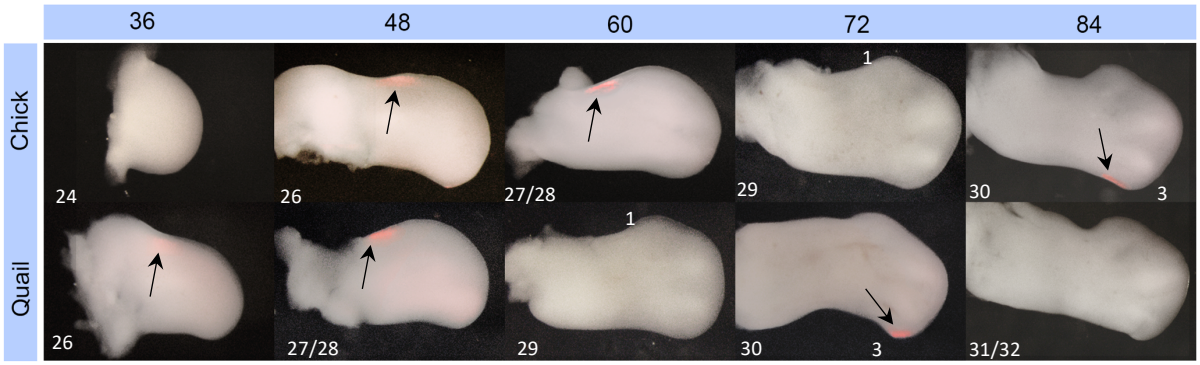

Figure 3.7. Cell death in the quail wing compared to the chick wing.

Chick and quail wing buds from 36 to 84 hours incubation were stained with Lysotracker (red) for apoptotic cells. Black arrows indicate the anterior necrotic zone seen in the quail at 36 hours and 48 hours and in the chick at 48 hours and 60 hours. The posterior necrotic zone is also indicated by black arrows at 72 hours in the quail and 84 hours in the chick. The contours associated with digits 1 and 3 are related to the anterior and posterior necrotic zones, respectively. *n* =3

3.3 Discussion

In this chapter, I have compared how quail and chick wings progress through development by analysing changes in morphology of the wing using the Hamburger Hamilton staging system. Both quail and chick embryos reach stage HH18/19 at day 3 incubation, noted at time 0 hours, when the wings buds are equivalently sized along the P-D axis. Interestingly, the accelerated development of the quail wing through the HH stages occurs during the initial 0 to 12 hours of wing outgrowth. By 12 hours incubation, the quail reaches HH22, however the chick does not reach this stage until 24 hours incubation. Furthermore, between the 0 and 12 hours, the rate of growth of the quail wing along the P-D axis is faster than that of the chick wing.

By comparing the outgrowth of quail and chick wing it became apparent that both species follow a similar pattern of P-D growth over time after 12 hours, which is independent from the timing of HH stages that are accelerated in the quail wing. For example, in both quail and chick wing, there is a period of faster growth between 12 and 48 hours, followed by a period of slower growth between 48 and 60 hours. However, this occurs between different HH stages in the chick wing (faster growth – HH22 to 26, slower growth - HH26 to HH27/28) and the quail (faster growth HH24-HH27/28, slower growth - HH27/28 to HH29) indicating that the acquisition of morphological landmarks is not coupled with growth rate and that developmental timing (HH stages) is accelerated relative to growth rate in the quail wing.

The quail wing maintains a significantly longer P-D axis compared to the chick wing, and as mentioned, this initial difference between the size of the wings appears to be set up early in development (0-12 hours), and is maintained until approximately 120 hours. Although a longer embryonic quail wing may seem counter-intuitive because the adult chick has a longer wing, this conclusion derives from making comparisons across incubation time rather than developmental time (HH stage). If developmental time is instead compared, the chick wing is longer, i.e. the quail wing at 60 hours is HH29 and measures 2.62mm, however

the chick wing at HH29 measures 3.51mm, although this occurs at 72 hours incubation. Therefore, this means that when quail wing growth decreases after 120 hours, the chick wing surpasses its length as it is developing at a slower rate. An implication of this data is that it is inaccurate to measure relative wing size across incubation time i.e. day 5 vs day 5, instead it is more accurate to compare across developmental time e g. HH29 vs HH29. My experiments are restricted to regulations stating that embryos can only be kept up until 2/3 of their incubation period. Therefore, I am unable to continue my comparisons in the later stages of development after 156 hours, as this would surpass 2/3 of the quail incubation period. It would, however, be interesting in future to analyse the growth of the wing past this time point and to compare how wings develop closer to hatching in both species.

Although my analysis of cell size revealed no significant difference between quail and chick undifferentiated mesenchyme, my analysis of proliferation reveals that the faster cell cycle rate seen at 12 hours in the quail wing could drive the faster outgrowth of the wing. However, between 0 and 12 hours both species have an average of 55% of cells in G1-phase – maintained 55% in the quail, compared to a 53 to 57 % decrease in the chick. It is therefore difficult to conclude whether faster proliferation rates in the early wing drive the faster outgrowth of the quail wing.

Coinciding with advanced developmental age from 12 hours onwards, cell proliferation appears to follow a similar pattern in chick and quail wing bud distal mesenchyme, but is 12 hours advanced in the quail i.e. the sharp decrease in cell cycle rates seen at HH27/28, and also the stabilisation of the cell cycle rate at approximately HH34. Taken together this suggests that cell cycle rates in the distal mesenchyme are linked to the developmental stage of the tissue, but surprisingly, are not directly linked to the P-D outgrowth of the wing bud.

Additionally, my analysis of apoptosis also reveals developmental time is accelerated in the quail wing. The anterior necrotic zone is present for the same duration of time (approximately 24 hours), however, it can be identified 12 hours earlier in the quail wing. This corresponds with the accelerated development of the quail wing such as the earlier

presence of distinct morphological features, such as the contour indicating digit 1 through the action of the anterior necrotic zone. Previously, it has been shown that the posterior necrotic zone can be seen at approximately HH30 in the chick wing (Pickering and Towers, 2016). My results correspond with these observations and show again that patterns of apoptosis occur 12 hours earlier in the quail. Thus, the data I have collected reveals that the sculpting and contouring of the wing bud by apoptosis (Hurle, Ros et al., 1996) occurs 12 hours earlier in the quail wing compared to the chick wing, and is coupled to the developmental age (HH stage) of the wing.

In summary, previous studies comparing quail and chick development have focused only on external, morphological features. During this chapter I have built on these studies and analysed cellular characteristics in order to determine how differences in development and formation of quail and chick wings occur. I revealed that development timing is accelerated by 12 hours in quail wings compared to the chick wing. This is associated with faster P-D outgrowth between 0 and 12 hours, cell proliferation and progression past HH20/21. Following this, developmental timing associated with apoptosis and cell proliferation occurs 12 hours earlier in the quail wing compared to the chick wing, but at the same rate in both species. However, developmental timing is uncoupled from incremental growth rates, which are instead linked to incubation time.

In order to gain a better understanding of how developmental events are timed in the quail and chick wing, in the next chapter I characterised the expression of molecular markers that are involved in pattern formation and growth during limb development.

Chapter 4.

Analyses of molecular markers in quail and chick wings

4.1 Introduction

In chapter 3 I used morphological and cellular assays to reveal that developmental timing is accelerated in the quail wing compared to the chick wing in terms of HH stages, cell proliferation and apoptosis. In this chapter, my aim was to investigate if accelerated developmental timing of the quail wing is associated with the expression of genes implicated in specification, patterning and differentiation. It is possible to detect the expression of genes whose products are implicated in specifying positional information of the different segments of the wing. These markers are sequentially expressed in discrete domains along the proximal to distal axis (proximal – humerus, to distal – digits) of the developing limb. Therefore, comparison of their expression in different species will illustrate if proximo-distal specification is co-ordinated with developmental timing in quail and chick wings. I have also analysed the expression of genes that characterise embryonic signalling centres to determine if their duration also correlates with the accelerated development of the quail wing bud compared to the chick wing bud. In addition, I have analysed the expression of markers of late stage developmental events in the wing including the formation of cartilage condensations and feathers follicles.

4.2 Results

4.2.1 Expression of proximo-distal positional markers reveal accelerated development of the early quail wing

The prospective regions of the wing are specified in a proximal (humerus) to distal (digits) sequence. *Meis1* is a considered to be a determinant of stylopod (humerus) fate and is induced in the wing bud by retinoic acid (RA), which is an extrinsic signal emanating from

the flank of embryo (Cooper, Hu et al., 2011, Swindell, Thaller et al., 1999). RA is then cleared from the distal region of the wing as it grows outwards after HH19, as indicated by downstream transcriptional targets of RA including *Meis1/2* (Mercader, Leonardo et al., 2000, Mic, Sirbu et al., 2004). Thus, at 0 hours *Meis1* expression can be seen throughout quail and chick wing buds that are close to the trunk of the embryo at HH18/19 (Figure 4.1). *Meis1* expression is then downregulated in the distal part of both chick and quail wings and becomes progressively restricted to more proximal regions including the trunk and prospective shoulder region of the embryo at approximately HH27/28 (48 hours quails, 60 hours chick) (Figure 4.1). My analysis of *Meis1* expression reveals that expression is lost in the distal part of the quail wing bud earlier than in the chick wing bud. Thus, although *Meis1* becomes undetectable in a distal band of mesenchyme cells at HH20/21 in both species, this occurs at 6 hours incubation in the quail and 12 hours incubation in the chick (marked with an asterisk). By measuring the percentage of the wing expressing *Meis1* I have also quantified its spatial distribution along the P-D axis as observed in the *in situ* data (Figure 4.1b, *n*=3). *Meis1* is detectable along 71.47% of the P-D axis by 6 hours - HH20/21 quail wing buds (compared to 96% in the chick at 6 hours - HH19). However, by 12 hours at HH20/21, the chick wing expresses *Meis1* (71.9%), which is comparable to the quail wing at HH20/21 (71.4%). Furthermore, there is an approximate 12 hour delay in *Meis1* downregulation in more-proximal regions of the chick wing, which can be seen when *Meis1* is expressed in approximately 50% of the wing. This occurs at HH22 in both species, i.e. 24 hours in the quail (52.28%) compared to 36 hours in the chick (50.07%) (Figure 4.1a and b).

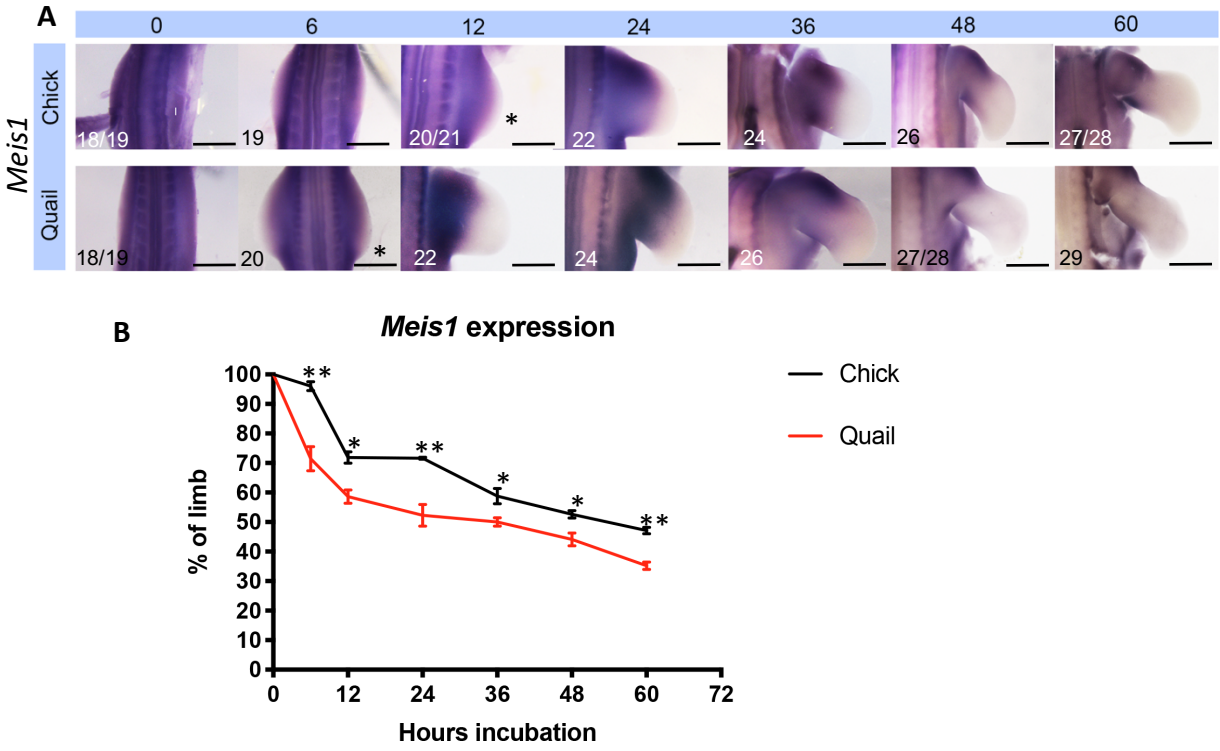

Figure 4.1. *Meis1* expression dynamics are accelerated in the quail wing.

Whole-mount *in situ* hybridisation was performed in quail and chick embryos incubated for an equivalent amount of time. At 0 hours, both wing buds are shown and from 12 hours only a close up of the right wing bud is shown. HH stages are noted for each time point. **A)** Expression of the proximal marker, *Meis1*, is downregulated at an earlier time point in the quail wing compared to the chick wing. Black asterisks indicate loss of *Meis1* in the distal wing bud. **B**) Quantification of the percentage of the wing expressing high-levels of *Meis1* along the proximo-distal axis was performed. Student's *t*-tests reveal that at 0 hours there is no significant difference between the limb bud *Meis1* expression, however, after this time, significantly less *Meis1* expression is seen in the quail wing compared to the chick wing from 6 to 60 hours. Scale bars = 500µm. *p* values: *=<0.05, **=<0.01 ***= <0.001 ****= <0.0001. *n*=3-8

Recent evidence suggests that there is a switch from the extrinsically controlled specification of the proximal wing segment by RA (indicated by *Meis1* expression), to an intrinsically timed programme of distal specification (Saiz-Lopez, Chinnaiya et al., 2015). The products of the 5' *Hoxa/d* genes are considered to be important in specifying positional

values early in the developing limb (reviewed (Tabin and Wolpert, 2007). In the limb bud, the genes of the *Hoxa/d* clusters are sequentially expressed in spatially restricted domains along the proximo-distal axis according to their chromosomal location in the 3' to 5' direction (Dolle and Duboule, 1989, Izpisua-Belmonte and Duboule, 1992, Zakany and Duboule, 1999). The most-5' *Hoxa* gene in the cluster, *Hoxa13*, is expressed in the most-distal regions of the limb bud and is required for normal development of the autopod (wrist and digits) (Nelson, Morgan et al., 1996, Vargesson, Kostakopoulou et al., 2001, Yokouchi, Nakazato et al., 1995, Zakany and Duboule, 1999), and has been shown to be expressed in an intrinsically-timed manner (Saiz-Lopez, Chinnaiya et al., 2015).

Hoxa13 expression becomes detectable at HH22 in the chick wing bud (Yokouchi, Sasaki et al., 1991). This is consistent with my data showing that *Hoxa13* is detectable at 24 hours (HH22) in the chick wing. However, this is approximately 12 hours after its expression is detectable in the HH22 quail wing bud (Figure 4.2 – 12 hour quail, compared to 24 hour chick - asterisks). In addition, the size of the domain of *Hoxa13* expression also increases over time, marking cells in the field of the prospective wrist and digits, which is noticeably more advanced in the quail compared to the chick (Figure 4.2).

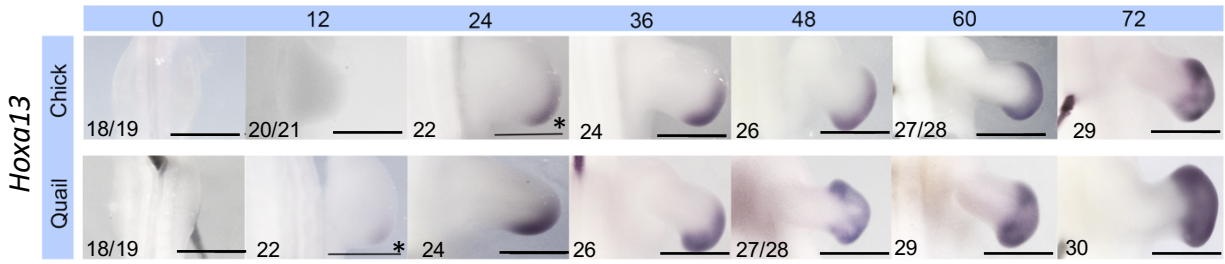

Figure 4.2. *Hoxa13* expression dynamics are accelerated in the quail wing.

Whole-mount *in situ* hybridisation was performed in quail and chick embryos incubated for an equivalent amount of time. At 0 hours both wing buds are shown, from 12 hours only a close up of the right wing bud is shown. HH stages are noted for each time point. The distal marker, *Hoxa13,* is expressed approximately 12 hours earlier in the quail compared to the chick. Black asterisks indicate *Hoxa13* upregulation in the distal wing bud *n*=4-8. Scale bars = 500µm

4.2.2 Genes are expressed in embryonic signalling centres for a shorter period of time in the quail wing compared to the chick wing

The polarising region and the apical ectodermal ridge are two major embryonic signalling centres in the developing limb bud. These centres produce signals which are involved in the specification of skeletal elements and in promoting growth (Reviewed in (Delgado and Torres, 2016, Fernandez-Teran and Ros, 2008, Tickle and Towers, 2017). The apical ectodermal ridge (AER) runs along the distal edge of the limb bud and expresses *Fgf8* which is involved in maintaining the outgrowth of the limb bud (Reviewed in (Tickle, 1995). As seen in Figure 4.3, *Fgf8* expression is detectable at 0 hours in both the quail and chick and is maintained as the wing bud develops in both species. However, *Fgf8* expression is downregulated at approximately HH29 and is therefore expressed at high levels for the shorter duration of 60 hours in the quail wing bud compared to 72 hours in the chick wing bud, although residual expression can be seen at later stages as the AER regresses (Figure 4.3).

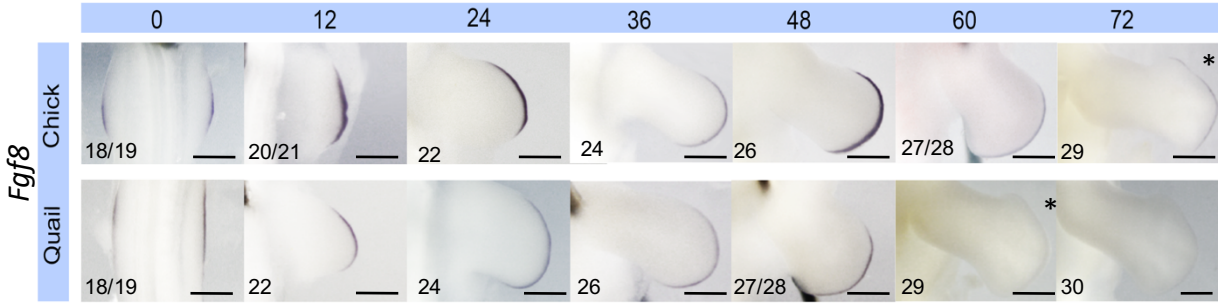

Figure 4.3. *Fgf8* in the apical ectodermal ridge is expressed for a shorter duration in the quail compared to the chick wing.

Whole-mount *in situ* hybridisation was performed in quail and chick embryos incubated for an equivalent amount of time. At 0 hours both wing buds are shown, from 12 hours only a close up of the right wing bud is shown. HH stages are noted for each time point. *Fgf8* expression in the apical ectodermal ridge can be seen from 0 hours, however is lost in the quail wing at 60 hours, compared to 72 hours in the chick, indicated by the black asterisk. *n*=4-8. Scale bars = 400µm

I have also analysed the expression of *Sonic hedgehog* (*Shh)* in the polarising region, which is detectable at HH18 (0 hours in quail and chick). As previously described, the polarising region is located in the posterior-distal mesenchyme of the wing bud and is defined by the expression of *Shh* (Charite, McFadden et al., 2000, Fernandez-Teran, Piedra et al., 2000, Riddle, Johnson et al., 1993). Shh emanates from the polarising region and is involved in specifying pattern and in stimulating growth along the antero-posterior axis (thumb to little finger) (Reviewed in (Tickle and Towers, 2017). At 0 hours, *Shh* expression is detectable in both quail and chick wing buds and is expressed strongly until HH26 - 48 hours in the chick wing, and 36 hours in the quail wing, and is then downregulated by HH27/28 - 60 hours in the chick wing and 48 hours in the quail wing. (Figure 4.4). This 12 hour difference in the expression duration of *Shh* is equivalent to the difference observed for *Fgf8* expression between chick and quail wings buds.

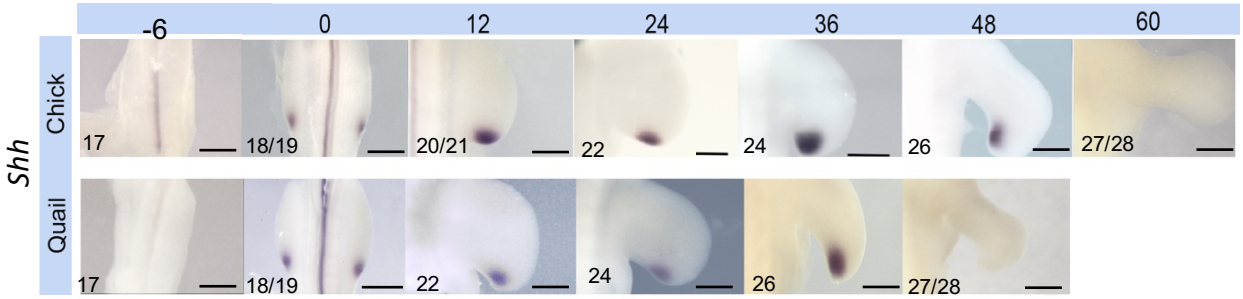

Figure 4.4. The polarising region expresses *Shh* for a shorter duration in the quail compared to the chick

Whole mount *in situ* hybridisation was performed in quail and chick embryos incubated for an equivalent amount of time. At -6 and 0 hours both wing buds are shown, from 12 hours only a close up of the right wing bud is shown. HH stages are noted for each time point. Expression of *Shh* in the polarising region is seen for approximately 60 hours in the chick compared to 48 hours in the quail. *n*=4-8. Scale bars = 250µm

4.2.3 Late stage developmental events occur earlier in the quail wing compared to the chick wing

I have also explored patterning events that occur at later stages of wing development, such as the formation of cartilage condensations of the skeletal elements and the emergence of feather follicles.

Sox9 is a marker of condensing cartilage cells during skeletogenesis, and first becomes distinct in chick wings at approximately HH22 (Healy, Uwanogho et al., 1999, Montero, Lorda-Diez et al., 2017). In my analysis, *Sox9* is detectable at HH22 in both species, which is equivalent to 24 hours in the chick and 12 hours in the quail (indicated by black arrows). A good example of the accelerated development in the quail can be seen when comparing the pattern of cartilage condensation at HH27/28 - 48 hours in the quail and 60 hours in the chick (marked by asterisks in figure 4.5). There is a clear similarity in the expression pattern at these two time points, demonstrating that cartilage condensation occurs 12 hours later in the chick wing, compared to the quail wing (Figure 4.5).

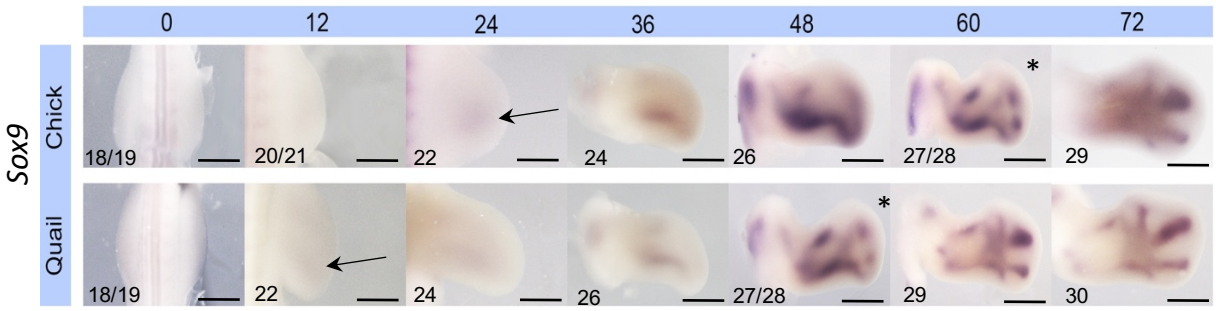

Figure 4.5. Cartilage condensation occurs earlier in the quail compared to the chick wing.

Whole-mount *in situ* hybridisation was performed in quail and chick embryos incubated for an equivalent amount of time. At 0 hours both wing buds are shown, from 12 hours only a close up of the right wing bud is shown. HH stages are noted for each time point. Expression of *Sox9* in condensing cartilage cells occurs 12 hours earlier in quail wing bud compared to the chick. Black arrows indicate the start of *Sox9* upregulation in the central wing bud *n*=4-8. Scale bars = 500µm.

I have also analysed *Bmp7* expression, which is necessary for the induction of epidermal feather placodes, and is therefore a useful early marker of feather development in avian species (Harris, Linkhart et al., 2004). In addition, Bmp7 is also one of the BMPs (along with Bmp2, Bmp4, and Bmp5) involved in creating interdigital necrotic zones which are areas of programmed cell death that separate the three digits of the wing (Kaltcheva, Anderson et al., 2016, Montero and Hurle, 2010). *Bmp7* expression reveals that the interdigital zones regress approximately 12 hours earlier in the quail wing compared to the chick wing as indicated by the green arrows (Figure 4.6). Strong expression of *Bmp7* in the interdigital zones can be seen up to approximately HH34 i.e. in the quail wing 108 hours, and in the chick wing, 120 hours (Figure 4.6).

With regard to feather development, *Bmp7* has an initial diffuse expression in the epidermis before becoming spatially segregated into spots of expression in the feather placodes, surrounded by non-expressing tissue *(Harris, Linkhart et al., 2004).* I have shown this initial diffuse expression can be seen at HH33/34, which is 96 hours in the quail, and 108 hours in the chick (black asterisks – Figure 4.6), again revealing 12 hours accelerated development in the quail wing. *Bmp7* expression can also be observed in distinct rows of spots at HH34/35 at in the quail wing 108 hours and at 120 hours in the chick wing. In addition, rows of *Bmp7*-expressing spots can then be detected on digit 1 (indicated by a black arrow) at 144 hours in the chick wing - HH35 and at 132 hours in quail wings – HH35 (Figure 4.6). At 144 hours, *Bmp7* expression is undetectable in the quail at this time point as quail feathers have begun to show black pigmentation.

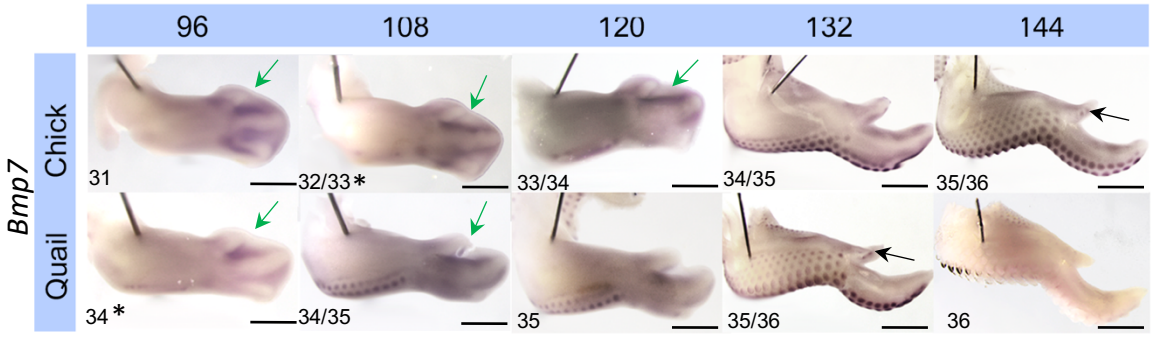

Figure 4.6. Late stage developmental events occur earlier in the quail compared to the chick wing.

Whole mount *in situ* hybridisation was performed in quail and chick embryos incubated for an equivalent amount of time. HH stages are noted for each time point. *Bmp7* expression can be seen marking areas of programmed cell death in interdigital regions, and rows of feather placodes in a posterior to anterior sequence. Green arrows indicate Bmp7 expression in the interdigital regions. Black arrows indicate forming feather placodes on digit 1. *n*=4. Scale bars = 1.25mm

4.3 Discussion

It is evident that chick and quail embryos develop differently sized wings during their distinct periods of incubation. However, it is largely unknown if patterning events are timed in relation to these morphological differences. Previous studies have described the embryonic development of different avian species without direct comparison to each other. In addition, these studies have only compared a short time-frame, or, alternatively, have observed broad morphological features rather than comparing cellular and molecular differences during embryonic wing development (Ainsworth, Stanley et al., 2010, Li, Bai et al., 2019, Padgett and Ivey, 1960, Sellier, 2006, Zacchei, 1961). It was therefore unknown

how developmental events are timed across the different incubation periods, and when differences in wing sizes become apparent in different species.

In this chapter I have analysed the timing and expression dynamics of a range of molecular markers and embryonic signalling centres essential for the patterning and development of the wing bud. The results I have presented indicate that gene expression is consistent with developmental time (Hamburger Hamilton stages), rather than incubation time, and that this is accelerated in the quail wing. This accelerated development is established during the first 12 hours of quail wing bud and is then maintained at later stages.

4.3.1 Analyses of molecular markers provide further evidence of accelerated quail wing development

In the current model of proximo-distal patterning there is a switch from the early proximal program (indicated by *Meis1* expression), which is specified by extrinsic signals at approximately HH19, to an intrinsically timed program which specifies the distal wing (indicated by *Hoxa13* and *Shh* expression). I have shown that there is an earlier downregulation of the proximal program marker, *Meis1,* in the quail wing during the first 12 hours of wing development. Downregulation of *Meis1* in the distal wing occurs as the limb grows outwards from the body wall, and away from proximalising RA signals (Cooper, Hu et al., 2011, Rosello-Diez, Ros et al., 2011). This occurs at the same developmental time in both species – HH20/21, however, quail wings reach this point faster than chick wings (6 hours, compared to approximately 12 hours, respectively). Therefore, downregulation of *Meis1* is accelerated in the quail wing consistent with acceleration of developmental time. Recent evidence suggests that the loss of the proximal RA, and *Meis* genes from the distal wing is necessary for the initiation of the intrinsically timed distal program and induction of *Hoxa13. Hoxa13* can then be detected at HH22 – 12 hours in the quail, 24 hours in the chick (Rosello-Diez, Arques et al., 2014, Saiz-Lopez, Chinnaiya et al., 2015). Therefore, the earlier induction of the distal program, indicated by earlier expression of *Hoxa13* in the quail wing, is likely to be a result of both the faster outgrowth and progression through Hamburger Hamilton

stages, and the subsequent earlier loss of *Meis1* expression. Thus, my data indicates that this switch between signal based (proximal) and timer based (distal) specification occurs earlier in the quail compared to the chick. This switch appears to occur at HH20/21 in both species and so, between the 0 and 12 hour time point.

At later stages, the accelerated development of the quail wing is maintained and results in the 12 hour earlier appearance of features typical of more advanced wing development, such as the emergence of cartilage (*Sox9)* and feathers (*Bmp7)* in the quail wing. *Bmp7* expression is also required for interdigital programmed cell death (Kaltcheva, Anderson et al., 2016). Expression of *Bmp7* in the interdigital necrotic zones is lost approximately 12 hours earlier in the quail compared to the chick. This observation correlates with my morphological data presented in chapter 3 showing that the digits separate and become distinct 12 hours earlier in the quail wing compared to the chick wing. Furthermore, I have shown that the condensation of cartilage and emergence of feathers is coupled to the developmental age of the wing, as opposed to incubation time. In addition, gene expression in embryonic signalling centres that are critical in patterning the wing, such as the polarising region and apical ectodermal ridge, are coupled to the developmental age of the tissue, and therefore are present for approximately 12 hours less in the quail wing compared to the chick wing. Taken together, my results show that developmental time is accelerated in the quail wing in terms of morphology (embryological staging), cell death, proliferation and gene expression (summarised in figure 4.7).

In the following chapter I have investigated how the switch from extrinsic (signal based) to intrinsic (timer based) specification occurs, and thus, how species-specific timing of limb patterning is achieved.

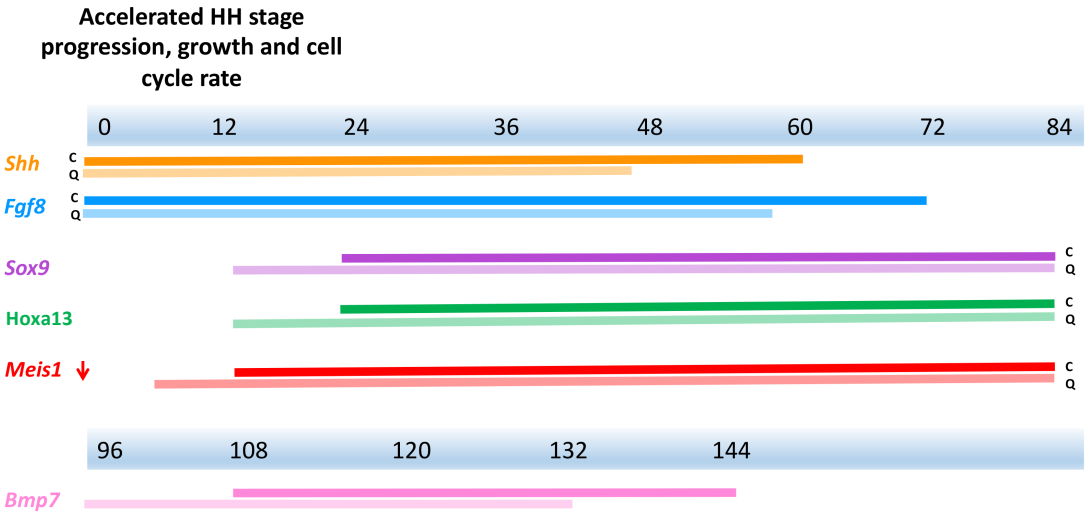

Figure 4.7. Schematic summarising the species-specific program of developmental events in the quail and chick

The first 84 hours of wing development are summarised in the schematic, with chick (C) represented by the darker bars, and the quail (Q) represented by the lighter coloured bars. The schematic illustrates the shorter duration of *Shh* and *Fgf8* in the quail, in addition, accelerated *Sox9* and *Hoxa13* expression and earlier *Meis1* downregulation. The first 12 hours are also highlighted as many important patterning events are set-up in this time-window in addition to the accelerated HH stage acquisition, limb outgrowth and faster cell cycle rate seen in the quail wing.

Chapter 5.

Determining the stability of species-specific timing in wing development.

5.1 Introduction

In chapters 3 and 4 I have described a species-specific program of development in quail and chick wings in relation to the incubation period, HH stages and wing growth. My findings reveal that developmental time (HH stages) and patterning of the quail wing is accelerated in comparison to the chick wing. I have also shown that this accelerated development occurs during the first 12 hours (0-12 hours incubation) and involves a faster rate of cell proliferation/wing outgrowth and the precocious downregulation of 'early' proximal limb markers, accompanied by delayed upregulation of 'late' distal limb markers. However, after the 12 hour time point growth of the wing is uncoupled from developmental time in different species. My findings indicate that the switch from proximal patterning by extrinsic signals, to an intrinsic timer which patterns the distal wing (Saiz-Lopez, Chinnaiya et al., 2015) occurs at approximately 6 hours incubation in the quail (HH20/21), and at 12 hours incubation in the chick (HH20/21).

Having shown that differences in timing of quail and chick wing development become apparent during the first 12 hour of outgrowth, this gave me an opportunity to investigate the underlying mechanisms. To understand how the timing of development is controlled and therefore differs between chick and quail wing buds, I performed a series of tissue grafts in which I reciprocally transplanted polarising regions between quail and chick wings buds at different time points. Tissue grafting is a classical method to investigate developmental timing, and some of the first experiments addressing this issue were conducted using whole limb bud grafts between different sized salamander species (Twitty, 1931). The authors of these early studies concluded that mechanisms intrinsic to the limb

bud were important in scaling species-specific development, and extrinsic signals from the body have a small but significant influence. However, since these experiments we performed, major advances have been made in understanding the molecular mechanisms of limb development. Therefore, gene expression and cellular analysis, combined with tissue grafts of polarising regions between species, could provide a useful technique to investigate patterning of the wing.

The polarising region is a developmental organiser located in the posterior-distal part of the limb bud which expresses *Shh* (Riddle, Johnson et al., 1993). Previous grafting experiments showed that *Sonic-hedgehog (Shh)* expression in the chick wing polarising region is intrinsically-regulated in a manner closely associated with cell proliferation parameters (Chinnaiya, Tickle et al., 2014, Saiz-Lopez, Chinnaiya et al., 2015). In Chapter 4, I showed that there is a species-specific duration of *Shh* in quail and chick wing development (Chapter 4, figure 4.4). Thus, *Shh* is initiated at an equivalent stage of wing development HH18/19 (0 hours) and is downregulated by HH27/28 in both species, however this occurs by 48 hours in the quail wing, and 60 hours in the chick wing. Therefore, grafts of the polarising region provide a useful assay to analyse the developmental timing in response to the extrinsic environment.

In this chapter I aim to elucidate the stability of species-specific developmental timing, by determining if donor polarising regions maintain their own parameters or reset them in response to the host environment. I will test this using two different grafting experiments between quail and chick wing buds: 1) when the distal intrinsic timer is running (after HH20/21, i.e. shortly after the 12 hour time point); 2) when wing bud cells are considered to be under the influence of the extrinsic proximal signalling environment (HH18/19 i.e. at the 0 hour time point).

5.2 Results

5.2.1 Polarising grafts provide a useful assay for exploring the influence of intrinsic mechanisms and extrinsic signals in wing development.

The grafting of polarising regions from one wing bud to the anterior margin of the wing bud of a host embryo is a well-established technique for understanding antero-posterior patterning (Stainton and Towers, 2018). The process involves removing the polarising region from a donor embryo and transplanting it to the anterior wing bud of a host embryo (see methods). This experiment can be seen in Figure 5.1a that shows a 12+ hour chick to chick (HH21) control polarising region graft made to the anterior margin of the right wing bud. *Shh* expression can be analysed using *in situ* hybridization 24 hours after the graft has been performed to ensure the correct cells have been transplanted (Figure 5.1b). By performing the grafts with a *Gfp*-expressing donor chick to a wild type host, shows that *Gfp* expression overlaps with polarising region cells in the graft, confirming that the grafted polarising region cells have successfully integrated into the host tissue (Figure 5.1b). This also shows that, as previously reported, grafts of the polarising do not induce the formation of another polarising region (Chinnaiya, Tickle et al., 2014)

In order to see if polarising region grafts behave normally when grafted to a host wing bud, I performed grafts between the same species at 12+ hours (defined at HH22 in the quail, and HH21 in the chick) and analysed the duration of *Shh* expression (CC – chick to chick, QQ- quail to quail) (Figure 5.1c). Performing grafts to the anterior margin of the host wing means that it is possible to compare *Shh* expression between grafted and host polarising regions. After performing the grafts, I analysed *Shh* expression 24 hours later (at the 36 hour time point) in both the quail and chick wings. In both CC (Figure 5.1ci) and QQ (Figure 5.1cii) grafts, *Shh* is expressed in the endogenous polarising region and in the anteriorly grafted polarising region. I then determined when *Shh* duration was terminated in the grafted polarising regions. In both CC and QQ grafts, *Shh* expression is downregulated simultaneously in the grafted and the endogenous polarising regions by 48 hours in the

quail (QQ), and 60 hours in the chick (CC). This result confirms that the grafting procedure does not affect *Shh* duration in the polarising region.

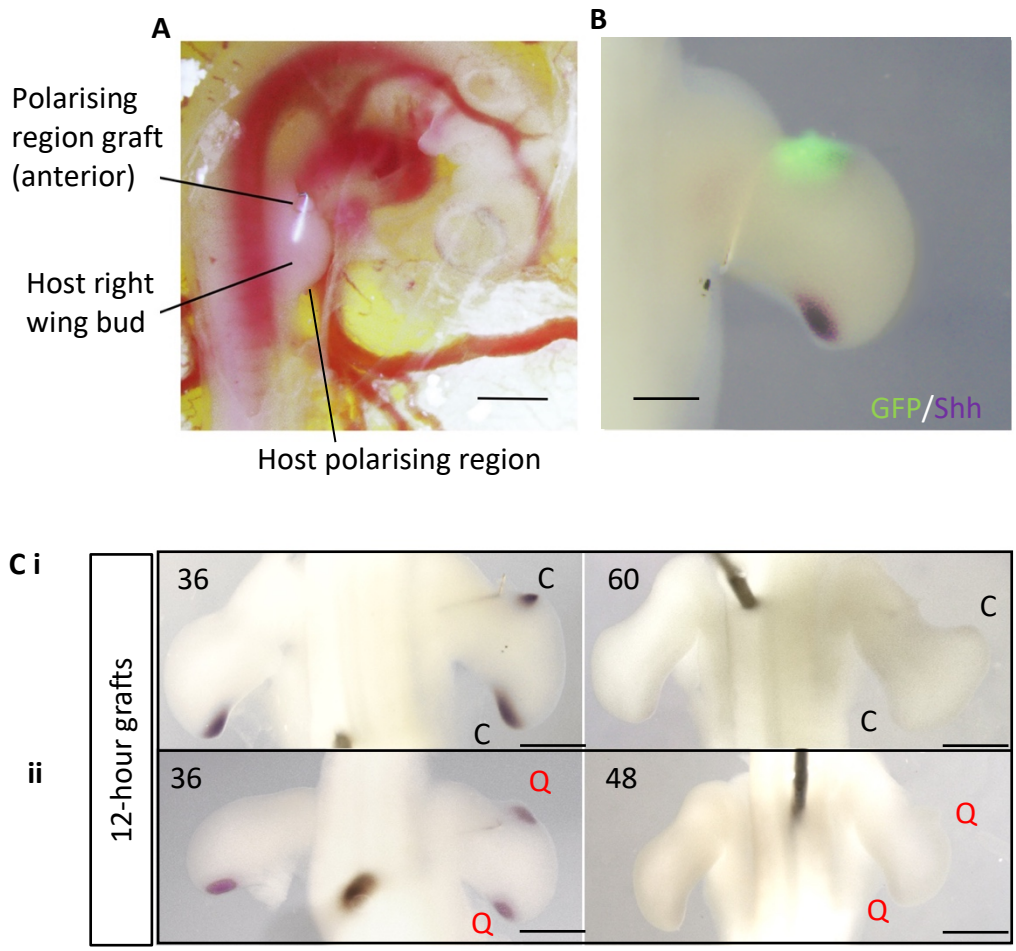

Figure 5.1. *Shh* maintains the correct duration in control grafts between the same species

A) Image taken shortly after a 12+ hour chick-chick control graft has been placed. The donor polarising region has been grafted to the anterior margin of the host right wing bud and held in place with a platinum pin. **B)** Overlay image of fluorescent *Gfp* expression in the anterior grafted polarising region with and whole mount *in situ* hybridisation of *Shh* expression which can be seen in both the endogenous polarising region and co-expressed with *Gfp* in the anterior grafted polarising region. Image taken at 36 hours (24 hours after the graft was performed). **C)** Same species graft performed at 12 hours (CC – chick to chick, QQ - quail to quail) **i)** CC graft at 36 hours shows strong *Shh* expression in the grafted and

endogenous polarising regions, which is then downregulated at 60 hours. **ii)** QQ graft at 36 hours shows strong *Shh* expression in the grafted and endogenous polarising regions, which is then downregulated at 48 hours. Scale bars in A and C = 500µm. Scale bar in B =300µm *n*=3

5.2.2 Intrinsic species timing of *Shh* is maintained in HH21+ polarising region grafts

I performed interspecies grafts at 12+ hours in both species i.e. HH22 in the quail and approximately HH21 in the chick. (Figure 5.2a – quail to chick (QC) and chick to quail (CQ)). My results presented in chapters 4 indicate that this is when the intrinsic timer is running in the distal part of the wing. As this process is intrinsically regulated, I therefore hypothesised that species-specific duration of *Shh* expression would be maintained in grafted tissue.

In grafts of a HH22 quail polarising region made to the anterior margin of a HH21 chick wing bud (12+ hours) – quail to chick (QC), *Shh* expression is switched off by the 48 hour time point, thus showing that its normal duration has been maintained (Figure 5.2b). However, *Shh* is still expressed in the endogenous chick wing host polarising region (posterior).

In the reciprocal graft in which a HH21 chick wing polarising region was made into a HH22 quail wing (CQ) *Shh* expression is maintained at the 48 hour time point, and its normal duration has been maintained (Figure 5.2c). However, *Shh* expression is terminated in the host quail polarising region at the 48 hour time point. This reveals that when grafts are performed after the 12 hour time point, the host environment is not able to influence species-specific timing of *Shh*.

Polarising region cell cycle rates have been shown to be intrinsically regulated and linked to the timing of *Shh* expression (Chinnaiya, Tickle et al., 2014). In chapter 3 I have also shown that the cell cycle rate in polarising region cells exhibits a distinct species-specific

pattern related to developmental age of the tissue. This therefore provides another assay to determine if species-specific timing is maintained in grafts. To understand if cell cycle rates are intrinsically maintained, I performed flow cytometric analyses 24 hours after the graft was performed - when the grafts have integrated into the tissue, but still can be easily defined by the pin holding the graft in place, allowing it to be easily dissected from the host wing bud.

In QC grafted polarising regions (QC12 grafted PR) there is a significant difference in cell cycle rates in the quail grafted polarising region compared to the endogenous chick polarising region - 63.3% of cells in G1-phase, compared to 71% cells, respectively (Figure 5.2d). However, there is no significant difference between the grafted quail polarising region cells and control quail polarising regions of the equivalent developmental age - 63.3% of cells in G1-phase, compared to 64% of cells in G1-phase (Figure 5.2d).

Similarly, in CQ grafts, cell cycle rates in the grafted chick polarising region (CQ12 grafted PR) are not significantly different from control chick polarising regions of the same incubation time - 72.6% in G1-phase compared to 71% in G1-phase, respectively. However, the cell cycle rates in the grafted chick polarising region are significantly different to the endogenous quail host – 72.6% compared to 64% Figure 5.2d. These results further indicate that polarising region cells intrinsically maintain their species-specific developmental timing at the 12+ hour time point.

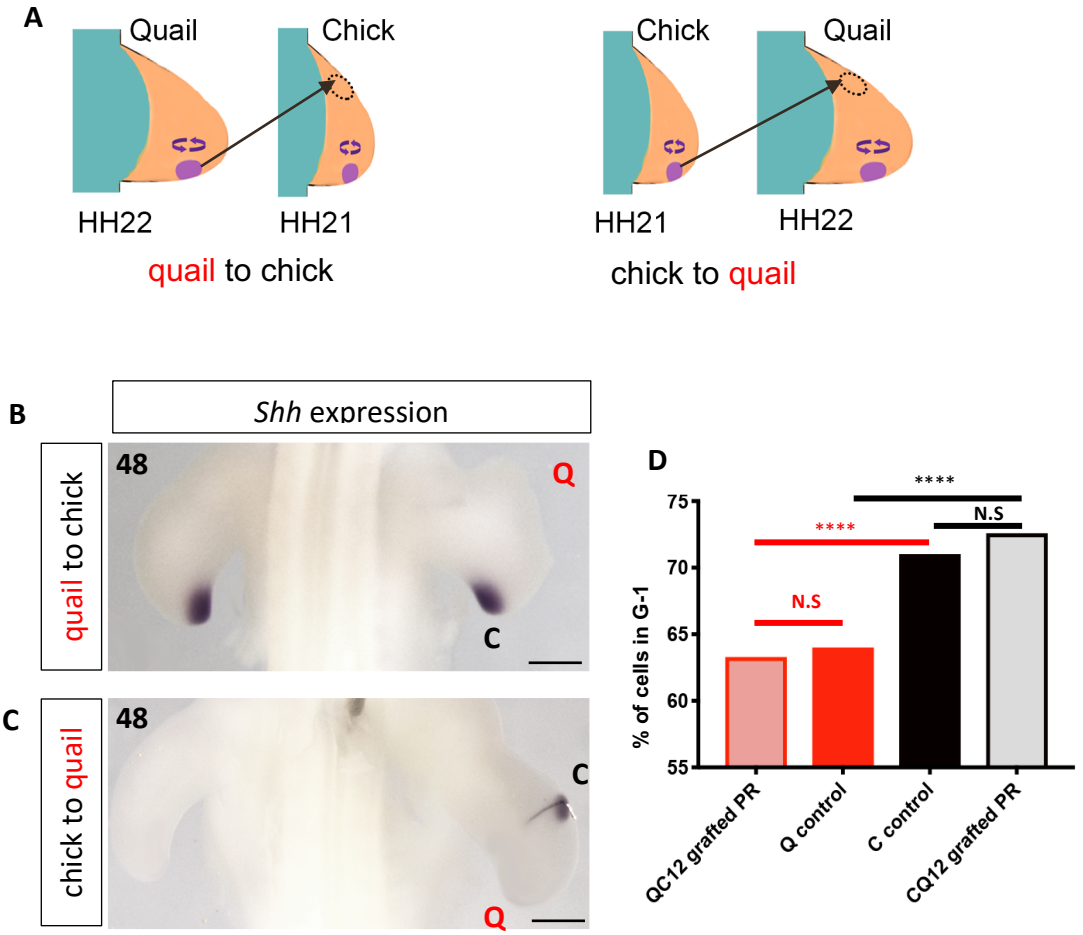

Figure 5.2. Species-specific timing is maintained in 12 hour polarising region grafts
A) Schematic depicting when the grafts were performed **B)** QC grafts were performed at the 12 hour time point and the expression of *Shh* analysed, at 48 hours the quail grafted polarising region has downregulated *Shh*, but *Shh* expression can still be seen in the endogenous chick polarising region. **C)** CQ grafts were performed at the 12 hour time point and the expression of *Shh* analysed, at 48 hours the chick grafted polarising region still expresses *Shh*, but *Shh* expression has been downregulated in the endogenous quail polarising region. **D)** The percentage of cells in G1 phase of the cell cycle in polarising regions were analysed by flow cytometry 24 hours after the graft was performed. Chi squared tests reveal QC12 grafted polarising regions (as in A) have 63.3% of cells in G1 compared to 64% of control quail polarising regions of the same age (not significant). However, have a significantly lower percentage of cells in G1 compared to control chick polarising regions (71%) *p*= <0.0001. CQ12 grafted polarising regions (as in B) have 72.6% of cells in G1 compared to 71% of control chick polarising regions of the same age (not significant). They also have a significantly higher percentage of cells in G1 compared to

control quail polarising regions (64%) *p*= <0.0001. *n*=3-5. *p* values: *=<0.05, **=<0.01 ***= <0.001 ****= <0.0001. Scale bars = 500µm

5.2.3 Intrinsic species timing of *Shh* can be reset during an early critical phase

I then performed grafts at 0 hours when both species are at the equivalent developmental age of HH18/19 (Figure 5.3a) and when *Shh* expression has just been induced in the polarising region (Chapter 4, figure 4.4). At this time point, the wing bud is influenced by proximal extrinsic signals from the flank of the embryo. I therefore hypothesised that the species-specific duration of *Shh* expression could be influenced by the host environment.

Indeed, when quail polarising regions were grafted to the chick wing at the 0 hour time point this resulted in a remarkable alteration in *Shh* expression in the grafted quail cells (Figure 5.3a). *Shh* is now strongly expressed at 48 hour time point in the quail donor polarising region (when it would normally be downregulated), similar to the expression seen in the chick host polarising region. This result shows that the duration of Shh has been reset to that of the host. (Figure 5.3b). A similar result can also be seen in the reciprocal graft, in which chick polarising region cells were grafted into a quail wing. *Shh* is no longer expressed at 48 hour time point in the chick donor polarising region (when it would normally be expressed) similar to the expression seen in the host quail polarising region (Figure 5.3c). These results reveal that when the grafts are performed at the 0 hour time point, the species-specific duration of *Shh* is reset in the grafted polarising region by the proximal host environment.

Furthermore, analysis of cell cycle rates 24 hours after the graft was performed also shows that species-specific timing can be reset by the proximal environment. In QC grafts (QC0 grafted PR) there is no significant difference between the endogenous host polarising region, and the grafted donor polarising region - 59% of cells are in G1-phase, compared to 60% of cells in G1-phase, respectively. However, cell cycle rates in QC grafted PRs is significantly different from control quail polarising regions (59% vs 56%).

In the reciprocal grafts of 0 hour chick polarising regions made to 0 hour quail wings, (CQ0 grafted PR) 54% of cells are in G1-phase compared to 56% in the host quail polarising region. Although this is significantly different, it is clear that the grafted chick polarising region cell cycle rate is more similar to the endogenous host (54% and 56% respectively), than to the control chick polarising region (60% of cells in G1-phase). These data show that, in polarising grafts performed at the 0 hour time point, intrinsic species-specific timing is reset by the host proximal environment, as indicated by *Shh* duration and cell cycle parameters.

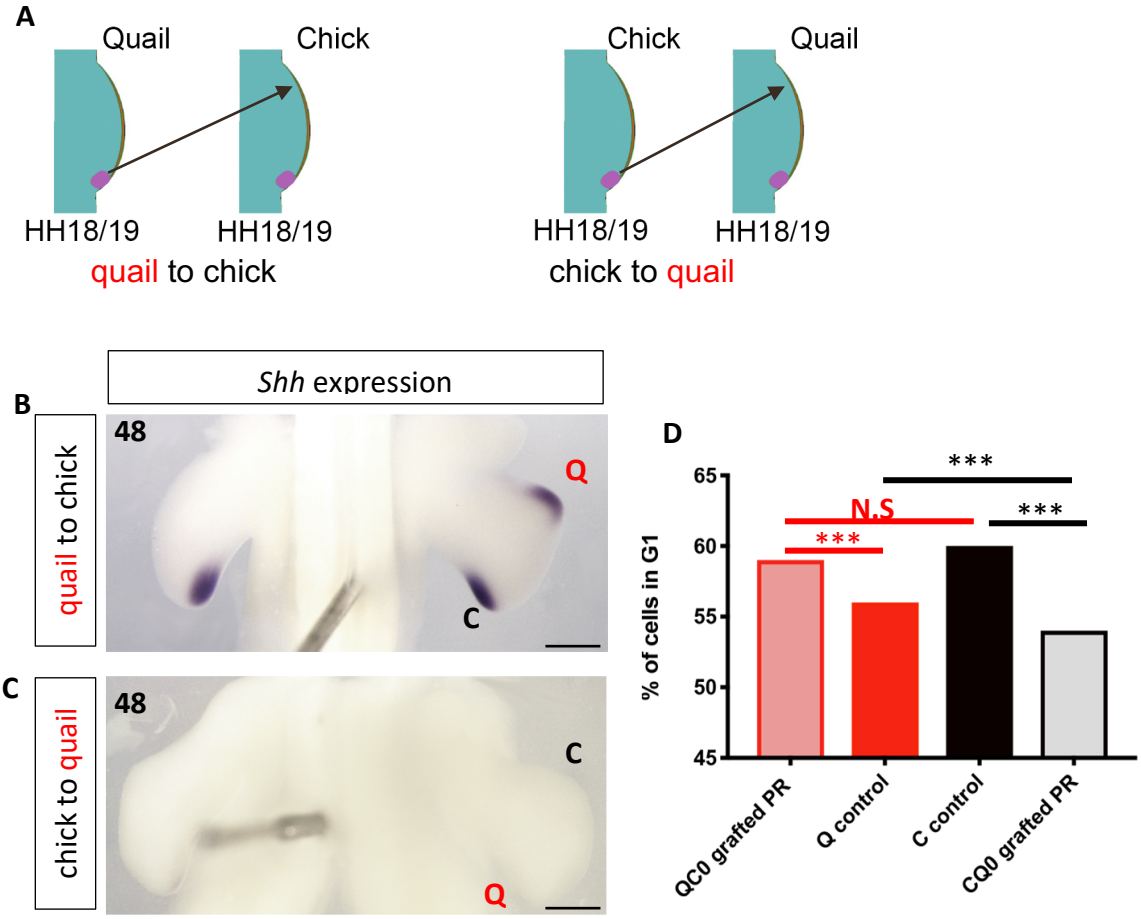

Figure 5.3. Species-specific timing is reset in 0 hour polarising region grafts
A) Schematic depicting when the grafts were performed **B)** QC grafts were performed at the 0 hour time point and the expression of *Shh* analysed, at 48 hours the quail grafted polarising region has strongly expresses *Shh*, similar to the host chick where

the endogenous polarising region still expresses *Shh*. **C)** CQ grafts were performed at the 0 hour time point and the expression of *Shh* analysed at 48 hours, the chick grafted polarising region now has downregulated *Shh*, corresponding with the endogenous host quail polarising region which has also downregulated *Shh* expression at this time point. **D)** The percentage of cells in G1 phase of the cell cycle in polarising regions were analysed by flow cytometry 24 hours after the graft was performed. Chi squared tests reveal QC0 grafted polarising regions (as in A) have 59% of cells in G1 compared to 56% of control quail polarising regions of the same age (p=<0.0001). However, are not significantly different from the host endogenous polarising region (C control - 60%). CQ0 grafted polarising regions (as in B) have 54% of cells in G1 compared to 60% of control chick polarising regions of the same age (p=<0.0001). They also have a significantly lower percentage of cells in G1 compared to control host quail polarising regions (56%) p= <0.0001. *n*=3-5. *p* values: *=<0.05, **=<0.01 ***= <0.001 ****= <0.0001. Scale bars = 500µm

5.2.4 Termination of *Shh* expression is intrinsically controlled in the polarising region

In the developing wing the two major embryonic signalling centres, the polarising region and the apical ectodermal ridge, work synergistically to couple patterning of the limb with outgrowth. A positive feedback loop operates between the polarising region and apical ectodermal ridge, in this feedback loop, Shh signalling maintains *Fgf4* expression in the apical ectodermal ridge by inducing *Gremlin* (*Grem1*) expression in the adjacent limb mesenchyme (Zuniga, Haramis et al., 1999). Gremlin is a Bmp 2,4 and 7 antagonist which acts to prevent Bmps from inhibiting *Fgf* expression in the apical ectodermal ridge (Pizette and Niswander, 1999). Subsequently, *Fgf4* expression in the apical ectodermal ridge feeds back and maintains *Shh* expression in the polarising region (Laufer, Nelson et al., 1994, Niswander, Jeffrey et al., 1994).

Termination of embryonic signalling centres is important in facilitating the precise sequence of patterning and growth in embryonic development. One model of how the termination of *Shh*-expression in the polarising region occurs indicates that this feedback loop is broken by the loss of maintenance of *Grem1* expression by a physical barrier of cells

separating *Grem1* competent cells from the polarising region. This is followed by the loss of *Fgf4* and finally the subsequent loss of *Shh* expression (Scherz, Harfe et al., 2004). However, a recent study grafting polarising regions between wing buds of different ages has provided evidence that *Shh* regulates its own expression, and termination of expression is intrinsically controlled. (Chinnaiya, Tickle et al., 2014)

My data Is consistent with the intrinsic termination model, as I have shown that species-specific duration of Shh is intrinsically maintained in polarising region grafts (Figure 5.2). In order to investigate this further I have analysed components of the feedback loop by a triple *in situ* of *Shh, Fgf4* and *Grem1* expression in QC grafted wing buds (Figure 5.4).

Interestingly, in QC polarising region grafts, *Fgf4* expression can be seen in the apical ectodermal ridge (arrow). In addition, the normal endogenous expression pattern of *Grem1* in the mesenchyme (black asterisk) can also be seen separated from *Shh* expressing polarising region cells by cells not expressing *Grem1*. In addition to this, duplicated *Grem1* expression (white asterisk) can be seen in the anterior mesenchyme adjacent to the grafted quail polarising region. Despite this, *Shh* expression can be seen in the endogenous chick polarising region, but has been downregulated in the grafted quail polarising region (Figure 5.4). Therefore, this result shows that termination of *Shh* expression does not require the physical displacement *Grem1* expressing cells from the polarising region and supports the model that *Shh* termination is intrinsically controlled.

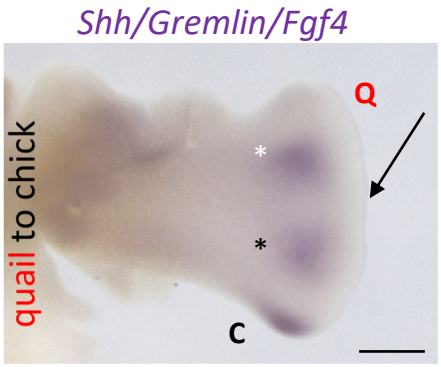

Figure 5.4. Termination of *Shh* is intrinsically controlled

QC grafts were performed at the 12 hour time point and at the 48 hour time point the expression of *Shh*, *Gremlin* (*Grem1*) and *Fgf4* was analysed. In the grafted quail polarising region *Shh* has been downregulated, but *Shh* expression can still be seen in the endogenous chick polarising region. Residual *Fgf4* expression can be seen in the apical ectodermal ridge indicated by the black arrow. Additionally, *Gremlin* expression is seen adjacent to endogenous *Shh* expression (black asterisk), and a duplicated field of *Gremlin* expression can also be seen adjacent to the grafted quail polarising region (white asterisk). Scale bar = 300µm *n*= 3

5.2.5 Whole wing bud grafts do not attain the final size of the contralateral wing

In reciprocal polarising region grafts, developmental timing – indicated by *Shh* expression and cell cycle rates, can be reset to host time in early 0 hour transplants (Figure 5.3), but not 12 hours grafts (Figure 5.2). To understand whether growth of the entire wing would follow a similar pattern I performed a series of whole wing bud grafts between quails and chicks at the 12 hour and 0 hour time points. Control grafts between the same species were performed at the 12 hour time point (CC= chick to chick, QQ= quail to quail). Embryos were then collected at day 9 incubation, at this time point the chick wing is at HH35 and on average measures 12.1mm +0.159, and the average quail wing is HH36 and measures 10.17mm +0.162.

In CC control grafts, a *Gfp*-expressing donor wing bud was transplanted into a wild type host and analyses were performed at day 9 (Figure 5.5). Cartilage staining reveals that

the grafted bud produces normal skeletal pattern (indicated by the arrow) and is integrated with the scapula and body of the host chick. Integration of the grafted bud to form the wing is also shown in GFP fluorescent microscopy imaging (Figure 5.5). This confirms that cells from the grafted bud grow and form a normal wing.

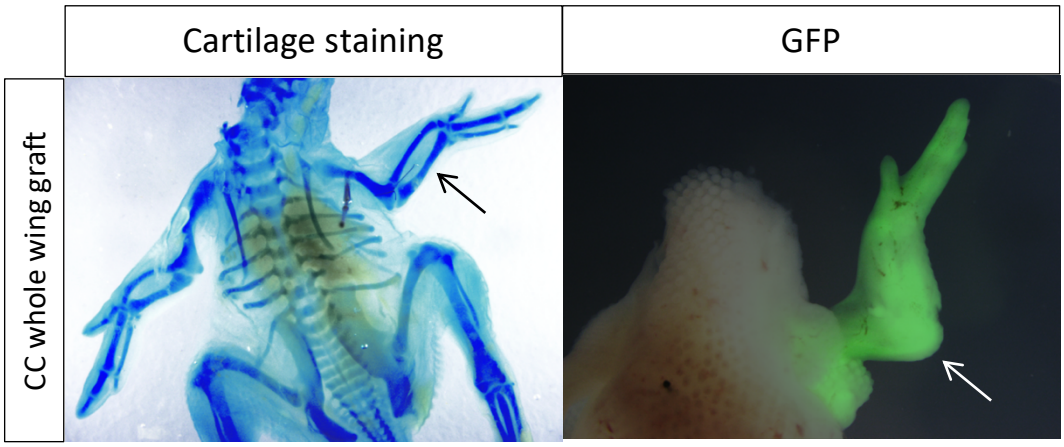

Figure 5.5. Whole wing bud grafts integrate and grow to form a normal wing.
Chick to chick (CC) whole wing bud graft between a *Gfp*-expressing donor wing bud and wild type host. Grafts of the right wing bud were performed at the 12 hour time point and collected at day 9, the wing from the grafted bud is indicated by a black (right) and white (left) arrow. Cartilage stains show a normally patterned skeleton of the wing, while GFP fluorescent imaging shows the graft has integrated into host body.

In the grafts conducted at the 12 hour time point, the size of the grafted wing (right) was compared to control (left) wings at day 9 (Figure 5.6). In CC grafts, the grafted wing (10.67mm) is significantly shorter than the control wing (12.68mm). However, in QQ grafts, there is no significant difference between the grafted and control wings (9.473mm and 10.35mm, respectively). I then performed interspecies whole wing bud grafts and compared the size of the wings. In both sets of grafts the grafted wing was significantly shorter than the host control wing (QC grafted quail wing = 9.773, control chick wing = 12.25; CQ grafted chick wing 7.32, control quail wing = 10.59) (Figure 5.6). This data suggests that, species-specific size does not appear to be maintained in grafted buds at day 9 incubation.

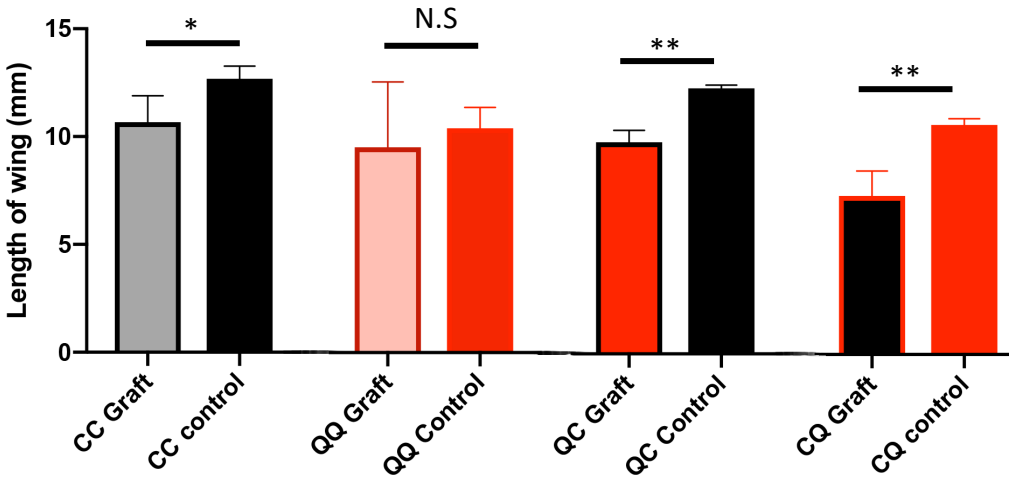

Figure 5.6. Whole wing bud grafts performed at 12 hours are smaller than the host wing at day 9.

Grafts of the right wing bud were performed at the 12 hour time point and collected at day 9. The measurement along the PD axis (combined lengths of the humerus, ulna and digit 2) was compared between the grafted right wing, and control contralateral left wing. CC= chick the chick graft, the grafted wing is significantly shorter than the control wing. QQ= quail to quail graft, there is no significant difference between the grafted and control wings. QC= quail graft into chick, the grafted wing is significantly shorter than the control wing. CQ= chick graft into quail, the grafted wing is significantly shorter than the control wing. Students *t*-tests were performed to determine if differences between the length of the wings are significantly different. *n*=3. *p* values: *=<0.05, **=<0.01 ***= <0.001 ****= <0.0001. *n*=3-4

Whole wing bud grafts were then performed at the 0 hour time point to determine if, growth could be influenced by proximal signals. The size of the grafted wing (right) was then compared to control (left) wings at day 9 (Figure 5.7). Similar to the 12 hour grafts in (Figure 5.6), in CC grafts the grafted wing (9.385mm) are significantly shorter than the control wing (12.7mm). Furthermore, in QQ grafts there is no significant difference between the grafted and control wings (9.067mm and 10.40mm, respectively). Additionally, in

interspecies whole wing bud grafts there is no significant difference between the size of the grafted wing and the host control wing. In QC grafts the grafted quail wing measures 10.56mm in comparison to the control host chick wing which measures 11.20mm. In CQ grafts, grafted chick wings measure 9.90mm, compared to control quail wings measuring 11.26mm (Figure 5.7). Therefore, this data appears to show that the time the whole wing bud grafts are conducted does not affect the growth of the wing during the time frame that I have analysed (day 9).

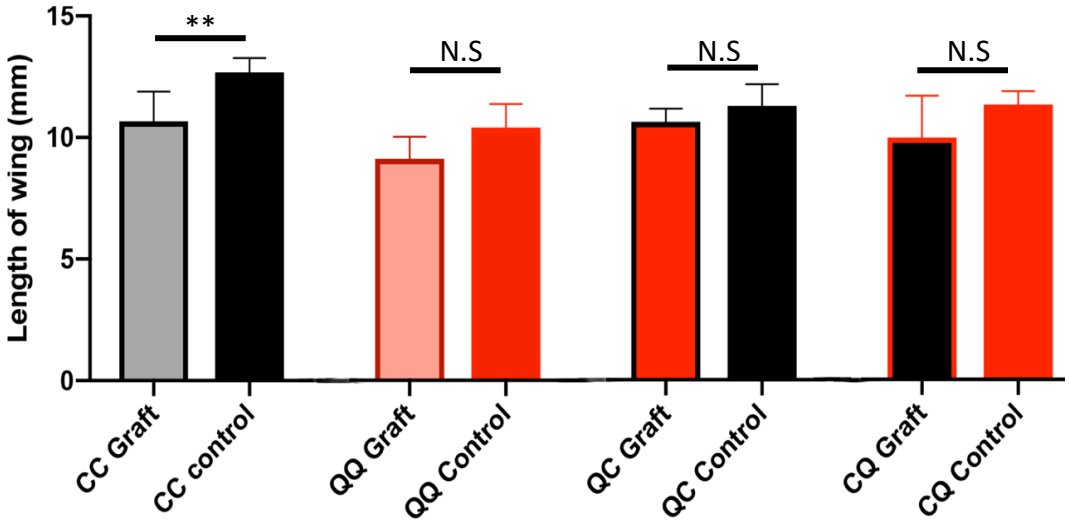

Figure 5.7. Wings from whole wing bud grafts performed at 0 hours are not significantly different in size from that of the host wing.

Grafts of the right wing bud were performed at the 0 hour time point and collected at day 9. The length along the PD axis (combined lengths of the humerus, ulna and digit 2) was compared between the grafted right wing, and control contralateral left wing. CC= chick the chick graft, the grafted wing is significantly shorter than the control wing. QQ= quail to quail graft, there is no significant difference between the grafted and control wings. QC= quail graft into chick, there is no significant difference between the grafted and control wings. CQ= chick graft into quail, there is no significant difference between the grafted and control wings. Students t-tests were performed to determine if differences between the length of the wings are significantly different. n=3. *p* values: *=<0.05, **=<0.01 ***= <0.001 ****= <0.0001.

Discussion

5.3.1 The proximal signalling environment is capable of resetting species-specific timing.

I have shown that when grafts are performed after the intrinsic timer has initiated in the wing after the 12 hour time point (after HH20/21), the species-specific duration of *Shh* and cell cycle rates are maintained in the grafted tissue. However, when the grafts are performed at the 0 hour time point at HH18/19 when the wing is close to the body wall and influenced by proximal extrinsic signals, species-specific timing reset to the host as shown by the duration of *Shh* in the grafted polarising region and cell cycle rates. This result suggests that the proximal environment at 0 hours (HH18/19), is capable of resetting species-specific intrinsic developmental timing, and thus acts to set distal timing such as *Shh* duration and associated cell cycle rates. In chapter 6 I will investigate the identity of this proximal signal.

5.3.2 Further evidence for the intrinsic termination of the polarising region

It has been suggested that termination of *Shh* expression in the polarising region relies on the breakdown of the Fgf/Shh loop between the polarising region and the apical ectodermal ridge. This is based on the observation that former *Shh* expressing cells - descendants of the polarising region - are unable to express *Grem1*, and as these cells proliferate, a physical barrier is formed separating *Grem1* expressing cells and the polarising region (Scherz, Harfe et al., 2004, Verheyden and Sun, 2008). When a 'critical distance' has formed between these populations, *Grem1* is no longer able to be maintained by Shh signalling, resulting in the breakdown of the loop and the subsequent de-repression of Bmps. Bmps then inhibit Fgfs in the apical ectodermal ridge, which leads to a loss of *Shh* in the polarising region. In this termination model, the initial loss of *Grem1* maintenance

would then be followed by the termination of *Fgf4* in the apical ectodermal ridge, and finally resulting in the loss of *Shh* in the polarising region (Scherz, Harfe et al., 2004) However, in this feedback-loop termination model, while maintaining the loop can temporarily increase *Shh* expression, it cannot extend *Shh* past its normal duration.

However, by transplanting polarising regions between species, I have shown that species-specific duration is maintained in different environments, this means that *Shh* expression from the quail polarising region is downregulated, despite *Shh* still being strongly expressed in the chick polarising region. Analysis of the components of the feedback loop, *Fgf4* and *Gremlin*, in the QC graft revealed that *Fgf4* expression was visible in the apical ectodermal ridge, as was a duplicated field of *Grem1* expression posterior to the grafted polarising region. The distance between the polarising regions (grafted and endogenous) appears to be at an equivalent distance from *Grem1* expression. This result is particularly interesting because if the feedback loop termination model were correct, then the donor quail polarising region should be reset and adapted to the host time by the overlying apical ectodermal ridge, and therefore *Shh* in the quail polarising region should still be strongly expressed whilst *Fgf4* is still active in the apical ectodermal ridge. However, this is not the case, and *Shh* is downregulated according to the age of the donor quail tissue. Furthermore, *Gremlin* expression can be seen at an equal distance away from grafted and endogenous polarising region; and *Shh* is still being strongly expressed in the endogenous polarising region.

Therefore, my data provides further evidence for an intrinsic termination model, whereby, *Shh* expression in the polarising region is linked to an intrinsic timer in the mesenchyme or potential cell cycle clock mechanism; terminating its expression intrinsically (Chinnaiya, Tickle et al., 2014, Pickering, 2019). Interestingly, other previous studies conducted in the mouse model have noted discrepancies in the feedback loop termination model, rather than *Gremlin* downregulating first as the model suggests, *Fgf4* is initially downregulated followed by *Shh* and finally *Gremlin* (Verheyden and Sun, 2008). This disorder in the sequence of events perhaps also challenges the feedback loop termination

model. Additionally, one study suggested Fgf4 signalling maintains *Shh* expression in the polarising region, however it was shown that this only occurs when RA signalling was also introduced in the wing (Niswander, Jeffrey et al., 1994). Therefore, *Fgf4* expression may play a role in allowing the induction of *Shh* but not necessarily controlling its expression or duration. Furthermore, alternative models for the termination of Shh have proposed a role for Tbx2 in repressing *Gremlin* expression, resulting in a breakdown signalling between the mesenchyme and the apical ectodermal ridge and thus, the subsequent termination of Shh expression (Farin, Ludtke et al., 2013). However, recently published data has determined that the overlying ectoderm does not dictate the age of the mesenchyme, but rather the distal mesenchyme behaves according to an intrinsic cell cycle clock timer and the apical ectodermal ridge acts permissively to allow outgrowth of the tissue (Pickering, Rich et al., 2018).

5.3.3 Wings from grafted buds are smaller than contralateral control wings.

In classical grafting experiments between salamander species it was shown that whole limb buds maintain the growth capacity of the donor species, with only a small influence from the body of the host (Twitty, 1931). However, in this study, controls grafts between the same species were not documented and experiments were only performed at one time point. In my analysis, control grafts at both 0 and 12 hours show that the grafted wing is slightly smaller than the reciprocal host wing. While these control grafts show that patterning of skeletal elements and integration of the grafted bud to the host is possible, it suggests that growth of the grafted buds may be delayed as the size of the wing does not match that of the host control wing.

One study from the early 90s explored the outcome of grafting whole wing buds between avian species by grafting whole chick wing bud grafts into quails (CQ grafts) at HH22 (equivalent to 12 hours quail, and 24 hours chick) (Martin, Ohki-Hamazaki et al., 1991). They find that species-specific growth is maintained when measuring the zeugopod (specifically, the ulna) a month after hatching. However, no data measuring the length of

the whole limb is described in the paper and the survival rate was low in the grafted wings. In my experiments, I find a similarly low rate of survival and integration, as only 20% of embryos with grafted wing buds survived until day 9 and many of these had abnormal or necrotic tissue where the grafts had not integrated properly. Measurements were therefore only taken from grafts with a normally patterned stylopod, zeugopod and autopod.

It is interesting to note that in all of the grafts performed, the grafted wings are shorter than the host control wings. This suggests that the grafted bud may not have integrated properly into the flank of the embryo or required more time for the program of growth to catch up with the host. In both the Twitty and Martin et al studies, measurements were taken after hatching, 1 month into post-natal development. Therefore, it may be useful in my analysis to also have analysed wing size after hatching of the quails and chicks.

The species-specific timing of patterning events is maintained in polarising region grafts at 12 hours, and reset in grafts performed at 0 hours. However, in whole wing bud grafts, the size of the wing is does not follow this pattern at least up until my analysis by day 9 (HH36 quail, HH35 chicks). This may imply that differences in the proximal signalling environment are not able to affect the growth of the wing. It may also suggest that either the grafting procedure is ineffective, or the graft takes a longer time to reach its growth potential than the scope of my experiments allowed. Due to my analysis being limited until day 9 incubation it is difficult to draw conclusions about the long-term growth potential of the grafted wing. It would therefore be useful to analyse the size of the wing across the same developmental time points (i.e. HH36 grafts compared to control HH36 wings) and also analyse wings from grafted buds later in the incubation period shortly before hatching, and then during post-embryonic development. This may allow more time for the graft to develop to the correct growth capacity.

Chapter 6.

Retinoic acid can determine species-specific developmental timing in the avian wing.

6.1 Introduction

In chapter 5 I used tissue grafting techniques to show that the host's proximal signalling environment is capable of resetting the species-specific *Shh* duration and cell cycle rates. Retinoic acid (all trans retinoic acid - RA) is an important signalling molecule in the embryonic development of the limb and has been implicated as the extrinsic signal which proximalises the limb through upregulation of *Meis1/Meis2* (Capdevila, Tsukui et al., 1999, Mercader, Leonardo et al., 1999, Mercader, Leonardo et al., 2000, Saiz-Lopez, Chinnaiya et al., 2015, Yashiro, Zhao et al., 2004). RA is cleared from the distal part of the chick wing after HH19 (shortly after 0 hours) by the action of Cyb26b1, which is induced by Fgfs in the apical ectodermal ridge (Cunningham and Duester, 2015, Yashiro, Zhao et al., 2004). In the current model of proximal-distal patterning, it is hypothesised that this loss of distal RA is involved in initiating the switch from proximal signal-based patterning to the intrinsic timer which patterns the distal part of the wing (Saiz-Lopez, Chinnaiya et al., 2015). The loss of RA in the wing bud coincides with the start of the intrinsic timer. RA therefore provides a candidate extrinsic signal which may be involved in setting the duration of the polarising region in 0 hour grafts (Chapter 5).

In this chapter I explore how RA affects the timing of limb development and growth and if it could be the proximal signal that resets the duration of *Shh* expression in polarising region grafts.

6.2 Results

6.2.1 RA treatment delays progression through Hamburger-Hamilton stages

In order to determine if RA effects the species-specific timing of development I implanted TTNPB soaked-beads into quail and chick wing buds - referred to as RA treatment (TTNPB is a stable isomer of RA and has the same properties (Stephens-Jarnagin, Miller et al., 1985)).

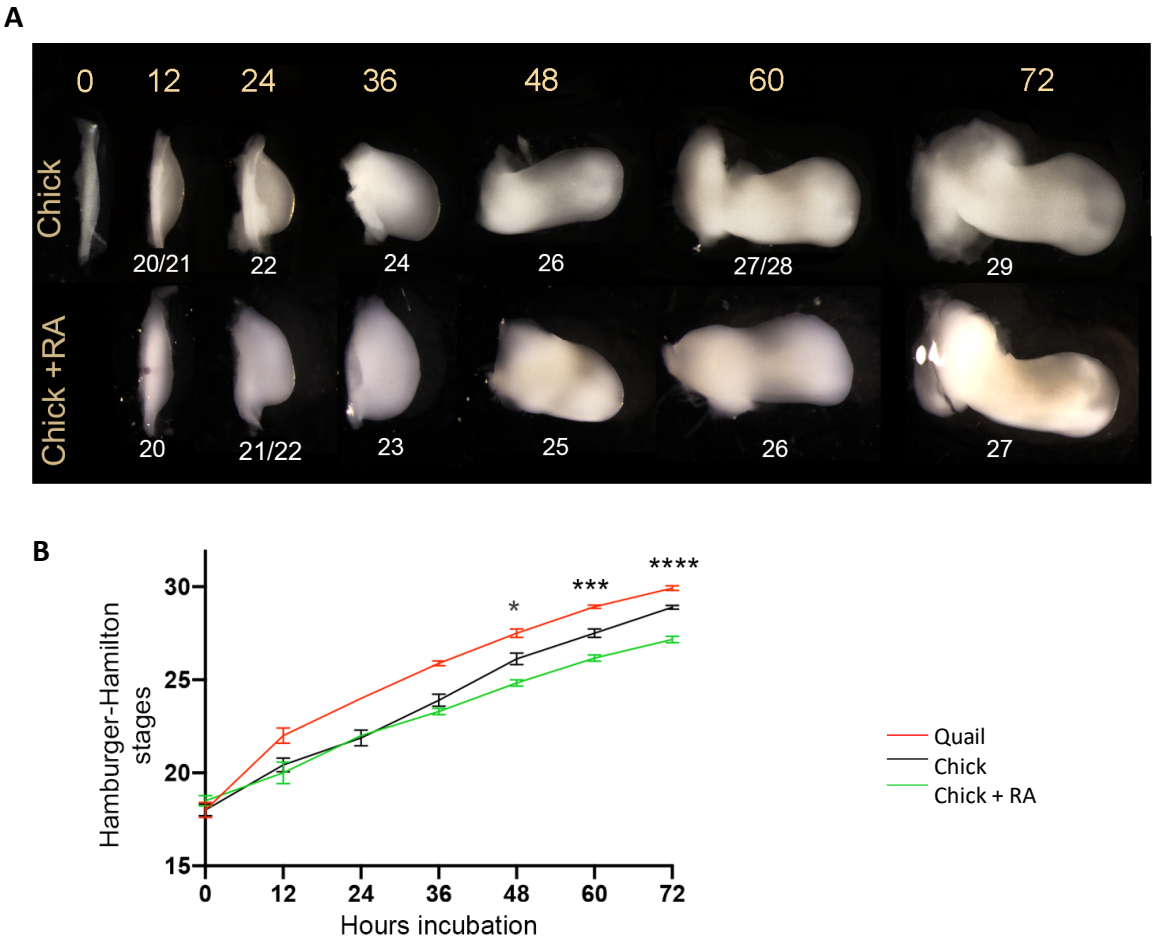

Figure 6.1. RA treated wings progress through Hamburger-Hamilton stages slower than untreated wings

Wing buds were treated with RA shortly after the 0 hour time point and analysed every 12 hours subsequently in comparison to control wings. **A)** Right wing buds from control chicks and RA treated chicks removed and photographed every 12 hours from 0

hours 72 hours. In RA treated wings no 0 hour image is shown as this is equivalent to untreated wings. Scale bars represent 1mm**. B)** Average Hamburger Hamilton stages were plotted against incubation time after 0 hours. Student *t*-tests reveal there is no significant difference is seen between control chicks and RA treated chicks until 48 hours when control chick wing buds are seen to progresses through the Hamburger Hamilton stages at a faster rate than the RA treated chick wing buds. P values: *=<0.05, **=<0.01 ***= <0.001 ****= <0.000 *n*=3.

To understand if RA could influence development timing, I analysed the morphological development of RA soaked bead-treated wing buds in comparison to control chick wings from time 12 to 72 hours (Figure 6.1a). It has been shown that RA disperses from the bead over an approximate 20 hour period (1984), therefore bead implantations extend RA signalling in the wing past the stage it would normally have been depleted. Note that for ease of comparison, data for RA treated quail wing buds can be found in the appendix. My analyses show that between 12 and 24 hours, RA treated chick wing buds are wider and have a slightly flatter appearance at the distal tip. By 72 hours incubation, the RA treated wing appears rounded at the distal tip, similar to what is seen at 60 hours in the control wings. However, control wing buds at 72 hours display a contour at the apical tip – indicating digit 1, in addition to a hooked contour in the distal posterior wing (digit 4 which later regresses). These observations suggest that RA slows the rate of development of the chick wing bud.

To better characterise theses morphological differences, I have staged the wing buds according to the Hamburger-Hamilton staging system (Figure 6.1b – also noted on Figure 6.1a). This analysis reveals that RA treated chick wing buds are delayed in terms of developmental age. For example at 36 hours, RA treated chick wing buds have only progressed to HH23, compared to HH24 in the control chick wing. Furthermore, at 60 hours, the RA treated wing bud is significantly less advanced compared to the control chick wing - HH26 compared to HH27/28, respectively.

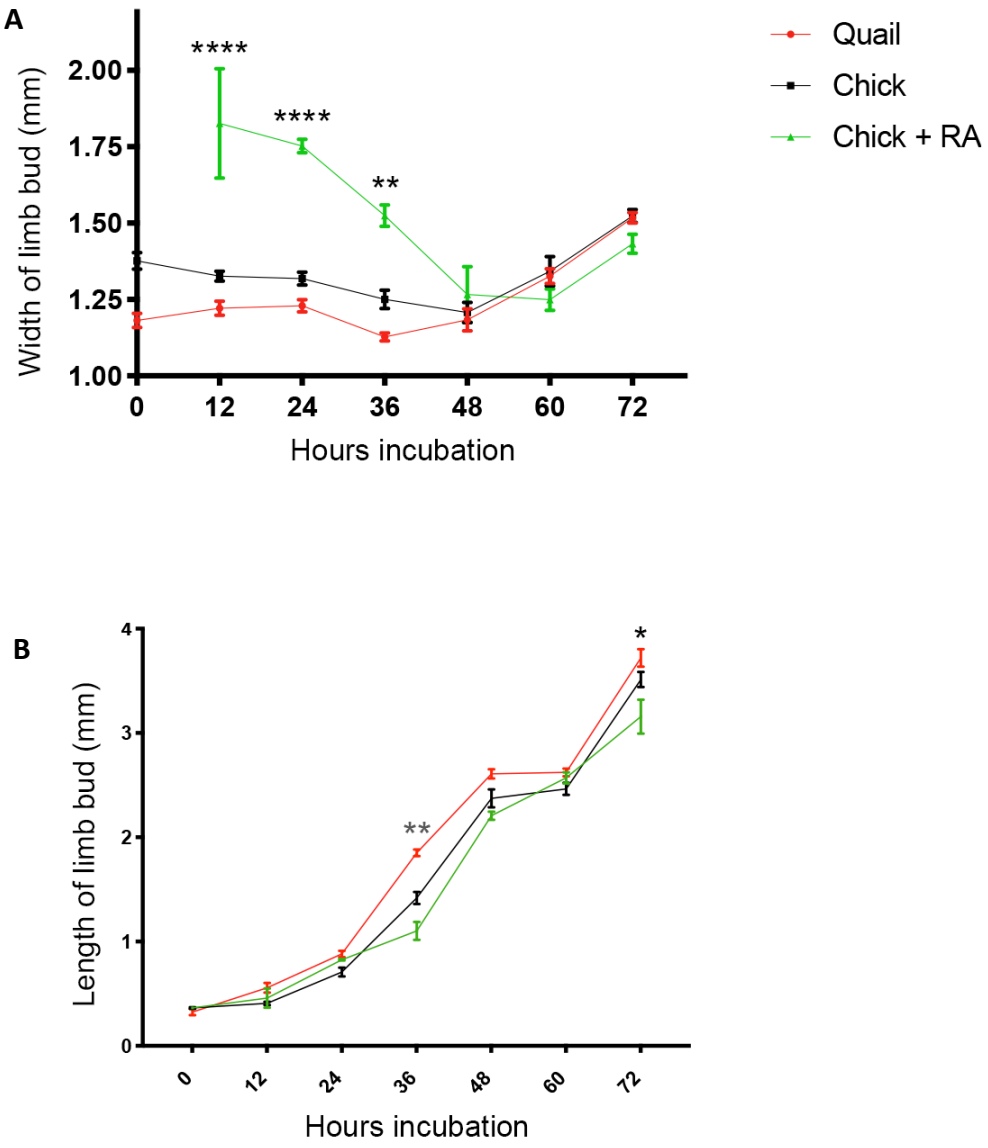

Figure 6.2. RA treated wings are increased in width along the antero-posterior axis, however proximo-distal length is unaffected.

Wing buds were treated shortly after the 0 hour time point and subsequently analysed every 12 hours in comparison to control wings. **A)** RA treated chick limb buds were measured along the anterior-posterior (A-P) axis (width of the limb bud) every 12 hours after the 0 hour time point. Student's *t*-tests reveal a significantly wider wing between 12 and 36 hours, however no significant difference in the width of the wing from 48 hours onwards. **B**) RA treated chick limb buds were measured along the proximo-distal (P-D) axis (body wall to tip of limb bud) every 12 hours after the 0 hour time point. Student *t*-tests show significant differences in limb lengths at 36 and 72 hours between control chicks and RA treated chick wing buds. *P* values: *=<0.05, **=<0.01 ***= <0.001 ****= <0.000 *n*=3.

RA treated chick wings at 12 hours (HH20) are significantly wider than control chick wings (HH20/21) - 1.827mm in RA treated wings compared to 1.327mm in control wings, which gradually decreases until 48 hours. From 48 hours onwards, the width of the antero-posterior axis is not significantly different between control (HH26) and RA treated (HH25) chick wings (Figure 6.2a). Furthermore, there appears to be little difference in the overall outgrowth of the wing (Figure 6.2b), however by 72 hours, the RA treated wing is significantly shorter along the P-D axis than control chick wings. The growth rate remains consistent between RA treated and control chick wings, for example there is a faster rate of rate of growth between 24-48 hours, then slower rate of growth between 48-60 hours, followed by faster rate of growth rate again from 60-72hours, independent of developmental stage.

One prediction is that, because developmental timing is delayed in RA treated chick wings, they could continue to grow at later stages when growth would normally slow down. Thus, at a later time in development, the length of the RA treated chick wings could surpass the length of the control chick wing (similar to the chick wing surpassing the growth if the quail wing at late stages). However, due to UK regulations, my analyses are limited to 2/3 of the incubation period. Analysis of the chick wing size at 144-216 hours (days 9 to 13) reveals no significant difference in the size of control and RA treated wings at these time points (Figure 6.3a). This is also the case when measuring the length of each skeletal elements at day 9. No significant difference is seen, apart from the ulna in RA treated wings which is slightly, but significantly, shorter than the ulna of control chick wings (Figure 6.3b). Taken together, these data show that RA treatment at 0 hours delays the progression of the wing through developmental stages, however it, does not appear to affect the growth of the wing in the time frame I have analysed.

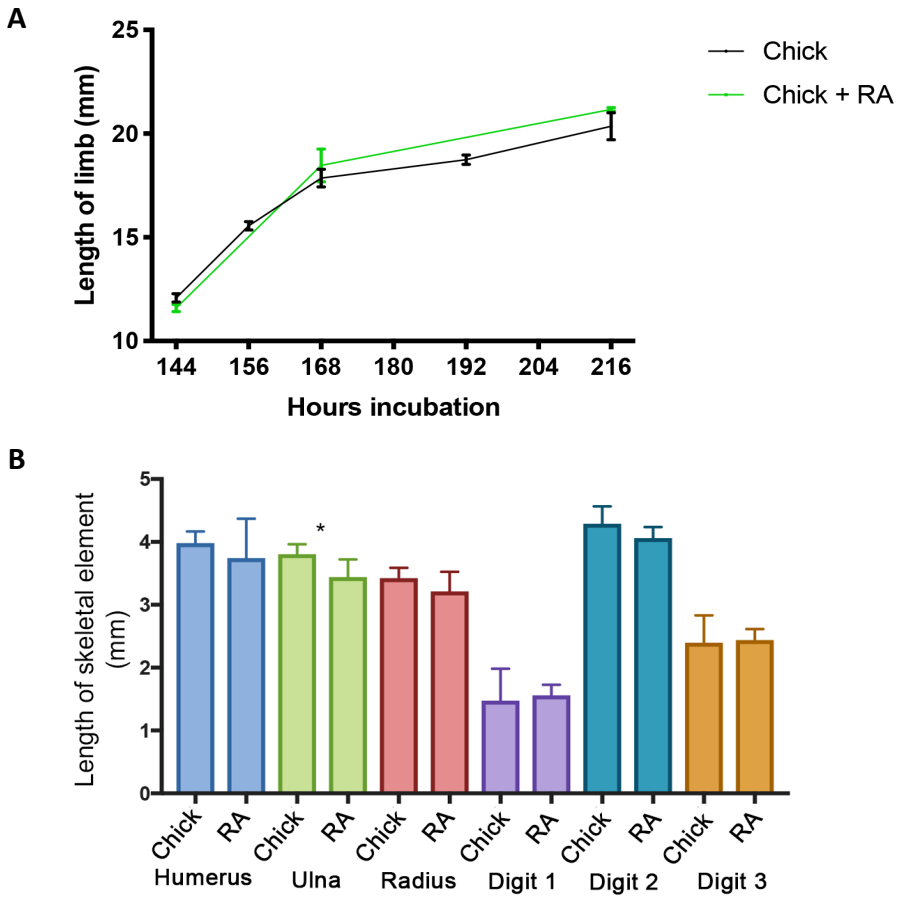

Figure 6.3. From 144 to 216 hours (day 9 to 13) the length of the wing is unchanged between RA treated and untreated chick wings.

Wing buds were treated shortly after the 0 hour time point and left to develop until day 9 incubation. The length of the wing was measured combining the lengths of the humerus, ulna and digit 2. **A)** Student *t*-tests reveal that at days 9-13 there is no significant difference in the overall size of the wing measuring the combined lengths of the humerus, ulna and digit2. **B)** Student t-tests reveal that there is no significant difference in the length of the humerus, radius, digit 1, digit 2 or digit 3 between RA treated and control chick wings at day 9, however the ulna in RA treated wings is significantly shorter than the control wing. *P* values: *=<0.05, **=<0.01 ***= <0.001 ****= <0.0001 *n*=3.

6.2.2 Maintained RA signalling delays the start of the intrinsic timer by delaying developmental progression.

Previous studies have noted that if RA signalling is prolonged in the wing beyond the stage it would normally be removed, then the duration of *Shh* is correspondingly extended (Chinnaiya, Tickle et al., 2014). In addition to this, the upregulation of the distal autopod marker, *Hoxa13* is delayed (Rosello-Diez, Arques et al., 2014) and *Meis1/2* in the wing is extended distally (Mercader, Leonardo et al., 2000). I have shown that RA treated wings are delayed in their progression through HH stages, and in chapter 4 I have shown that gene expression is linked to the HH stage of the wing. Therefore, a possible re-interpretation of this data is that RA delays the developmental stage of the wing, and thus, genes are expressed according to the developmental age of the tissue, rather than gene expression is extended to a later HH stage.

To understand if gene expression is indeed coupled to the developmental age of the RA treated wings, I have analysed the expression of a number of genes involved in patterning the wing. In RA treated wing buds, RA signalling is extended past its normal duration, and is depleted in the distal wing at a later time point. Analyses of *Meis1* expression shows that it extends to distal regions of RA treated wing buds (Figure 6.4a). Due to the high expression of *Meis1* in the wing during this time point, a further increase in expression is difficult to detect using *in situ* hybridisation. However, qPCR data confirms that chick wing buds treated with RA at the 12 hour time point and then analysed 12 hours later, have significantly increased *Meis1* expression in the distal part of the wing bud, as seen by the 4.19 fold increase compared to the control untreated wing of the same age (Figure 6.4aii). Furthermore, *Shh* expression is extended past its normal duration by approximately 12 hours in both quail and chick RA treated wing buds (Figure 6.4b). Thus, RA treated quail wing buds downregulate *Shh* by 60 hours; and RA treated chick wing buds downregulate *Shh* by 72 hours. However, *Shh* is still downregulated at the HH27/28 stage in RA treated wings, therefore revealing that the extended expression is due to developmental timing being slowed down by approximately 12 hours.

Sox9 expression in condensing cartilage cells is also delayed in RA treated chick wings (Figure 6.4c). In control wings, expression of *Sox9* can be seen in proximal elements, the ulna and radius and also the autopod, however, expression is limited to only the proximal elements and the ulna in RA treated wings. This pattern is comparable to *Sox9* expression seen at a 12 hour earlier developmental stage in the wing and also confirms that RA delays developmental progression. In addition, the onset of *Hoxa13* expression occurs in control wings at HH22 (Vargesson, Kostakopoulou et al., 2001), which is delayed for approximately 12 hours in quail and chick wings treated with RA. This is likely due to RA treatment delaying developmental progression by 12 hours, and thus the longer time taken to reach HH22 (Figure 6.4d).

Furthermore, in Chapter 3 I have shown that the cell cycle rate decreases as development time progresses in the polarising region. I have therefore analysed the effect that prolonged RA signalling has on cell cycle rates of quail and chick wings buds by applying RA beads shortly before the 12 hour time point and analysing cell cycle rates 24 hours later, in comparison to the contralateral control wing. Polarising regions in RA treated quail wing buds show on average a lower percentage of cells in G1-phase compared to control quail wings (60% of cells compared to 64.2%), however, this is not statistically significant. On the other hand, polarising regions in RA treated chick wing buds have a significantly lower percentage of cells in G1-phase compared to control wings of the same developmental age (62.66% of cells compared to 71%). A lower percentage of cells in G1-phase Is indicative of a faster cell cycle rate in RA treated wings, thus suggesting that cells in RA treated wings are at an earlier stage of development (Figure 6.5).

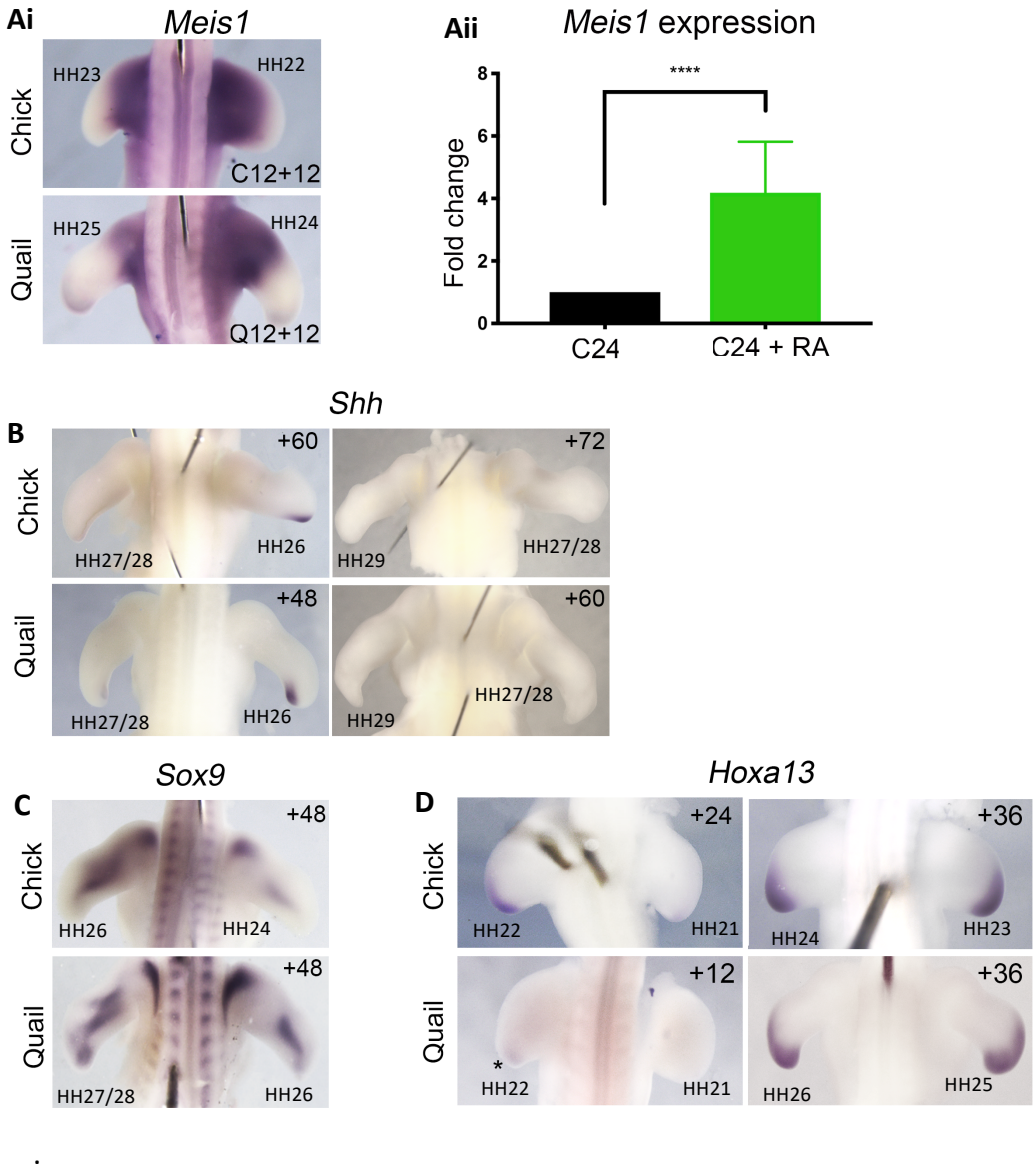

.

Figure 6.4. In RA treated wings the proximal program is extended, and the distal program is delayed.

Whole mount *in situ* hybridisation images showing RA treated (right wing) vs control (left wing) expression in quail and chicks. **A)** Analysis of the proximal patterning. TTNPB beads were placed at the 12 hour time point and *Meis1* was analysed 12 hours later, **i)** Meis1 is extended distally in RA treated wings. **ii)** qPCR analysis of *Meis1* expression in RA treated chick wings (C24 + RA) and control chick wings of the same age (C24). Data was normalised by the amount of *18S* mRNA. Means were collected from triplicate data (*n*=3) **B-D** Analysis of distal patterning. TTNPBB beads were placed at 0 hours and gene expression analysed at subsequent time points. **B)** *Shh* expression at 60 hours in the chick and 48 hours in the quail shows RA treated wings expressed *Shh* past the normal duration, *Shh* is downregulated by 72 hours in the chick and 60 hours in the quail. **C)** *Sox9* expression 48 hours after bead placement. *Sox9* staining can be seen in the shoulder and ulna in RA treated quail and chick

wings, in left control wings staining can be been in the autopod, ulna and radius. **D)** *Hoxa13* expression at 24 hours in the chick and 12 hours in the quail shows RA treated wings have delayed *Hoxa13* expression, *Hoxa13* is then visible by 36 hours in the chick and quail wings. HH stages are also noted for each wing. *n*= 3

Taken together, these results suggest that prolonged RA signalling in the wing delays progression through developmental stages with associated changes in gene expression, cell cycle rates and morphology. My interpretation of the RA treated wing data is that delayed HH stage progression, extended *Meis1* expression and delayed *Hoxa13* expression reveal that the switch from the extrinsic programme, to the intrinsic distal programme is delayed in RA treated wings (depicted in Figure 6.6). However, this is still relative to a fixed growth rate.

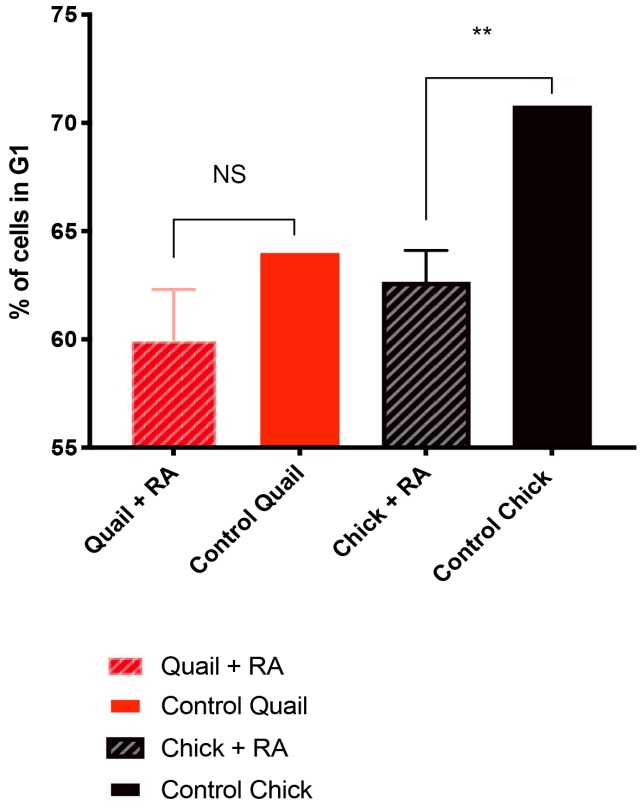

Figure 6.5. RA treated wing buds maintain a faster rate of proliferation in the polarising region.

Quail and chick wing buds were treated shortly before the 12 hour time point and the cell cycle rate in the polarising region was analysed 24 hours later. Student's *t*-tests reveal no significant difference in the cell cycle rate of quail polarising regions treated with

RA in comparison to the chick, however a significantly lower percentage of cells in G1 in the chick polarising regions in RA treated wings. P values: *=<0.05, **=<0.01 ***= <0.001 ****= <0.0001 *n*=3.

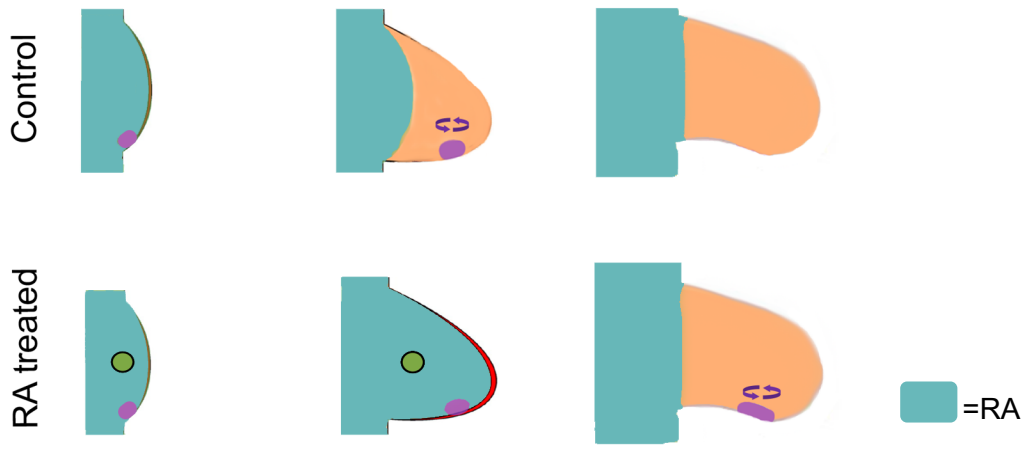

Figure 6.6. Schematic depicting 'control' vs 'RA treated' wings.
In the early wing bud (approximately 0 hours) RA signalling is present throughout the whole limb bud, then as the wing grows outwards RA is lost from the distal part of the wing. At this point there is a switch from extrinsic patterning to an intrinsic timing based patterning programme. The control wing bud was left to develop as normal (left wing). The 'RA treated' wing buds (right wing) were implanted with a bead soaked in 0.05mg/ml TTNPB shortly after the 0 hour time point to extend RA signalling in the wing past its normal duration and thus delay the start of the intrinsic timer indicated by the polarising region (purple).

6.2.3 RA treatment adapts chick developmental time to turkey developmental time.

My data above shows that RA treatment delays the developmental timing of the chick wing by 12 hours, but does not affect its growth along the P-D axis. Since developmental timing is accelerated by 12 hours in the smaller species - the quail, compared to the chick wing, I went on to determine whether RA treated chick wings replicate timing found in a species with larger wings. The length of the adult chick wing is approximately twice the length of a quail wing (31 cm vs. 17.5 cm), however the adult

turkey wing is approximately twice the length of a chick wing (65 cm vs. 31 cm). In addition, the incubation period in the quail is 14 days compared to 21 days in the chick, the turkey incubation period also is a week longer than the chick at 28 days. Therefore, my hypothesis was that RA treated chick wings may replicate the developmental timing of the larger turkey (Figure 6.7).

In contrast to the quail and chick, where HH18/19 occurs at day 3, the equivalent stage of limb development in the turkey occurs 24 hours later (day 4) and therefore has a different '0 hour' time point (See materials and methods – Chapter 2).

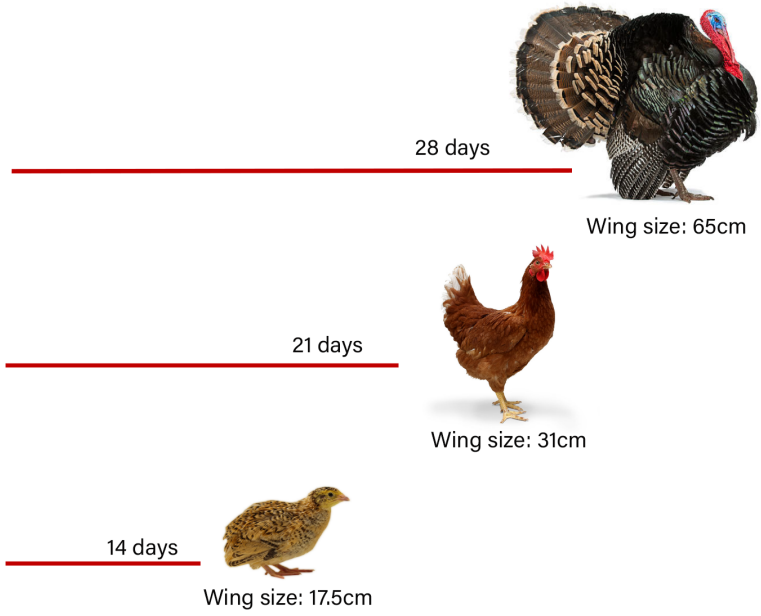

Figure 6.7. Development of the turkey wing provides a good comparison to quail and chick wings.

Schematic depicting the incubation period until hatching in the quail (14 days), chick (21 days) and turkey (28 days), in addition to the average length of an adult wing for the quail chick and turkey; 17.5cm, 31cm, and 65cm, respectively. Pictures are not to scale.

To understand how developmental progression of RA treated chick wings compares with that of turkey wings, I have analysed the progression through Hamburger Hamilton stages. These morphological stages can be viewed in Table 6.1 and in Figures 6.8a, b. At 0 hours, equivalent stage HH18/19, there is no significant difference in the stage of the limb in all three species – quail, chick and turkey. After this point, the quail wing appears to progress through the Hamburger-Hamilton stages faster than the wings buds of the two larger species, and the turkey progresses at the slowest rate. However, for ease of comparison, I will continue to focus on comparing the turkey, chick and RA treated chick wings.

Hours incubation	Quail	Chick	Turkey	Chick + RA
0	HH18/19	HH18/19	HH18/19	HH18/19
12	HH22	HH20/21	HH20	HH20
24	HH24	HH22	HH21	HH21/22
36	HH26	HH24	HH23	HH23
48	HH27/28	HH26	HH25	HH25
60	HH29	HH27/28	HH26	HH26
72	HH30	HH29	HH27	HH27
84	HH32	HH30	HH28	
96	HH34	HH31	HH28/29	
108	HH34/35	HH32/33	HH29	
120	HH35	HH33/34	HH30	
132	HH35/36	HH34/35	HH30/31	
144	HH36	HH35/36	HH31	
156		HH36	HH31/32	

Table 6.1. Turkey wing development is slower compared to the quail and chick.
Using the Hamburger-Hamilton staging system the embryonic stages are noted from day 3 egg incubation in the quail and chick and from the equivalent time point at day 4 in

the turkey, then every 12 hours subsequently. The turkey progresses through the HH stages at a slower rate compared to the chick and quail, but at a similar rate to chick + RA.

The turkey wing follows a similar temporal progression through the Hamburger Hamilton stages as RA treated chick wings, with no significant difference between stages during the 0-72 hour time points (RA treated wings referred to as Chick + RA in figures). For example, at 12 hours incubation both reach HH20 (in comparison to HH20/21 in the chick), and at 36 hours both turkey and RA treated chick wings are at HH23, compared to the chick which is at HH24. (Table 6.1; Figure 6.8b – also noted in 8a). By 48 hours, incubation the turkey and RA treated chicks are at a significantly less advanced developmental stage than the control chick. At 60 hours the chick reaches HH27/28 and both the turkey and RA treated chick wings at HH26 (Table 6.1 and Figure 6.8a,8b).

I have measured the outgrowth of the wing bud from 0 to 72 hours, and then at the 216 hour time point (due to constraints in embryo numbers I have only measured up until this point). The data shows that from the equivalent stage HH18/19 (0 hours) to 72 hours there is no significant difference between the size of the turkey wing compared to the control chick wing and RA treated chick wing. The growth rate of the turkey wing appears to show a similar pattern compared to the chick, and again (as with chick and quails), the growth rate appears uncoupled from developmental age. A large amount of growth can be seen between 24 and 48 hours, despite differences in developmental ages (HH22 to HH26 in the chick, and HH21 to HH25 in the turkey and RA treated chicks), then a slower growth period between 48 and 60 hours (HH26 to HH27/28 – chick, compared to HH25 to HH26 – turkey and RA treated chicks). Although at 72 hours the turkey wing is significantly smaller (3.11mm) than the chick wing (3.49mm), this relates to a different developmental age HH29 – chick and HH27 – turkey (Figure 6.9a). However, the turkey wing at HH27 is significantly larger than the chick at HH27/28 (Figure 6.9a).

By 216 hours, the chick and RA treated chick wings are at a similar developmental age of HH39, determined by the observation that no discernible difference could be seen between control and RA treated chick wings. This suggests that RA treated wings may have caught up to control wings, although further work is needed to determine an accurate

staging of HH39 wings. In comparison, at 216 hours the turkey is at HH34/35. The length of the P-D axis at 216 hours reveals there is no significant difference between chick wings and RA treated chick wings (20.35mm vs 21.17mm), however the turkey wing is significantly smaller (13.40mm - Figure 6.9b). The chick wing surpasses the growth of the quail wing after 132 hours (Chapter 3), therefore it is likely that the turkey will exceed the growth of the chick wing. However, my data shows that at the final time point measured, 216 hours, the turkey wing has not yet surpassed the growth of wing in the smaller species, the chick.

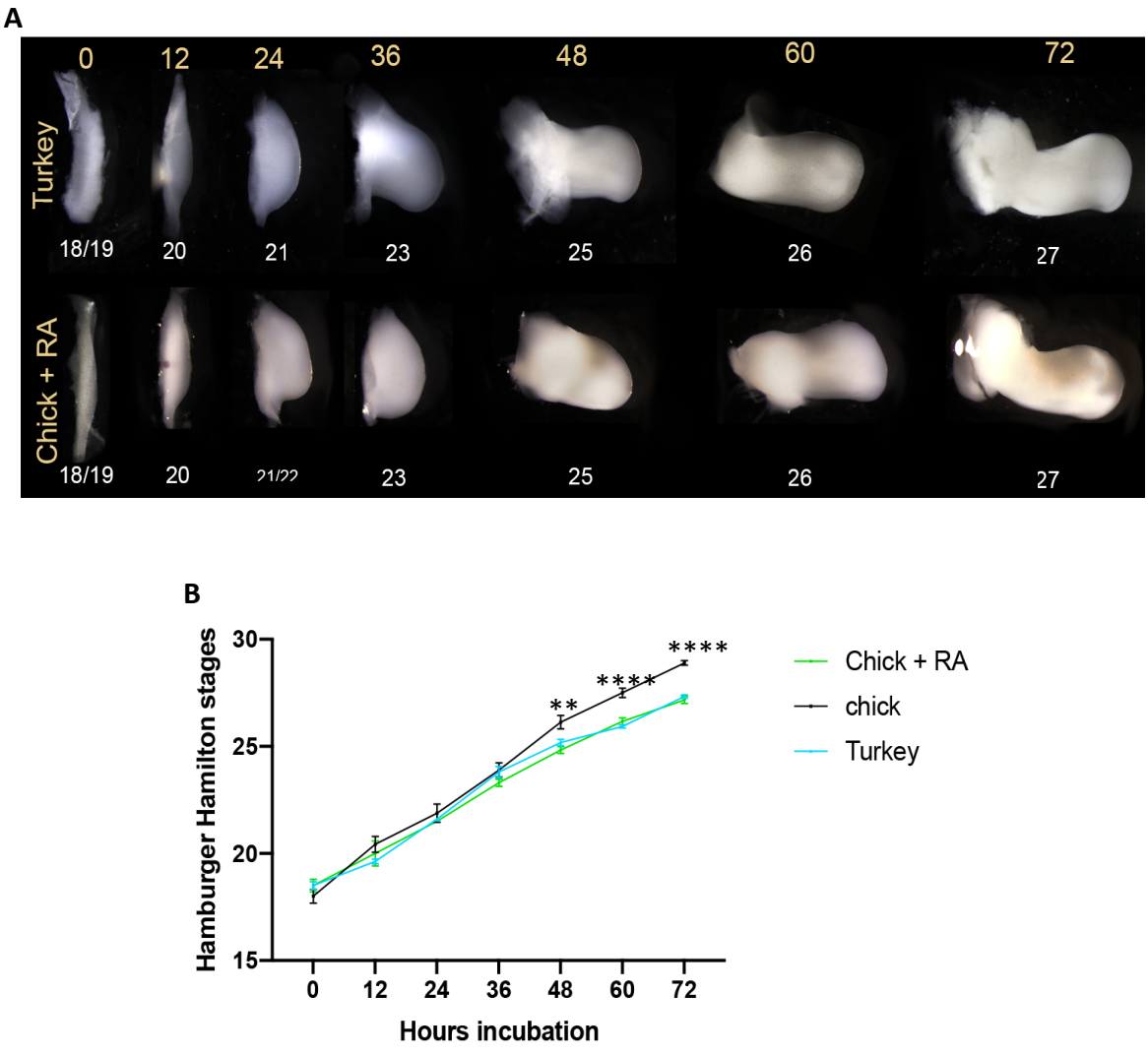

Figure 6.8. The turkey wing progresses through Hamburger Hamilton stages slower compared to the chick and at a similar rate as chick + RA.

A) Embryos were incubated for equivalent times. RA treatment (chick + RA) was performed at the 0 hour time point. Right wing buds from turkeys, chick + RA and untreated control chicks were then removed and photographed every 12 hours of wing development from 0 hours to 72 hours. Hamburger Hamilton stages are also recorded below each wing bud. Scale bars represent 1mm. **B)** Hamburger Hamilton stages were plotted against incubation time 0 hours. My observations show that at 0 hours there is no significant difference between Hamburger Hamilton stage in the chick, chick + RA and turkey. (Student's *t*-test *P* values: *=<0.05, **=<0.01 ***= <0.001 ****= <0.0001) *n*=3.

To determine if gene expression is also linked to progression through HH stages in the turkey, I have analysed the expression of *Shh. Shh* expression in the polarising region is a particularly good molecular marker to assess, as its location and expression dynamics are well-defined. Expression can be seen from HH18/19 (0 hours) until it is downregulated by HH27/28, in the quail this occurs by 48 hours, compared to 60 hours in the chick. My analysis of *Shh* in the turkey wing reveals that expression can be seen at 0 hours (HH18/19). However, *Shh* is expressed in the polarising region for a longer period of time – up to 72 hours, although this sill relates to the developmental age of HH27 in the wing (Figure 6.10). Interestingly, *Shh* is also expressed until 72 hours incubation in RA treated wings (Figure 6.2b). However, both RA treated chick wings and turkey wings are at HH27 at 72 hours. Therefore, these observations reveal that RA treated chick wings have the same developmental timing as turkey wings.

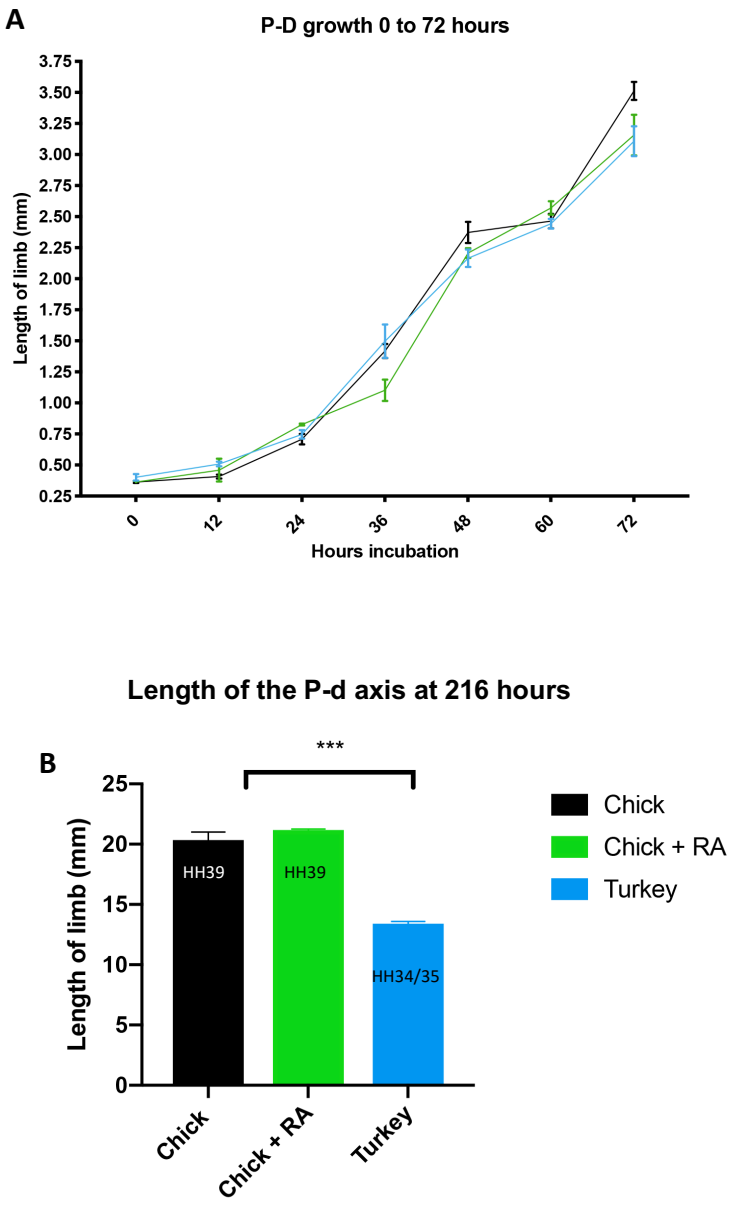

Figure 6.9. PD outgrowth of the wing is equivalent in RA treated chick wings and turkey wings.

A) Turkey, chick and chick + RA limb buds were measured along the proximo-distal (P-D) axis (body wall to tip of limb bud) every 12 hours after the 0 hour time point until 72 hours. Student's t-tests reveal that there is no significant difference in the outgrowth of the RA treated chick wing compared with turkey wings. **B)** At 216 hours, turkey, chick and chick + RA limb buds were measured along the proximo-distal (P-D) axis by combining the lengths of thee humerus, ulna and digit 2. Student's *t*-tests show that turkey wings are significantly shorter that chick and chick+ RA wings. *n*=3-5 *p* values: *=<0.05, **=<0.01 ***= <0.001 ****= <0.000

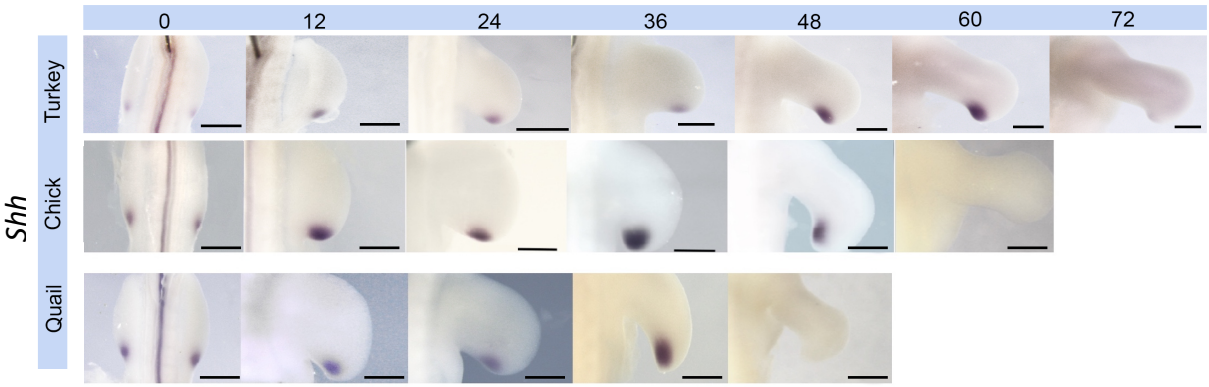

Figure 6.10. The polarising region is active for a longer duration in the turkey compared to the chick and quail

Whole mount *in situ* hybridisation was performed in turkey, quail and chick embryos incubated for an equivalent amount of time after limb initiation. Expression of *Shh* in the polarising region is seen for approximately 72 hours in the turkey, 60 hours in the chick and 48 hours in the quail. *n*=3-6. Scale bars = 500µm.

6.2.4 Retinoic acid is involved in setting species-specific timing in the wing bud

In chapter 5, I have shown that polarising region grafts into the proximal environment at 0 hours – HH18/19 resets the duration of *Shh* and cell cycle rates in the donor polarising region to that of the host. However, in 12+ hour grafts (HH21+) the duration of *Shh* expression and cell cycle rates are maintained. In this chapter, I have identified RA as a proximal extrinsic signal which when maintained in the wing, is capable of altering developmental timing and associated gene expression and cell cycle rates. In order to investigate further if RA is the proximal signal at the 0 hour time point which resets the species-specific duration of *Shh*, I have maintained RA levels in the wing of 12+ hour grafts to see if species-specific timing can be reset. To do this, I implanted a bead soaked in RA at the 0 hour time point and performed grafts between quail and chick wings at the 12+ hour

time point (Figure 6.11a). As a reminder, in 12+ hour grafts developmental timing and *Shh* duration is maintained in grafted tissue, therefore *Shh* is downregulated by 48 hours in the quail grafted polarising region (Figure 6.11b). However, when the 12+ hour grafts are performed after RA signalling has been maintained in the wing, the results show that *Shh* duration is no longer downregulated by the 48 hour time point in the grafted quail polarising region. Instead, increased RA signalling is sufficient to adapt the developmental age of the quail graft tissue and 'reset' it to the developmental age of the control chick (HH26/27 - as seen in the left wing bud – Figure 6.11c). The duration seen in the chick host right wing has also been affected by RA treatment, as seen by the stronger expression of *Shh* in the right wing bud (approximately HH25) compared to the left untreated wing bud (HH26/27 - Figure 6.11c). Therefore, RA treatment has influenced the duration of *Shh* in both host and donor polarising regions. This indicates that RA signalling in the early proximal environment is able to set species-specific timing of patterning events.

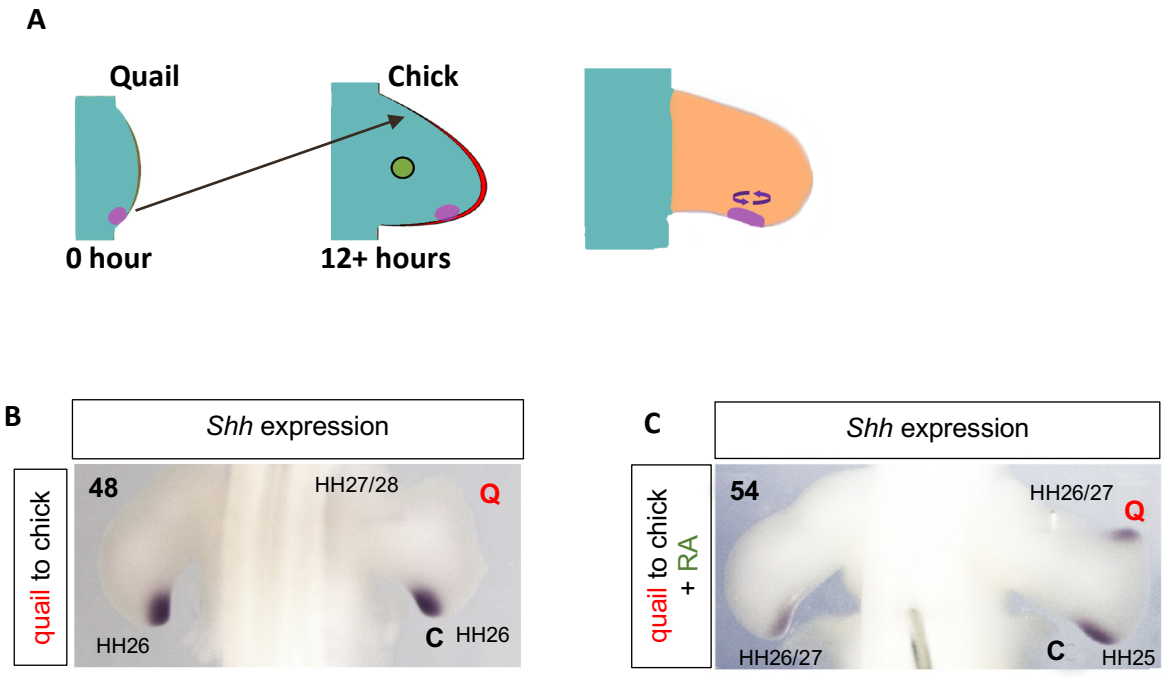

Figure 6.11. Species-specific timing is reset in RA treated 12 hour grafts

A) An RA soaked bead was implanted in the wing bud shortly after the 0 hour time point to extend RA signalling past the normal duration. QC grafts were then performed at the 12 hour time point. **B)** QC grafts were performed at the 12 hour time point and the

expression of *Shh* analysed, at 48 hours the quail grafted polarising region has downregulated *Shh*, but *Shh* expression can still be seen in the endogenous chick polarising region **C)** After bead implantation at 0 hours, QC grafts were performed at the 12 hour time point and the subsequent expression of *Shh* analysed at approximately 54 hours. At this point the quail grafted polarising region now has strong expression of *Shh*, similar to the normal control expression in the left host chick wing. *Shh* expression is also expressed more strongly in the RA treated (right) chick polarising region. *n*=4

I have shown that maintaining RA signalling delays the start of the intrinsic timer and slows the progression through developmental stages in the chick wing. These data suggest that developmental progression in RA-treated chick wings results in patterning being timed in a similar way to the larger species, the turkey. Therefore, one explanation could be that larger species maintain extrinsic signalling by RA for longer and thus delays the initiation of the intrinsic distal program. To determine if RA is lost at a later time point in the wing buds of larger species, I have begun to analyse RA degradation in quail and chick wings.

RA is cleared from the distal part of the chick wing by the action of Cyb26b1, which is induced by Fgfs in the apical ectodermal ridge (Cunningham and Duester, 2015, Yashiro, Zhao et al., 2004). I have performed preliminary experiments analysing the expression of the RA degrading enzyme, *Cyp26b1*, in wing buds of quails and chicks (Figure 6.12). A comparative time course of *Cyp26b1* expression in whole wing buds between 0 and 24 hours shows that it is upregulated earlier in the quail compared to the larger chick. In the quail wing bud, *Cyp26b1* has a 7-fold increase between 0 and 6 hours, but there is no substantial change in *Cyp26b1* expression in the chick between these time points. However, between 6 and 12 hours, an 11-fold increase in *Cyp26b1* expression is seen in the chick wing bud. By 24 hours, *Cyp26b1* is increased by 32.7-fold in the quail wing bud, compared to a 12.6-fold increase in the chick (Figure 6.12). This data only has an *n* of 1, and therefore conclusions cannot be drawn at this stage. However, it indicates that *cyp26b1* is upregulated earlier in the quail wing, and thus RA is degraded earlier in the distal wing of the quail wings compared to chick wings.

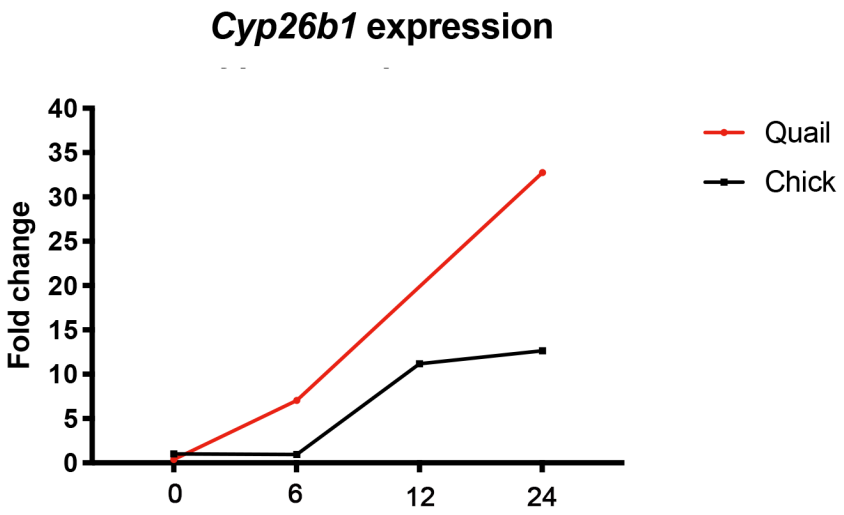

Figure 6.12. Analysis of Cyp26b1 expression suggests RA is degraded earlier in the quail wing compared to the chick wing.

qPCR analysis of *Cyp26b1* expression in quail and chick whole wing buds from 0 to 24 hours. Data for each time point was normalised by the amount of *18S* mRNA. Time 0 in the chick wing (no expression of *Cyp26b1*) was used as a standard, with fold increases from this time point. Data was collected from triplicate for each time point. 10 pooled whole wing buds were used for each point. *n*=1

6.3 Discussion

6.3.1 RA signalling duration can influence species developmental timing in the wing

My analyses of gene expression and morphological features demonstrates that RA treatment of the chick wing at 0 hours retards the progression through Hamburger-Hamilton stages. Since RA treated chick wings take longer to reach HH20/21 than untreated wings, this suggests that the proximal programme is extended and the switch to the intrinsic distal programme is delayed. Furthermore, the delay in *Hoxa13* expression in RA treated

wings corresponds with the release of RA from the bead implanted in the wing, which has been shown to disperse from the bead over approximately 20 hours (1984), suggesting that after RA signalling is removed from the wing the distal program is able to initiate. This therefore implies that loss of RA is required in the wing to allow the distal intrinsic timer to start. However, it is interesting to note that addition of multiple beads sequentially could not inhibit *Hoxa13* indefinitely, suggesting that the intrinsic programme timing *Hoxa13* expression is eventually able to over-ride the extrinsic signals (See appendix). Rosello-Diaz et al, also found that *Hoxa13* expression is inhibited by RA signalling, however, they also demonstrate that *Hoxa13* cannot be precociously activated by inhibition of RA, further suggesting that an intrinsic timing mechanism is a necessary factor in *Hoxa13* expression (Rosello-Diez, Arques et al., 2014).

My analyses revealed that RA treated chick wings emulate developmental timing of turkey wings. Previously it has been shown that turkey development in the first few days after oviposition is significantly slower than that of the chick (Gupta and Bakst, 1993, Sellier, 2006). My data is consistent with these findings as turkey wing buds develop 24 hours after quail and chick wing buds. However, development of the turkey wing, in terms of progression through HH stages, is delayed compared to the chick, but is not significantly different from RA treated wings between 0 and 72 hours. This result shows that although RA treatment extends *Shh* expression for 12 incubation hours, this corresponds to the same developmental time. For example, in the polarising region, *Shh* is downregulated at HH27/28. I have shown that RA treatment slows developmental time, and therefore in RA treated wings *Shh* is not extended past HH27/28, rather the wing takes 12 hours longer to reach HH27/28 - in control chick wings, it takes approximately 60 hours to reach HH27/28. However, RA treated chick wings do not reach HH27 until 72 hours incubation. This also corresponds with when the turkey wing downregulates *Shh*, providing further evidence to suggest that RA treatment delays developmental time in the chick wing bud.

These results implicate RA as a proximal signal capable of influencing developmental timing. I then returned to interspecies polarising region grafts and demonstrated that RA

treatment is sufficient to reset *Shh* duration at a time-point at which cells would normally be measuring their own intrinsic developmental time. Therefore, this suggests that RA can set the species-specific distal timing in the wing by delaying the switch to the intrinsic distal timer.

6.3.2 Patterning of the wing is uncoupled from growth rates between different species.

While RA induces faster proliferation rates in the wing between 0 and 72 hours, there is little difference in the P-D outgrowth of the chick wing. However, between 12-36 hours the RA treated chick wing grows wider along the antero-posterior axis. This is consistent with the idea that changes in proliferation preferentially affect AP growth during early wing bud development (Towers, Mahood et al., 2008).

There appears to be only a negligible difference in the outgrowth of the control and RA treated chick wing between 0 and 72 hours. Thus, although RA treatment affects developmental timing and associated and gene expression, it does not influence the outgrowth of the wing during the time points I have analysed. An alternative explanation is that because the developmental age of the RA treated wing resembles that of the turkey, then at later points the RA treated wing may emulate turkey growth and overtake the size of the control chick wing. However, until the last time point measured at 216 hours (i.e. day 13), there is no significant difference between the size of the RA treated wing and control chick wing. Furthermore, at 216 hours, while the turkey wing is larger than the chick at the equivalent stage of HH34/35 - 13.4mm compared to 12.1mm, it has not yet surpassed the growth of the chick in terms of incubation hours. My experiments are restricted to regulations stating that embryos can only be kept up until 2/3 of their incubation period. Therefore, I am unable to continue my comparisons after day 13 in the chick. It would, however, be interesting in future to analyse the growth of the wing at later time points and after hatching. Furthermore, analysis of the size of the turkey wing until 21 days incubation

would be useful, but due to the limited number of turkey embryos available this was not possible in the time frame of the study.

In summary, in this chapter I have shown that loss of RA in the distal part of the wing triggers the switch from extrinsic signal-based proximal patterning, to an intrinsic timing mechanism which patterns the distal wing. I have also shown evidence that RA signalling in the proximal environment sets the specific-specific duration of developmental events, and prolonging RA signalling delays the progression of wings through developmental stages. Thus, chick wings treated with RA develop according to the developmental time of a larger species – the turkey. However, RA does not affect growth rates between species.

Chapter 7.

Discussion

7.1 Conclusions

- Development of the quail wing is accelerated compared to the chick wing during the 0 – 12 hour time point.

- Hamburger-Hamilton developmental stages are linked to the timing of gene expression, proliferation and apoptosis, but are uncoupled from growth rates between species.

- The switch from extrinsic signal-based proximal specification to intrinsically-timed distal patterning occurs at approximately HH20/21, but at an earlier incubation time in the quail compared to the chick.

- The proximal signalling environment (before HH18/19) can reset species-specific timing in polarising region grafts.

- Once distal cells are measuring intrinsic time (after HH20/21) species-specific timing is maintained in polarising region grafts.

- RA signalling delays the switch from extrinsic signal based proximal specification to intrinsically-timed distal patterning in the wing.

- Prolonged RA signalling slows developmental timing but does not affect wing outgrowth.

- RA signalling is implicated in setting species-specific timing in the avian wing.

7.2 Timing limb development in different sized avian wings

The Hamburger-Hamilton staging system (HH stages) describes the morphological stages the embryo progresses through during development, and is characterised by distinct features and morphological landmarks, which are present at each stage. It is therefore a useful system to compare development, and previous studies have shown that it is applicable to a range of avian species (Ainsworth, Stanley et al., 2010, Li, Bai et al., 2019, Sellier, 2006). In my research, I have shown that the timing of several events during the embryonic development of the wing, including proliferation, apoptosis and the expression of genes involved in the specification and patterning of the limb segments, are linked to the developmental (Hamburger-Hamilton -HH) stage in quail, chick and turkey wings.

Interestingly, during the patterning phase (H18/19 - HH29), wing development is accelerated in the smaller quail by approximately 12 hours compared to the larger chick. This acceleration occurs between 0 and 12 hours incubation, when the quail wing develops from HH18/19 to HH22, compared to the chick wing, which only develops from HH18/19 to HH20/21. This acceleration is associated with maintained proliferation rates, faster outgrowth and more advanced gene expression (e.g. earlier downregulation of *Meis1).* In addition, chick wing development is accelerated compared to the larger turkey wing, which only develops from HH18/19 to HH20 during the 0-12 hour time point.

I have therefore shown that smaller avian species display accelerated development during the 0-12 hour time point compared to larger species. This conflicts with previously published data which suggested that patterning and development of the embryo is equivalent between avian species until HH28, after which point, HH stage progression is accelerated in smaller species (Ainsworth, Stanley et al., 2010, Li, Bai et al., 2019). However, these studies were based on examining the broad morphology of the embryo. In comparison, my research is focused on wing development and I have integrated morphological observations with measurements of the principle developmental axes of the wing, apoptosis, proliferation and analysis of gene expression dynamics.

After the 0-12 hour time point, development progresses at a constant rate, but is now approximately 12 hours advanced in the quail compared to the chick. It is worth noting that accelerated events may not always follow this 12 hour pattern. For example, the down-regulation of *Meis1* expression in the distal part of the quail wing bud appears to occur only 6 hours prior to its downregulation in the chick wing bud. However, although *Meis1* downregulation is difficult to quantify at early stages, it subsequently resolves in to a clear 12 hour difference in timing between chick and quail wings. Furthermore, after the 0- 12 hour time point, comparative growth rates between the species are independent of developmental stage and instead are linked to the hours of incubation.

7.2.1 The proximal RA signal delays intrinsic distal developmental timing

In the quail wing, the earlier progression to HH20/21 and the loss of *Meis1* expression indicates that the switch from extrinsic signal-based specification of proximal elements (indicated by *Meis1*), to an intrinsic timer patterning distal elements (indicated by *Hoxa13*) is accelerated in the quail and takes place at approximately 6 hours (HH20/21), compared to approximately 12 hours in the chick (HH20/21). Additionally, analysis of the turkey wing revealed that it reaches HH20/21 at approximately 18 hours incubation, suggesting a possible time point for the switch to occur in turkeys. Work is currently ongoing to confirm the timing of proximal and distal specification (*Meis1* and *Hoxa13*, respectively). However, due to the seasonal nature of attaining turkey eggs, this was not possible in the timeframe of my PhD thesis.

The switch from extrinsic to intrinsic based patterning is an important element of the current model of P-D patterning of the wing (Saiz-Lopez, Chinnaiya et al., 2015). My research has therefore built on this study by revealing the approximate time that this switch occurs in the quail, chick and turkey wings. However, it would also be useful to compare upregulation of *Hoxa11* or *Shox* expression in quail, chick and turkey wings, as the expression of these genes mark prospective zeugopod cells, which are specified before the autopod (*Hoxa13 expression*). Thus, the timing of their expression could add further evidence for when the distal timer begins in the wings of both species. Upregulation of gene

expression (e.g. *Hoxa11*) is also easier to determine than the downregulation (e.g. of *Meis1)* and therefore may provide a more precise readout of when the distal timer is initiated.

Having shown that the switch from extrinsic signal-based proximal patterning to intrinsic timer-based distal patterning is accelerated in the quail wing, I went on to determine what causes this switch. Using interspecies polarising region transplants I have shown that grafting into the proximal environment, before the intrinsic distal timer has started (HH18/19 – 0 hours) can reset developmental timing - *Shh* duration and cell cycle rates. I have also shown that polarising grafts performed after the intrinsic distal timer has started (12+ hour grafts - HH21+), instead result in the temporal pattern of *Shh* expression, and cell cycle rates being maintained. Timing of *Shh* and cell cycle rates are not reset in these grafts because polarising region cells are now behaving autonomously, and thus, progression through developmental stages is maintained.

In normal wing development, RA is present in the wing at HH19 and then lost shortly after this point. I have implicated RA as a proximal signal in the wing bud that may be involved in resetting developmental events. Transiently maintaining RA signalling slows down developmental timing in the wing. This is indicated by delayed HH stage progression, the maintenance of a faster proliferation rate, increased *Meis1* expression, and delayed expression of markers of distal development (e.g. *Sox9*, *Hoxa13*) in RA treated wings. While previous studies have noted some of these effects when RA signalling is prolonged in the wing, it was thought that gene expression is extended until a later developmental stage, for example *Shh* expression until HH29 (Chinnaiya, Tickle et al., 2014, Hu, Li et al., 2017, Mercader, Leonardo et al., 2000, Rosello-Diez, Arques et al., 2014). However, I have provided evidence that RA acts instead by delaying the progression of the wing bud through developmental stages (chick wing buds see chapter 5; quail wing buds see appendix). Therefore, in RA treated wings, *Shh* is still expressed until HH27/28, but the wing takes 12 hours longer to reach this developmental stage. Delayed developmental timing by prolonged RA signalling therefore extends the proximal programme and delays the start of the distal intrinsic timer. This indicates that in normal development, the loss of RA is required for the initiation of the intrinsic distal programme. Thus, my results suggest that

proximal RA signalling from the host resets developmental age in 0 hour polarising region grafts – after HH20/21 the developmental age is dictated by when RA is lost in the host wing. This is because loss of RA sets the length of the distal intrinsic timer and thus the progression through HH stages. Furthermore, I have shown that *Shh* duration can also be reset in 12+ hour grafts made to an environment in which I prolonged RA signalling. This reveals that loss of the proximal signal, implicated to be RA, is required to initiate the intrinsic timer in the distal wing, and is sufficient to reset developmental timing.

Interestingly, progression through developmental stages and the duration of *Shh* expression in RA treated chick wings emulates the developmental timing of a larger species, the turkey. This provides further evidence that RA treatment delays developmental time in the chick wing bud.

7.3 Setting species-specific wing growth

My results indicate that RA determines developmental timing of the avian wing bud relative to a fixed growth rate between species. Therefore, RA may indirectly regulate the size of the wing by influencing developmental progression during the incubation period i.e. the patterning phase runs from HH18/19 to HH29, but this occurs in different sized wings. At HH29 quail, chick and turkey wings measure 2.6mm, 3.6mm and 4.5mm, respectively, and these proportions could therefore be maintained during later development and influence the final size of the wing.

Until day 8, the quail wing is longer than the chick wing, however because the timing of chick development has been retarded, it eventually grows larger. In my analysis I have also measured up until 216 hours in chick and turkey wings, however the turkey wing by this point has not yet surpassed the growth of the chick wing, therefore it would be useful to measure later time points in future experiments to determine when this occurs. Maintained RA signalling in chick wings delays progression through developmental stages, so the chick wing instead emulates the developmental timing of the larger species, the turkey. It is

therefore possible to speculate that RA treated chick wing growth may also follow that of the turkey wing. However, the size of the RA treated wing at the last point measured is not significantly different from the control chick wing (21.17mm and 20.35mm, respectively) and both control and RA treated wings appear to be equivalent in their appearance – HH39. Considering these results, the RA treated chick wing does not follow the growth of the turkey wing, which at the equivalent incubation time point (216 hours) measures 13.1mm - HH34/35. This suggests that the RA treated wing catches up to the developmental stage of the control wing. For example, it has been shown that after manipulation early in development, compensatory mechanisms can act at later stages to correct limb size (Rosello-Diez, Madisen et al., 2018). However, further work is required to determine if this occurs in RA treated chick wings. Furthermore, in the Hamburger-Hamilton staging system characteristics of the wings at later stages (after HH36) become indistinct, so accurately measuring the HH39 stage is difficult. Therefore, further analysis of skeletal development may be needed to determine if both control and RA treated chick wings are indeed at an equivalent stage.

My research presents a model which differs from the generally accepted idea that the patterning duration is the same between species, followed by a growth period which differs between species. Instead, I suggest that the patterning phase is also accelerated in smaller avian species and this occurs in relation to a fixed growth rate. Further work could be done to understand how the fixed growth rate is controlled between species. This may involve other extrinsic factors, apart from RA. Studies have proposed that growth pathways including the Hippo, mTOR, and IGF signalling may be involved in sensing organ size and regulating growth. Modifications to these pathways between species could therefore result in the organs being scaled to the size of the body (Boone, Colombani et al., 2016, Crickmore and Mann, 2008). Furthermore, IGF signalling has been implicated in scaling the size of limb growth (Qin, Cimildoro et al., 2002, Sears, Patel et al., 2012). While this is not within scope of my PhD thesis, analysis of mTOR and IGF pathways in determining wing size is an area of research which would be interesting to explore in future.

7.4 Model for how wing development is timed in different species

I have shown that initiation of the distal timer depends on the loss of RA from the distal wing. The different duration of *Shh* expression in quail, chick and turkey polarising regions also offers a robust readout of this intrinsic distal timer in the wing bud. My model states that RA is lost from the distal part of the wing at earlier time points in smaller avian species, and this accelerates developmental timing in relation to fixed growth rates between species. For example, in the quail wing faster progression to HH20/21, associated gene expression, and outgrowth to approximately 0.4mm moves the distal part of the wing away from RA emanating from the flank of the embryo, therefore causing an earlier loss of RA (Figure 7.1). The earlier depletion of RA in the quail wing causes the precocious activation of the intrinsic distal timer, e.g. resulting in the shorter duration of *Shh*. In this model, early growth of the wing bud may dictate the length of the proximal programme (however, after HH20/21 the length of the wing appears uncoupled from growth rates). I therefore hypothesise that the length of time the wing is exposed to RA dictates the duration of the intrinsic distal timer, and loss of RA triggers the timer to initiate (Figure 7.1). This distal timer runs until the end of the patterning phase at HH29 when the apical ectodermal ridge regresses, so from 6-60 in quail (54hrs), and 12-72 in the chick (60hrs). Although this appears to be a small difference in the duration of the distal timer, it results in a 12 hour difference in proximal and distal specification between quail and chick wings. Further analysis of patterning events is needed in the turkey, however I would predict that proximal specification takes 18 hours, and that distal specification takes 72 hours. Thus, patterning of the turkey wing is 12 hours delayed compared to the chick wing (Figure 7.1). My model allows the timing of the patterning phase to be altered relative to a fixed growth rate and the length of the incubation period. For example, the earlier switch to the intrinsic timing mechanism in the quail wing allows the patterning phase (HH18/19-HH29) to occur over a 12 hour shorter time period compared to the chick wing (Figure 7.1). Furthermore, patterning is achieved in different sized wings by HH29: 2.6mm quail wings and 3.6mm chick

wings (predicted 4.5mm turkey wings). Therefore, RA is implicated in setting species-specific developmental timing so that patterning is scaled to the eventual size of the wing (Figure 7.1).

7.4.1 Potential mechanisms underpinning the loss of RA in the distal wing

The switch from proximal specification, to distal specification depends on the loss of RA signalling in the distal part of the wing. In my model this occurs at different time points between different avian wings. However, there are multiple possibilities for how differential loss of RA occurs between species, which I have started to investigate. The quail and chick wing buds at HH20/21 measure approximately 0.4mm at 6 hours in the quail and 12 hours in the chick. This may suggest that 0.4mm is the length of outgrowth required to allow loss of RA in the distal wing and thus the switch to the autonomous timer. In preliminary experiments I aimed to restrain wing bud growth through the transient inhibition of proliferation in wing bud cells at HH18/19 using the cell cycle inhibitor PD0332991 (commercially known as Palbociclib). This resulted in the extension of *Shh* past its normal duration (see appendix). This finding is similar to what is seen when RA signalling is maintained in the wing bud. Therefore, one possible explanation for the extension of *Shh* is that PD0332991 inhibits that proliferative growth of the wing bud, which prolongs RA exposure, and delays developmental timing. Further work is required in repeating the experiment and analysing the growth and developmental progression of the PD0332991 treated wings.

However, the turkey wing bud, measures 0.58mm at HH20/21 when the switch from extrinsic to intrinsic specification occurs, which is significantly different in length compared to quail and chicks wing buds. This suggests that there could be other factors involved in the depletion of RA in the distal wing in addition to growth away from the RA source. One possible mechanism is degradation of RA by Cyp26b1 enzymes (Yashiro, Zhao et al., 2004). Preliminary data analysing *Cyp26b1* expression indicates it is upregulated earlier in quail wings compared to chick wings, suggesting this may be a potential mechanism for the

earlier loss of distal RA. However, more repeats are needed, and analysis would also need to be undertaken in the turkey wings.

Another possible explanation for the differential loss of RA in the distal parts of the wings of quails, chicks and turkeys could be differences in overall levels of RA in the embryo, with lower levels in smaller species leading to an earlier loss of RA in the distal wing. To quantify RA levels, high performance liquid chromatography – mass spectrometry (LC-MS) can be used. Although the extraction of RA (specifically, *all-trans* retinoic acid) from wing tissue is difficult due to the highly unstable nature of the molecule and its multiple isomers, I have performed preliminary experiments which have determined that extraction of RA from quail and chick wings is possible and I am currently working to determine if my data is reproducible. It would be worthwhile to perform further experiments quantifying RA levels in quail, chick, turkey across different time points.

One other possible explanation for the loss of RA in the distal region of the wing could be altered sensitivity to RA in different sized HH20/21 wings. For example, it was shown that patterning by a morphogen gradient is scaled in different sized avian neural tubes through altered ratios of transcriptional regulators (Uygur, Young et al., 2016). Thus, a similar mechanism may be altering RA sensitivity in different sized wing buds. In the larger turkey wing, altered sensitivity to RA could be involved in allowing the switch from proximal to distal specification at HH20/21 despite the larger wing bud, a possible approach to explore this would be to analyse the distribution of RARs (retinoic acid receptors) in distal regions of the wing bud.

Finally, I have shown that the earlier loss of proximal signals (implicated to be RA) in wing buds results in a shorter species-specific duration of *Shh* (i.e. transplanting chick polarising regions into quail wing buds at HH18/19 – 0 hours). Another experiment to provide further evidence that loss of RA triggers the switch from extrinsic specification to an intrinsic timer and that this occurs earlier in quail wing buds, could be to remove RA signalling in the chick distal wing at an earlier time point through the use of RA inhibitors. This would determine whether loss of RA is sufficient to precociously activate the intrinsic distal programme and thus change species-specific timing of patterning events. There are

multiple possible inhibitors of RA signalling which could be used to explore this including inhibitors of RA synthesis e.g. DEAB, or antagonists of the retinoic acid receptor (RAR) e.g. AGN193109 and BMS493 (Chute, Muramoto et al., 2006, Mercader, Leonardo et al., 2000, Rosello-Diez, Arques et al., 2014). However, while this experiment may be useful as a proof of concept, the levels of RA required to initiate the intrinsic programme are not yet known, therefore tissue grafting experiments which I have already performed provide a more robust and physiologically relevant readout of altering the extrinsic environment on intrinsic timing mechanisms.

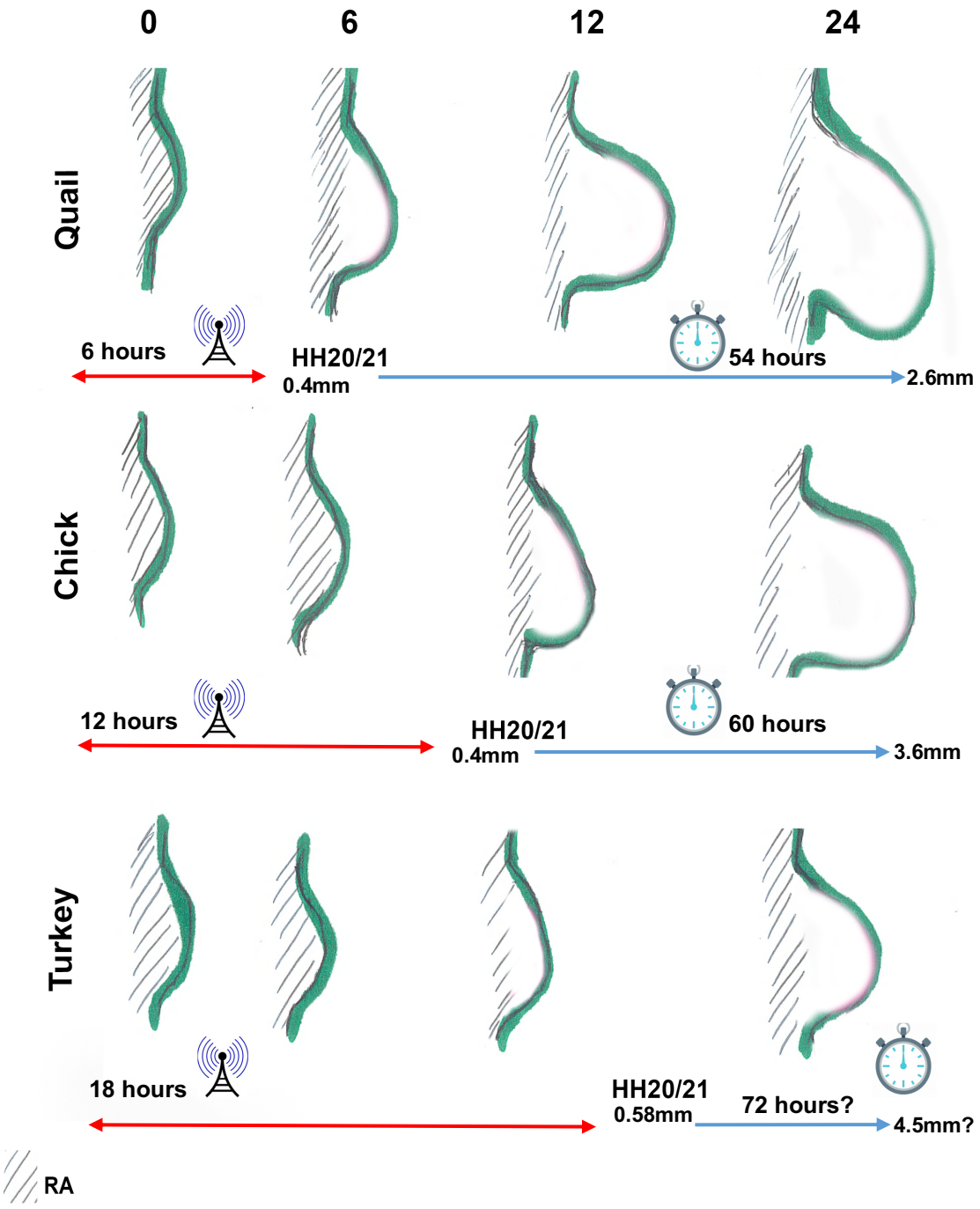

Figure 7.1. Model of setting species-specific timing in early wing development.

Schematic depicting the outgrowth of the wing bud in quail, chicks and turkeys from 0 hour to 24 hours. Black hatching marks RA signalling in the proximal limb. The switch from extrinsic signal based proximal specification to the intrinsic timer occurs at HH20/21 when the wing bud has lost RA signalling in the distal wing. The proximal signal-based specification is indicated by the red arrow and occurs from 0-6 hours (quail), 0-12 hours (chick) and 0-18

hours (predicted turkey). After RA is lost from the wing, specification by an autonomous timing runs for a set duration until HH29, 6-60 hours – quail (54 hours) ending in 2.6mm wings, 12-72 hours – chick (60 hours) 3.6mm wings, 18-84 -predicted turkey (66 hours) predicted ending in 4.5mm wings.

7.5 Further work

In addition to analysing *Meis1* and *Hoxa13* expression in the turkey, I have also started to analyse whether developmental timing events in the forelimb bud are also mirrored in human limb bud development. In a collaboration with the Institute of Child Health, it has been shown that in human embryonic limb development, *Shh* expression can be detected from approximately Carnegie stage (CS) 13 until CS16 (i.e. 9 days) which is about 3-4 times the duration seen in the chick (Figure 7.2). Determining a full time-course of expression in human limb buds is difficult due to the limited availability and sensitive nature of attaining embryos. However, the longer expression seen in human limb buds correlates with the longer gestation period for humans and also larger limbs.

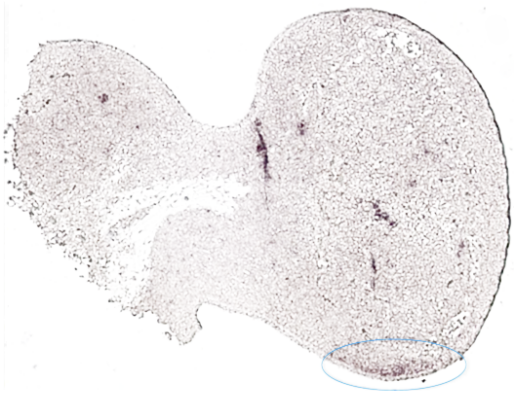

Figure 7.2. *Shh* expression in the human forelimb bud.
Shh expression in the developing human limb bud Carnegie stage 16 (day 39). Image courtesy of the Institute of Child Health, London.

It would be fascinating to also to determine the timing of proximal and distal specification in human limb bud development and determine whether the switch from extrinsic based patterning to an intrinsic timer also occurs. As how the limb bud is timed in human development, and whether this is scaled to the gestation period is currently unknown.

7.5.1 The potential mechanism underpinning the autonomous timer in the distal wing

In my thesis I have built on previous studies and provided evidence for an autonomous timing mechanism which operates in the distal wing and patterns the zeugopod and autopod (Pickering, Rich et al., 2018, Saiz-Lopez, Chinnaiya et al., 2015, Saiz-Lopez, Chinnaiya et al., 2017, Summerbell, Lewis et al., 1973). This autonomous timer is initiated by the loss of RA in the distal wing, and depending on when this occurs, appears to set species-specific timing of patterning wing development. The mechanism underpinning this process is unclear, however there is evidence that the cell cycle clock could provide the basis of this intrinsic timer that controls the distal program (Chinnaiya, Tickle et al., 2014, Lewis, 1975, Towers, Mahood et al., 2008).

Cell cycle clocks have also been implicated in other developing systems. For example, oligodendrocyte precursor cells cultured *in vivo* require a mitogen to induce proliferation. The precursors then require a hydrophobic signal in order to triggers cells to start 'counting' a particular number of cell divisions (in this case, 8) before differentiating. Interestingly, along with thyroid hormone, RA has been implicated as this hydrophobic signal. While it remains unclear what the molecular mechanism underlying this phenomenon is, it has been suggested that RA signalling triggers the timing mechanism regulated by the accumulation of cell cycle inhibitors over time, thus leading to a set number of cell divisions (Barres, Lazar et al., 1994, Durand and Raff, 2000, Temple and Raff, 1986). RA could therefore be acting in a similar nature in my model in order to initiate the intrinsic cell cycle clock in the distal mesenchyme.

Furthermore, it has recently been shown that Shh controls the expression of genes whose products either stimulate proliferation (D cyclins) or inhibit proliferation (D cyclin inhibitors) in the chick wing polarising region. However, Shh regulates these genes with different temporal dynamics, and therefore forms the basis of an autoregulatory mechanism which has been proposed to control timing of the cell cycle clock in the polarising region (Pickering, 2019).

Although there are examples indicating the role cell cycle clocks play in measuring time in development, this may not be the full picture. In some embryonic tissues timing of development appears uncoupled from the cell cycle. In cerebral development, it was shown through analysis of gene expression indicating particular cell identities, that progression through progenitor identities occurs even when the cell cycle is arrested, suggesting in this case, that timing is independent of the cell cycle. Although the actual mechanism remains unclear, *in vitro* studies of single cells compared to neurospheres (multiple cells) suggested that this timing was largely cell autonomous, but could also be affected or fine-tuned by extrinsic signals (Okamoto, Miyata et al., 2016).

Furthermore, one well studied example of timing in development is somitogenesis - the segmentation and periodic formation of body segments (somites) from the presomitic mesoderm. The periodicity of somite formation and the number produced is species-specific, for example somites form approximately every 30 minutes in zebrafish, 90 minutes in chicks, 2 hours in mice and 5 hours in humans. Timing of somite formation is driven by oscillations of gene expressions - *Hes7* in the mouse (Dequeant and Pourquie, 2008, Hubaud and Pourquie, 2014). Research into how species-specific oscillation periods are achieved have highlighted a role of cell autonomous mechanisms, for example it was shown that the kinetics of mRNA splicing, degradation rates, and transcription differs between species, with the larger species exhibiting delayed mRNA processing (Hoyle and Ish-Horowicz, 2013, Matsuda, Hayashi et al., 2019). However, the actual mechanism underpinning differences in biochemical rates and mRNA processing is unclear, and whether this is linked to the cell cycle, or epigenetic regulation is yet to be determined (Chavez, Garcia-Martinez et al., 2016, Mushegian, 2016).

7.6 Summary

To summarise, in my thesis I have shown that the patterning of the wing bud in smaller avian species is accelerated in comparison to larger avian species. This accelerated development appears to occur during the progression from HH18/19 to HH20/21, when the switch from extrinsic signal-based specification of proximal elements, to an intrinsic-based timer specifying distal elements occurs. This switch is initiated by the loss of RA in the distal wing, and therefore the extrinsic signal, RA, is involved in setting the species-specific timing in the wing. Maintenance of RA in the wing results in the delayed progression through developmental stages and associated gene expression. Thus, when chick wings are treated with RA they develop according to developmental timing of the larger species, the turkey. RA appears to be involved in setting the duration of distal patterning events in the wing relative to a fixed growth rate, therefore patterning is completed in different sized wings between species which may influence adult wing size. However, maintaining RA signalling does not appear to change the size of the wing as growth and developmental stages appear to catch up in later development in RA treated wing buds.

Appropriate timing of the loss of RA from the distal part of the wing appears to be due to a combination of outgrowth from the source of RA signalling in the flank of the embryo, and the upregulation of *Cyp26b1* in the distal mesenchyme. However additional work is needed in this area. Furthermore, the mechanism underpinning the nature of the autonomous timer operating in the distal mesenchyme, including the polarising region is unclear, however there is evidence for a cell cycle clock in timing patterning events (Chinnaiya, Tickle et al., 2014, Pickering, 2019, Summerbell, Lewis et al., 1973).

Appendix

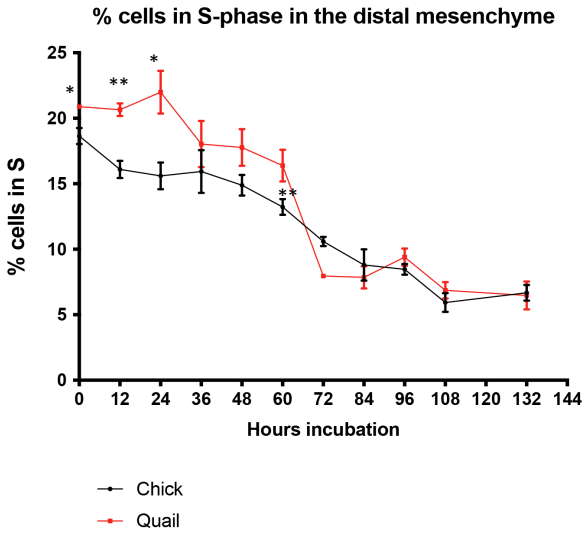

Figure 1. Cell cycle rates in quail and chick wing bud distal mesenchyme

The proportion of cells in S phase (DNA replication) shows there is a significant reduction in proliferating cells approximately 12 hours earlier in the quail compared to chick distal wing bud cells. Student t tests were performed on the percentage of cells in each phase of the cell cycle. *N*=3 experimental repeats each containing *n*=8-12 pooled blocks of distal mesenchyme. *p* values: *=<0.05, **=<0.01 ***= <0.001 ****= <0.0001.

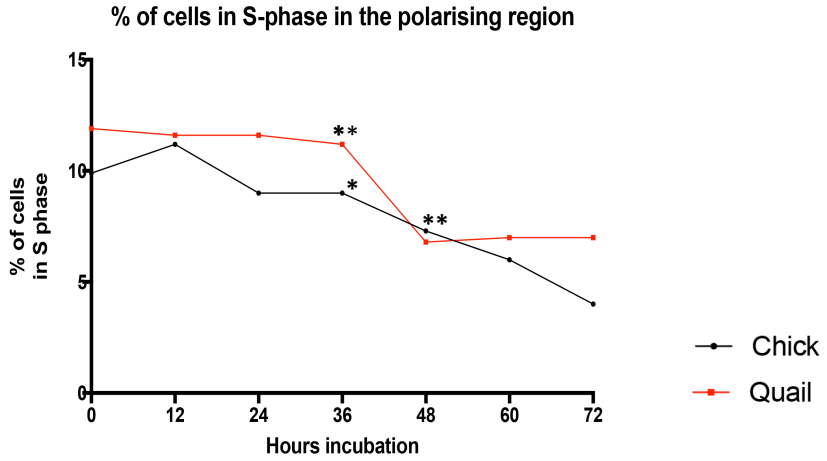

Figure 2. Cell cycle rates in quail and chick polarising regions.

The proportion of cells in S phase (DNA replication) shows there is a significant reduction in proliferating cells at approximately 36 hours in the quail compared to 48 hours in the chick polarising region cells, coinciding with when high levels of Shh signalling downregulates. Student t tests were performed on the percentage of cells in each phase of

the cell cycle. *n*=8-12 pooled blocks of distal mesenchyme. *p* values: *=<0.05, **=<0.01 ***= <0.001 ****= <0.0001.

A

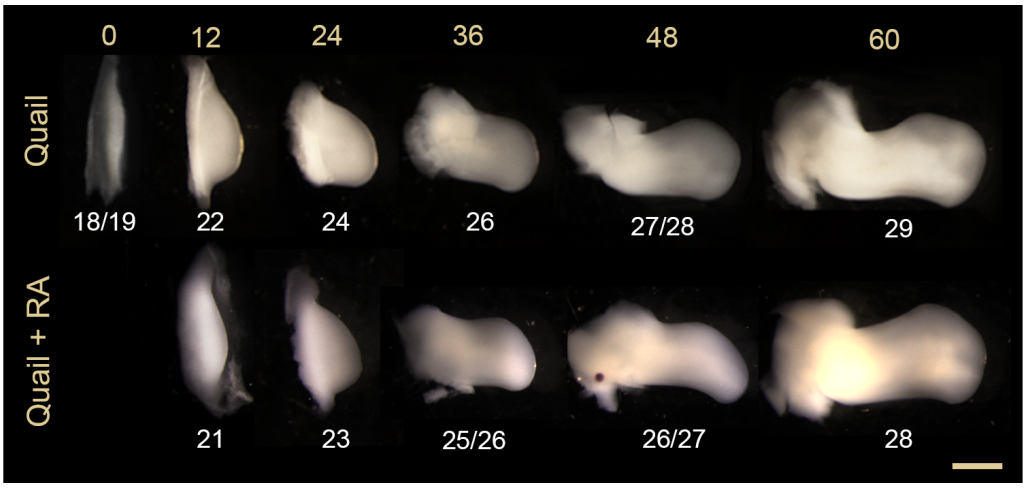

B

Hours incubation	Quail	Quail + RA	Chick
0	HH18/19	HH18/19	HH18/19
12	HH22	HH21	HH20/21
24	HH24	HH23	HH22
36	HH26	HH25/26	HH24
48	HH27/28	HH26/27	HH26
60	HH29	HH28	HH27/28
72	HH30	HH29	HH29

Figure 3. RA treated quail wings progress through Hamburger-Hamilton stages slower than untreated quail wings and at a similar rate to chick wings.

Quail wing buds were treated at the 0 hour time point and analysed every 12 hours subsequently in comparison to control wings. **A)** Right wing buds from control quail and RA treated quails were removed and photographed every 12 hours from 0 hours 60 hours. In RA treated limb no 0 hour image is shown as this was equivalent to untreated wings. Scale bars represent 500µm**. B)** Using the Hamburger-Hamilton staging system the embryonic stages are noted from 0 hours incubation then every 12 hours subsequently. The quail + RA progresses through the HH stages at a slower rate compared to the quail, but at a similar rate compared to the chick. *n*=3-10

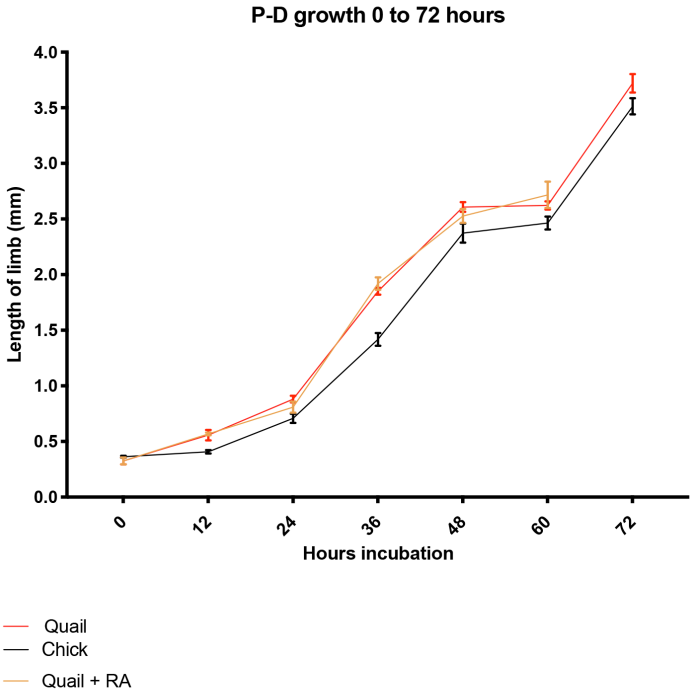

Figure 4. Proximo-distal outgrowth is unchanged in RA treated quail wings compared to control quail wings.
Wing buds were treated shortly after the 0 hour time point and analysed every 12 hours subsequently in comparison to control wings. RA treated quail limb buds were measured along the proximo-distal (P-D) axis (body wall to tip of limb bud) every 12 hours after the 0 hour time point. Student t tests show no significant differences in limb lengths between control quail and RA treated quail wing buds. P values: *=<0.05, **=<0.01 ***= <0.001 ****= <0.000 *n*=3

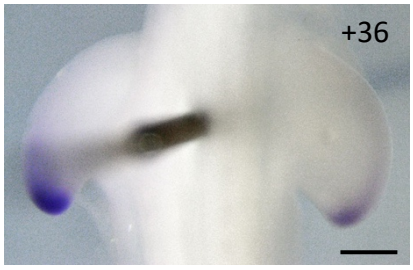

Figure 5. Multiple RA beads sequentially placed cannot indefinitely delay *Hoxa13* expression in chick wings

Whole mount *in situ* hybridisation images showing RA treated (right wing) vs control (left wing) expression in chicks. TTNPBB beads were placed at 0 hours, then at 12 hours and

gene expression analysed at approximate 36 hour time point. Maintaining RA in the wing through bead implantation is insufficient to indefinitely delay *Hoxa13* expression. Scale bar=500µm *n*=4

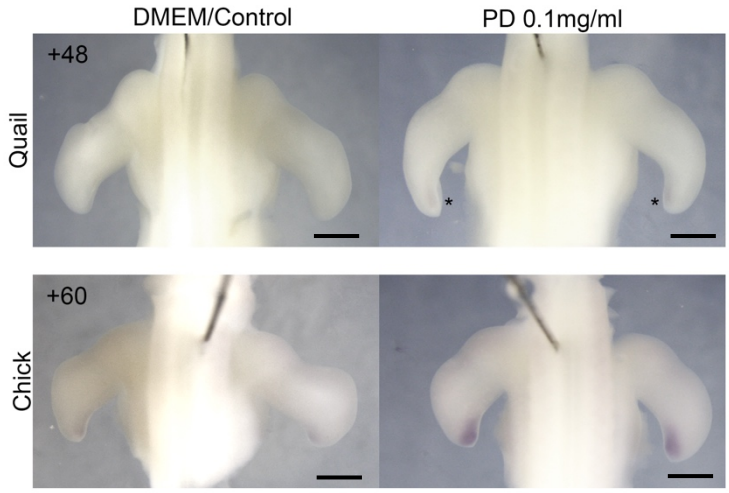

Figure 6. Treatment with PD0332991 extends the expression of *Shh* in quail and chick wings.

HH18/19 (0 hour) quail and chick wing buds were treated with 0.1mg/ml PD0332991 or control DMEM and left to develop until the stage when *Shh* is downregulated, 48 hour time point – quail, or the 60 hour time point - chick. *Shh* expression was detected using *in situ* hybridisation. Control quail wings downregulate *Shh* at 48 hours but slight expression can be seen in PD treated wings (marked by black asterisks). Control chick wings downregulate *Shh* at 60 hours, however strong expression can be seen in PD treated wings Scale bars =. 500µm *n*=2

References

(1984). Microcontrolled release of biologically active compounds in chick embryos: Beads of 200-µm diameter for the local release of retinoids. *Analytical Biochemistry* 142(2) 542 - 555.

Agarwal, P., et al. (2003). Tbx5 is essential for forelimb bud initiation following patterning of the limb field in the mouse embryo. *Development* 130(3) 623-633.

Ainsworth, S. J., R. L. Stanley and D. J. Evans (2010). Developmental stages of the Japanese quail. *J Anat* 216(1) 3-15.

Barres, B. A., M. A. Lazar and M. C. Raff (1994). A novel role for thyroid hormone, glucocorticoids and retinoic acid in timing oligodendrocyte development. *Development* 120(5) 1097-1108.

Boehm, B., et al. (2010). The role of spatially controlled cell proliferation in limb bud morphogenesis. *PLoS Biol* 8(7) e1000420.

Boone, E., et al. (2016). The Hippo signalling pathway coordinates organ growth and limits developmental variability by controlling dilp8 expression. *Nat Commun* 7 13505.

Burke, A. C., et al. (1995). Hox genes and the evolution of vertebrate axial morphology. *Development* 121(2) 333-346.

Capdevila, J., et al. (1999). Control of vertebrate limb outgrowth by the proximal factor Meis2 and distal antagonism of BMPs by Gremlin. *Mol Cell*. United States. 839-849.

Charite, J., D. G. McFadden and E. N. Olson (2000). The bHLH transcription factor dHAND controls Sonic hedgehog expression and establishment of the zone of polarizing activity during limb development. *Development* 127(11) 2461-2470.

Chavez, S., et al. (2016). The importance of controlling mRNA turnover during cell proliferation. *Curr Genet*. United States. 701-710.

Chinnaiya, K., C. Tickle and M. Towers (2014). Sonic hedgehog-expressing cells in the developing limb measure time by an intrinsic cell cycle clock. *Nature Communications* 5.

Chute, J. P., et al. (2006). Inhibition of aldehyde dehydrogenase and retinoid signaling induces the expansion of human hematopoietic stem cells. *Proc Natl Acad Sci U S A* 103(31) 11707-11712.

Collier, J. L. (2000). FLOW CYTOMETRY AND THE SINGLE CELL IN PHYCOLOGY. *J Phycol* 36(4) 628-644.

Cooper, K. L., et al. (2011). Initiation of proximal-distal patterning in the vertebrate limb by signals and growth. *Science* 332(6033) 1083-1086.

Crickmore, M. A. and R. S. Mann (2008). The control of size in animals: insights from selector genes. *Bioessays* 30(9) 843-853.

Crowley, L. C., G. Chojnowski and N. J. Waterhouse (2016). Measuring the DNA Content of Cells in Apoptosis and at Different Cell-Cycle Stages by Propidium Iodide Staining and Flow Cytometry. *Cold Spring Harb Protoc* 2016(10).

Cunningham, T. J. and G. Duester (2015). Mechanisms of retinoic acid signalling and its roles in organ and limb development. *Nat Rev Mol Cell Biol* 16(2) 110-123.

Cygan, J. A., R. L. Johnson and A. P. McMahon (1997). Novel regulatory interactions revealed by studies of murine limb pattern in Wnt-7a and En-1 mutants. *Development* 124(24) 5021-5032.

Dahn, R. D. and J. F. Fallon (2000). Interdigital regulation of digit identity and homeotic transformation by modulated BMP signaling. *Science*. United States. 438-441.

Dealy, C. N., et al. (1993). Wnt-5a and Wnt-7a are expressed in the developing chick limb bud in a manner suggesting roles in pattern formation along the proximodistal and dorsoventral axes. *Mech Dev* 43(2-3) 175-186.

Delgado, I. and M. Torres (2016). Gradients, waves and timers, an overview of limb patterning models. *Semin Cell Dev Biol*. England, 2015 Elsevier Ltd. 109-115.

Dequeant, M. L. and O. Pourquie (2008). Segmental patterning of the vertebrate embryonic axis. *Nat Rev Genet*. England. 370-382.

Dolle, P. and D. Duboule (1989). Two gene members of the murine HOX-5 complex show regional and cell-type specific expression in developing limbs and gonads. *Embo j* 8(5) 1507-1515.

Dudley, A. T., M. A. Ros and C. J. Tabin (2002). A re-examination of proximodistal patterning during vertebrate limb development. *Nature* 418(6897) 539-544.

Durand, B. and M. Raff (2000). A cell-intrinsic timer that operates during oligodendrocyte development. *Bioessays*. United States, 2000 John Wiley & Sons, Inc. 64-71.

Eichele, G. and C. Thaller (1987). Characterization of concentration gradients of a morphogenetically active retinoid in the chick limb bud. *J Cell Biol* 105(4) 1917-1923.

Eichele, G., C. Tickle and B. M. Alberts (1985). Studies on the mechanism of retinoid-induced pattern duplications in the early chick limb bud: temporal and spatial aspects. *J Cell Biol* 101(5 Pt 1) 1913-1920.

Farin, H. F., et al. (2013). Tbx2 terminates shh/fgf signaling in the developing mouse limb bud by direct repression of gremlin1. *PLoS Genet* 9(4) e1003467.

Fernandez-Teran, M., et al. (2000). Role of dHAND in the anterior-posterior polarization of the limb bud: implications for the Sonic hedgehog pathway. *Development* 127(10) 2133-2142.

Fernandez-Teran, M. and M. A. Ros (2008). The Apical Ectodermal Ridge: morphological aspects and signaling pathways. *Int J Dev Biol*. Spain. 857-871.

Fernandez-Teran, M. A., J. R. Hinchliffe and M. A. Ros (2006). Birth and death of cells in limb development: a mapping study. *Dev Dyn* 235(9) 2521-2537.

Fogel, J. L., T. Z. Thein and F. V. Mariani (2012). Use of LysoTracker to detect programmed cell death in embryos and differentiating embryonic stem cells. *J Vis Exp*(68).

Gierer, A. and H. Meinhardt (1972). A theory of biological pattern formation. *Kybernetik* 12(1) 30-39.

Gupta, S. K. and M. R. Bakst (1993). Turkey embryo staging from cleavage through hypoblast formation. *J Morphol* 217(3) 313-325.

Hamburger, V. and H. L. Hamilton (1951). A series of normal stages in the development of the chick embryo. *Dev Dyn* 195(4) 231-272.

Harfe, B. D., et al. (2004). Evidence for an expansion-based temporal Shh gradient in specifying vertebrate digit identities. *Cell*. United States. 517-528.

Harris, M. P., B. L. Linkhart and J. F. Fallon (2004). Bmp7 mediates early signaling events during induction of chick epidermal organs. *Dev Dyn* 231(1) 22-32.

Harrison, R. G. (1924). Some Unexpected Results of the Heteroplastic Transplantation of Limbs. *Proc Natl Acad Sci U S A* 10(2) 69-74.

Healy, C., D. Uwanogho and P. T. Sharpe (1999). Regulation and role of Sox9 in cartilage formation. *Dev Dyn*. United States. 69-78.

Hornbruch, A. and L. Wolpert (1970). Cell division in the early growth and morphogenesis of the chick limb. *Nature* 226(5247) 764-766.

Hoyle, N. P. and D. Ish-Horowicz (2013). Transcript processing and export kinetics are rate-limiting steps in expressing vertebrate segmentation clock genes. *Proc Natl Acad Sci U S A* 110(46) E4316-4324.

Hu, Q. X., et al. (2017). All-trans-retinoic acid activates SDF-1/CXCR4/ROCK2 signaling pathway to inhibit chondrogenesis. *Am J Transl Res* 9(5) 2296-2305.

Hubaud, A. and O. Pourquie (2014). Signalling dynamics in vertebrate segmentation. *Nat Rev Mol Cell Biol*. England. 709-721.

Hurle, J. M., et al. (1996). Morphology and significance of programmed cell death in the developing limb bud of the vertebrate embryo. *Microsc Res Tech*. United States. 236-246.

Hurle, J. M., et al. (1995). Cell death in the embryonic developing limb. *Scanning Microsc* 9(2) 519-533; discussion 533-514.

Izpisua-Belmonte, J. C. and D. Duboule (1992). Homeobox genes and pattern formation in the vertebrate limb. *Dev Biol* 152(1) 26-36.

Izpisua-Belmonte, J. C., et al. (1991). Expression of the homeobox Hox-4 genes and the specification of position in chick wing development. *Nature* 350(6319) 585-589.

Kaltcheva, M. M., et al. (2016). BMPs are direct triggers of interdigital programmed cell death. *Dev Biol*. United States, 2016. Published by Elsevier Inc. 266-276.

Kuchipudi, S. V., et al. (2012). 18S rRNA is a reliable normalisation gene for real time PCR based on influenza virus infected cells. *Virol J* 9 230.

Laufer, E., et al. (1994). Sonic hedgehog and Fgf-4 act through a signaling cascade and feedback loop to integrate growth and patterning of the developing limb bud. *Cell*. United States. 993-1003.

Le Douarin, N. M., et al. (2000). Interspecific chimeras in avian embryos. *Methods Mol Biol* 135 373-386.

Lee, R. T., Z. Zhao and P. W. Ingham (2016). Hedgehog signalling. *Development*. England, 2016. Published by The Company of Biologists Ltd. 367-372.

Lewis, J. H. (1975). Fate maps and the pattern of cell division: a calculation for the chick wing-bud. *J Embryol Exp Morphol* 33(2) 419-434.

Li, S., et al. (2019). Comparison of whole embryonic development in the duck (Anas platyrhynchos) and goose (Anser cygnoides) with the chicken (Gallus gallus). *Poult Sci*. England, 2019 Poultry Science Association Inc.

Litingtung, Y., et al. (2002). Shh and Gli3 are dispensable for limb skeleton formation but regulate digit number and identity. *Nature* 418(6901) 979-983.

Loomis, C. A., et al. (1996). The mouse Engrailed-1 gene and ventral limb patterning. *Nature* 382(6589) 360-363.

Martin, C., et al. (1991). Successful xenogeneic transplantation in embryos: induction of tolerance by extrathymic chick tissue grafted into quail. *Dev Immunol* 1(4) 265-277.

Matsuda, M., et al. (2019). Species-specific oscillation periods of human and mouse segmentation clocks are due to cell autonomous differences in biochemical reaction parameters. *bioRxiv* 650648.

McGrew, M. J., et al. (2004). Efficient production of germline transgenic chickens using lentiviral vectors. *EMBO Rep* 5(7) 728-733.

Mercader, N., et al. (1999). Conserved regulation of proximodistal limb axis development by Meis1/Hth. *Nature* 402(6760) 425-429.

Mercader, N., et al. (2000). Opposing RA and FGF signals control proximodistal vertebrate limb development through regulation of Meis genes. *Development* 127(18) 3961-3970.

Mic, F. A., I. O. Sirbu and G. Duester (2004). Retinoic acid synthesis controlled by Raldh2 is required early for limb bud initiation and then later as a proximodistal signal during apical ectodermal ridge formation. *J Biol Chem*. United States. 26698-26706.

Minguillon, C., et al. (2012). Hox genes regulate the onset of Tbx5 expression in the forelimb. *Development* 139(17) 3180-3188.

Montero, J. A. and J. M. Hurle (2010). Sculpturing digit shape by cell death. *Apoptosis* 15(3) 365-375.

Montero, J. A., et al. (2017). Sox9 Expression in Amniotes: Species-Specific Differences in the Formation of Digits. *Front Cell Dev Biol* 5 23.

Moon, A. M. and M. R. Capecchi (2000). Fgf8 is required for outgrowth and patterning of the limbs. *Nat Genet* 26(4) 455-459.

Moreau, C., et al. (2019). Timed Collinear Activation of Hox Genes during Gastrulation Controls the Avian Forelimb Position. *Curr Biol* 29(1) 35-50 e34.

Mushegian, A. A. (2016). Regulating the rate of mRNA degradation. *Science Signaling* 9(448) ec231-ec231.

Nakajima, Y. (2019). Retinoic acid signaling in heart development. *Genesis* 57(7-8) e23300.

Nakane, Y. and M. Tsudzuki (1999). Development of the skeleton in Japanese quail embryos. *Dev Growth Differ* 41(5) 523-534.

Nardi, J. B. a. S. D. L. (1984). Surface properties of regenerating limb cells: Evidence for gradation along the proximodistal axis. *Differentiation* 25(1-3) 27--31.

Nelson, C. E., et al. (1996). Analysis of Hox gene expression in the chick limb bud. *Development* 122(5) 1449-1466.

Newman, S. A. and H. L. Frisch (1979). Dynamics of skeletal pattern formation in developing chick limb. *Science* 205(4407) 662-668.

Niederreither, K., et al. (2002). Embryonic retinoic acid synthesis is required for forelimb growth and anteroposterior patterning in the mouse. *Development* 129(15) 3563-3574.

Nishimoto, S., et al. (2015). RA Acts in a Coherent Feed-Forward Mechanism with Tbx5 to Control Limb Bud Induction and Initiation. *Cell Rep* 12(5) 879-891.

Niswander, L., et al. (1994). A positive feedback loop coordinates growth and patterning in the vertebrate limb. *Nature* 371(6498) 609-612.

Noji, S., et al. (1991). Retinoic acid induces polarizing activity but is unlikely to be a morphogen in the chick limb bud. *Nature* 350(6313) 83-86.

Ohki-Hamazaki, H., et al. (1997). Control of the limb bud outgrowth in quail-chick chimera. *Dev Dyn*. United States. 85-91.

Okamoto, M., et al. (2016). Cell-cycle-independent transitions in temporal identity of mammalian neural progenitor cells. *Nat Commun* 7 11349.

Padgett, C. S. and W. D. Ivey (1960). The normal embryology of the Coturnix quail. *Anat Rec* 137 1-11.

Parr, B. A. and A. P. McMahon (1995). Dorsalizing signal Wnt-7a required for normal polarity of D-V and A-P axes of mouse limb. *Nature* 374(6520) 350-353.

Pickering, J., et al. (2018). An intrinsic cell cycle timer terminates limb bud outgrowth. *Elife* 7.

Pickering, J. and M. Towers (2016). Inhibition of Shh signalling in the chick wing gives insights into digit patterning and evolution. *Development* 143(19) 3514-3521.

Pickering, J. a. C. K. a. T. M. (2019). An autoregulatory cell cycle timer integrates growth and specification in chick wing digit development. *eLife* 8 e47625.

Pizette, S. and L. Niswander (1999). BMPs negatively regulate structure and function of the limb apical ectodermal ridge. *Development* 126(5) 883-894.

Qin, P., et al. (2002). PBX, MEIS, and IGF-I are potential mediators of retinoic acid-induced proximodistal limb reduction defects. *Teratology* 66(5) 224-234.

Raspopovic, J., et al. (2014). Modeling digits. Digit patterning is controlled by a Bmp-Sox9-Wnt Turing network modulated by morphogen gradients. *Science* 345(6196) 566-570.

Riddle, R. D., et al. (1995). Induction of the LIM homeobox gene Lmx1 by WNT7a establishes dorsoventral pattern in the vertebrate limb. *Cell*. United States. 631-640.

Riddle, R. D., et al. (1993). Sonic hedgehog mediates the polarizing activity of the ZPA. *Cell*. United States. 1401-1416.

Rosello-Diez, A., et al. (2014). Diffusible signals and epigenetic timing cooperate in late proximo-distal limb patterning. *Development*. England. 1534-1543.

Rosello-Diez, A., et al. (2018). Cell-nonautonomous local and systemic responses to cell arrest enable long-bone catch-up growth in developing mice. *PLoS Biol* 16(6) e2005086.

Rosello-Diez, A., M. A. Ros and M. Torres (2011). Diffusible signals, not autonomous mechanisms, determine the main proximodistal limb subdivision. *Science*. United States. 1086-1088.

Rubin, L. and J. W. Saunders, Jr. (1972). Ectodermal-mesodermal interactions in the growth of limb buds in the chick embryo: constancy and temporal limits of the ectodermal induction. *Dev Biol*. United States. 94-112.

Saiz-Lopez, P., et al. (2015). An intrinsic timer specifies distal structures of the vertebrate limb. *Nature communications* 6.

Saiz-Lopez, P., et al. (2017). Intrinsic properties of limb bud cells can be differentially reset. *Development* 144(3) 479-486.

Sato, K., et al. (2007). Specification of cell fate along the proximal-distal axis in the developing chick limb bud. *Development*. England. 1397-1406.

Saunders, J. (1948). The proximo-distal sequence of origin of the parts of the chick wing and the role of the ectoderm. *Journal of Experimental Zoology Part A:Ecological and Integrative Physiology*. 363-403.

Saunders, J. and M. Gasseling (1968). Ectodermal mesenchymal interactions in the origin of limb symmetry. Epithelial Mesenchymal Interactions, Fleischmaje R, Ž Billingham RE. 78-97.

Saunders, J. W., Jr. and M. T. Gasseling (1962). Cellular death in morphogenesis of the avian wing. *Dev Biol*. United States. 147-178.

Scherz, P. J., et al. (2004). The limb bud Shh-Fgf feedback loop is terminated by expansion of former ZPA cells. *Science*. United States. 396-399.

Sears, K. E., et al. (2012). Disparate Igf1 expression and growth in the fore- and hind limbs of a marsupial mammal (Monodelphis domestica). *J Exp Zool B Mol Dev Evol* 318(4) 279-293.

Sellier, N. a. B. J. P. a. D. V. a. B. M. R. (2006). Comparative Staging of Embryo Development in Chicken, Turkey, Duck, Goose, Guinea Fowl, and Japanese Quail Assessed from Five Hours After Fertilization Through Seventy-Two Hours of Incubation. *The Journal of Applied Poultry Research* 15(2) 219-228.

Sheth, R., et al. (2012). Hox genes regulate digit patterning by controlling the wavelength of a Turing-type mechanism. *Science* 338(6113) 1476-1480.

Smith, J. C., C. Tickle and L. Wolpert (1978). Attenuation of positional signalling in the chick limb by high doses of gamma-radiation. *Nature* 272(5654) 612-613.

Stadler, H. S., K. M. Higgins and M. R. Capecchi (2001). Loss of Eph-receptor expression correlates with loss of cell adhesion and chondrogenic capacity in Hoxa13 mutant limbs. *Development* 128(21) 4177-4188.

Stainton, H. and M. Towers (2018). Polarizing Region Tissue Grafting in the Chick Embryo Limb Bud. *Methods Mol Biol* 1863 143-153.

Stephens-Jarnagin, A., D. A. Miller and H. F. DeLuca (1985). The growth-supporting activity of a retinoidal benzoic acid derivative and 4,4-difluororetinoic acid. *Arch Biochem Biophys*. United States. 11-16.

Stratford, T., et al. (1999). Abnormal anteroposterior and dorsoventral patterning of the limb bud in the absence of retinoids. *Mech Dev*. Ireland. 115-125.

Summerbell, D. (1974). Interaction between the proximo-distal and antero-posterior co-ordinates of positional value during the specification of positional information in the early development of the chick limb-bud. *J Embryol Exp Morphol*. 227-237.

Summerbell, D. and J. H. Lewis (1975). Time, place and positional value in the chick limb-bud. *J Embryol Exp Morphol* 33(3) 621-643.

Summerbell, D., J. H. Lewis and L. Wolpert (1973). Positional information in chick limb morphogenesis. *Nature* 244(5417) 492-496.

Swindell, E. C., et al. (1999). Complementary domains of retinoic acid production and degradation in the early chick embryo. *Dev Biol* 216(1) 282-296.

Tabin, C. and L. Wolpert (2007). Rethinking the proximodistal axis of the vertebrate limb in the molecular era. *Genes Dev*. United States. 1433-1442.

Tamura, K., et al. (1997). Retinoic acid changes the proximodistal developmental competence and affinity of distal cells in the developing chick limb bud. *Dev Biol*. United States. 224-234.

te Welscher, P., et al. (2002). Progression of vertebrate limb development through SHH-mediated counteraction of GLI3. *Science* 298(5594) 827-830.

Temple, S. and M. C. Raff (1986). Clonal analysis of oligodendrocyte development in culture: evidence for a developmental clock that counts cell divisions. *Cell*. United States. 773-779.

Tickle, C. (1981). The number of polarizing region cells required to specify additional digits in the developing chick wing. *Nature* 289(5795) 295-298.

Tickle, C. (1995). Vertebrate limb development. *Curr Opin Genet Dev* 5(4) 478-484.

Tickle, C., J. Lee and G. Eichele (1985). A quantitative analysis of the effect of all-trans-retinoic acid on the pattern of chick wing development. *Dev Biol* 109(1) 82-95.

Tickle, C., D. Summerbell and L. Wolpert (1975). Positional signalling and specification of digits in chick limb morphogenesis. *Nature* 254(5497) 199-202.

Tickle, C. and M. Towers (2017). Sonic Hedgehog Signaling in Limb Development. *Front Cell Dev Biol* 5 14.

Towers, M., et al. (2008). Integration of growth and specification in chick wing digit-patterning. *Nature*. England. 882-886.

Towers, M., et al. (2011). Insights into bird wing evolution and digit specification from polarizing region fate maps. *Nat Commun*. England. 426.

Turing, A. (1952). Philosophical the royal biological transqfctions society sciences. *Phil. Trans. R. Soc. Lond. B* 237 37-72.

Twitty, V. C. a. S. J. L. (1931). The growth of eyes and limbs transplanted heteroplastically between two species of Amblystoma. *Journal of Experimental Zoology* 59(1) 61--86.

Uygur, A., et al. (2016). Scaling Pattern to Variations in Size during Development of the Vertebrate Neural Tube. *Dev Cell* 37(2) 127-135.

Vargesson, N., et al. (2001). Characterisation of hoxa gene expression in the chick limb bud in response to FGF. *Dev Dyn* 220(1) 87-90.

Verheyden, J. M. and X. Sun (2008). An Fgf/Gremlin inhibitory feedback loop triggers termination of limb bud outgrowth. *Nature* 454(7204) 638-641.

Vogel, A., et al. (1995). Dorsal cell fate specified by chick Lmx1 during vertebrate limb development. *Nature* 378(6558) 716-720.

Wada, N. (2011). Spatiotemporal changes in cell adhesiveness during vertebrate limb morphogenesis. *Dev Dyn* 240(5) 969-978.

Wada, N. and H. Ide (1994). Sorting out of limb bud cells in monolayer culture. *Int J Dev Biol* 38(2) 351-356.

Wanek, N., et al. (1991). Conversion by retinoic acid of anterior cells into ZPA cells in the chick wing bud. *Nature* 350(6313) 81-83.

Wang, B., J. F. Fallon and P. A. Beachy (2000). Hedgehog-regulated processing of Gli3 produces an anterior/posterior repressor gradient in the developing vertebrate limb. *Cell* 100(4) 423-434.

Wolpert, L. (1969). Positional information and the spatial pattern of cellular differentiation. *J Theor Biol* 25(1) 1-47.

Wolpert, L., C. Tickle and M. Sampford (1979). The effect of cell killing by x-irradiation on pattern formation in the chick limb. *J Embryol Exp Morphol* 50 175-193.

Yang, Y., et al. (1997). Relationship between dose, distance and time in Sonic Hedgehog-mediated regulation of anteroposterior polarity in the chick limb. *Development* 124(21) 4393-4404.

Yang, Y. and L. Niswander (1995). Interaction between the signaling molecules WNT7a and SHH during vertebrate limb development: dorsal signals regulate anteroposterior patterning. *Cell*. United States. 939-947.

Yashiro, K., et al. (2004). Regulation of retinoic acid distribution is required for proximodistal patterning and outgrowth of the developing mouse limb. *Dev Cell*. United States. 411-422.

Yokouchi, Y., et al. (1995). Misexpression of Hoxa-13 induces cartilage homeotic transformation and changes cell adhesiveness in chick limb buds. *Genes Dev* 9(20) 2509-2522.

Yokouchi, Y., H. Sasaki and A. Kuroiwa (1991). Homeobox gene expression correlated with the bifurcation process of limb cartilage development. *Nature* 353(6343) 443-445.

Zacchei, A. M. (1961). [The embryonal development of the Japanese quail (Coturnix coturnix japonica T. and S.)]. *Arch Ital Anat Embriol* 66 36-62.

Zakany, J. and D. Duboule (1999). Hox genes in digit development and evolution. *Cell Tissue Res* 296(1) 19-25.

Zhao, X., et al. (2009). Retinoic acid promotes limb induction through effects on body axis extension but is unnecessary for limb patterning. *Curr Biol* 19(12) 1050-1057.

Zhu, J., et al. (2008). Uncoupling Sonic hedgehog control of pattern and expansion of the developing limb bud. *Dev Cell*. United States. 624-632.

Zuniga, A., et al. (1999). Signal relay by BMP antagonism controls the SHH/FGF4 feedback loop in vertebrate limb buds. *Nature* 401(6753) 598-602.

Zwilling, E. a. H. L. A. (1956). Interaction between limb bud ectoderm and mesoderm in the chick embryo. III. Experiments with polydactylous limbs. *Journal of Experimental Zoology* 132(2) 219--239.